# UNDERSTANDING POST DISASTER RECOVERY THROUGH ASSESSMENT OF LAND COVER AND LAND USE CHANGES USING REMOTE SENSING

MOHAMMADREZA SHEYKHMOUSA
February, 2018

SUPERVISORS:
Prof. Dr. N. Kerle
Dr. M. Kuffer

ADVISOR:
S. Ghaffarian, PhD Candidate

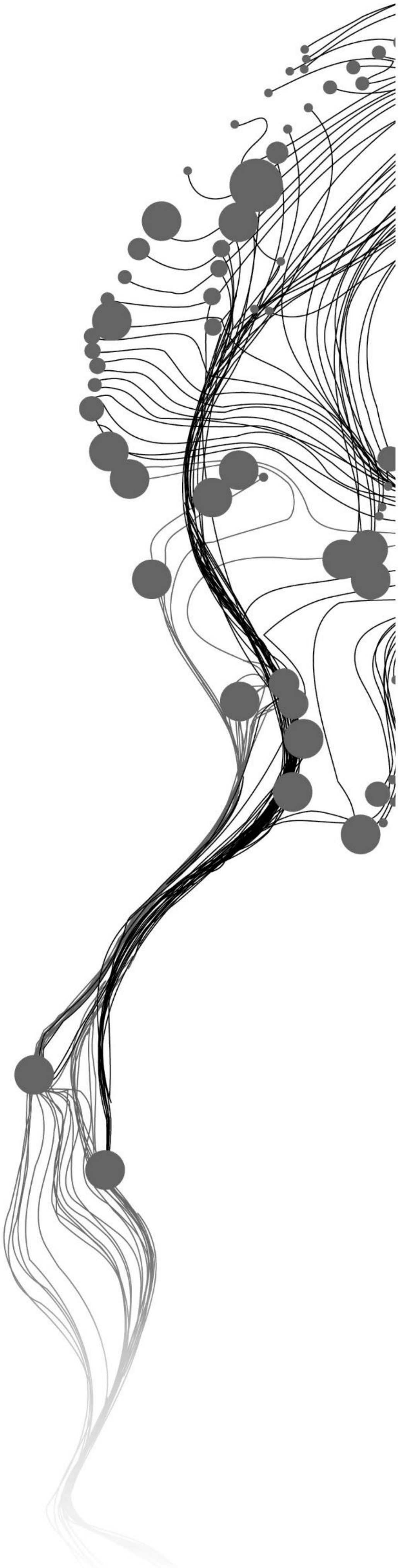

# UNDERSTANDING POST DISASTER RECOVERY THROUGH ASSESSMENT OF LAND COVER AND LAND USE CHANGES USING REMOTE SENSING

MOHAMMADREZA SHEYKHMOUSA
Enschede, The Netherlands, February, 2018

Thesis submitted to the Faculty of Geo-Information Science and Earth Observation of the University of Twente in partial fulfilment of the requirements for the degree of Master of Science in Geo-information Science and Earth Observation.
Specialization: Applied Earth Sciences

SUPERVISORS:
Prof. Dr. N. Kerle
Dr. M. Kuffer

ADVISOR:
S. Ghaffarian, PhD Candidate

THESIS ASSESSMENT BOARD:
Prof. Dr. V. Jetten (Chair)
Dr. Maik Netzband (External Examiner, University of Wuerzburg)

# ABSTRACT

Post-disaster recovery is a complex phenomenon, and distinct from physical reconstruction (physical recovery) in that it includes relevant processes such as economic and social (functional recovery). The recovery is reported to be the least understood phase of disaster cycle, where existing literature mostly focus on physical recovery, neglecting functional recovery. Disasters introduce changes to the affected land and in subsequent post-disaster activities through land cover and land use change (LCLUC). LCLU information extracted from satellite imagery is widely used in the RS disciplines. However, the value of this information in the recovery context has not yet been explored.

The main purpose of this study was to support the recovery assessment through LCLUC analysis using RS and specifically to investigate the value of LCLU information in the recovery assessment. Tacloban city in the Philippines was selected as a test area. On 8 November 2013, Tacloban city was devastated by super typhoon Haiyan, the strongest typhoon on record to make landfall. Despite the crippling damage, the local government tried to coordinate recovery efforts towards a more resilient city. The available data were 3 WV2 images from 8 months before, right after, and 4 years after typhoon Haiyan. First, a methodology was developed based on a generic, action-oriented, forward-looking conceptual framework (CF), comprised of transition patterns (TPs) to characterize different recovery statuses. Here it is understood that recovery information is a geographic phenomenon and related TPs are geographic objects. Moreover, it is found that some TPs can specifically characterize short- and some long-term recovery. Second, for classification purposes support vector machine (SVM) was employed, and a detailed comparison of the performance of linear- and RBF-based SVM relying on the various settings of hand-crafted features was conducted. The best combination of SVM with image features (SVM+GLCM+NDVI2, SVM+LBP+NDVI2; LC and LU tasks respectively) were applied in 3 time-span images to produce LCLU maps. The result showed (OA: 89.4%, 82.2%, 90.8%; 76.3%, 69.9%, 77.8%; LC and LU respectively) that well designed hand-crafted features could show competitive performance in a complex task involving classes from simple and small to abstract and big regarding complexity and size, respectively. However, more investigation is needed when it comes to vegetation related classes in "use" level.

Lastly, The LCLU maps were stacked and, based on the developed CF, different TPs from the stacked LC and LU maps were extracted. The final products are LC- and LU-based recovery maps which were further up-scaled to a region level. It was found that the characteristic of the post-Haiyan recovery in Tacloban city can be explained through the LCLUC information. Results of this study showed that 168 ha of the area had positively recovered by the time of the most recent image, while 69 ha showed negative recovery in both LC- and LU-based recovery maps. Positive recovery was mainly related to the recovery projects and was in part effective to build back the damaged area and build impervious surfaces back better. However, the recovery project fails where slum areas were rebuilt again along the coastline, where study suggests considering slum areas in the readjustment projects. Additionally, it is concluded that the general understanding of the recovery could be provided by LC information and LU information can be used, where LC information cannot provide useful recovery evidence (area of uncertainty). The other finding was that due to the different recovery rate of regions and practicality issues, an adaptive approach should be considered for the timing of the imagery. Meaning that while a 3-time-based framework provides an initial recovery (assessment) insight of a region, a 5-time-based framework can be used as a normal framework which can give an overall assessment of the area, when the timing of the imagery should be well adjusted with different recovery rate of specific activities (adaptive approach). Another important purpose of this research was to establish the relation between the existing recovery indicators

and advanced RS methods. The study provides 3 tables, where all relevant indicators are grouped based on their utilities ranging from low and medium to high; micro, meso, and macro indicators, respectively.

The overall findings emphasis that the LC-based recovery map contributes to the general recovery understanding, while detailed functional recovery is revealed by LU-based recovery map.

**THESIS IN ONE SENTENCE**: LCLU-based information is useful in the most aspects of recovery measurement, while also providing (from a basic to a deep) understanding of recovery assessment.

# ACKNOWLEDGEMENTS

Thank God for finally writing this thesis! One of the most challenging and at the same time fruitful periods in my life. Sincere appreciation to my supervisors Prof. Norman Kerle and Dr. Monika Kuffer, and my advisor Saman Ghaffarian, who have dedicated their time and effort to guide me through this thesis.

I would also like to thank the UT-ITC for the opportunity given to me through the excellence scholarship. This unique opportunity enabled me to pursue my dreams at ITC. In addition, I salute my classmates from all over the world, with whom we toiled daily.

The satellite imagery were provided from Digital Globe Foundation, which were granted for an ongoing project at ITC entitled "post-disaster recovery assessment using remote sensing data and spatial economic modeling."

Lastly, I extend the warmest appreciation to my dear parents in Iran for their constant support, to my lovely balio for always being there and providing moral support, to other members of family and friends, and I dedicate this to Ghochak. "This is us!"

*Follow Your Dreams!*

# LIST OF ABBREVIATION

| | |
|---|---|
| Build Back Better | BBB |
| Change Detection | CD |
| Conceptual Framework | CF |
| Comprehensive Land use Plan | CLP |
| Convolutional Neural Network | CNN |
| Disaster Risk Management | DRM |
| Food and Agriculture Organization of the United Nations | FAO |
| Geographic Information System | GIS |
| Grey Level Co-occurrence Matrix | GLCM |
| Hilbert-Schmidt Independence Criterion | HSIC |
| Local Binary Pattern | LBP |
| Land Cover Land Use Change | LCLUC |
| Light Detection and Ranging | LIDAR |
| Machine Learning | ML |
| Overall Accuracy | OA |
| Object-Based Change Detection | OBCD |
| Object-Based Image Analysis | OBIA |
| Open Street Maps | OSM |
| Producer Accuracy | PA |
| Pixel-Based Change Detection | PBCD |
| Random Forest | RF |
| Remote Sensing | RS |
| Support Vector Machine | SVM |
| Transition Pattern | TP |
| User Accuracy | UA |
| Volunteered Geographic Information | VGI |
| Very High Resolution | VHR |
| World View 2 | WV2 |

# TABLE OF CONTENTS

1. Introduction....1
1.1. Background....1
1.2. Research Motivation....2
1.3. Research Identification....3
1.4. Objectives and Research Questions....3
1.5. Thesis Structure....4
2. Understanding post disaster recovery....5
2.1. Post Disaster Recovery....5
2.2. Physical vs. Functional Recovery....6
2.3. Importance of Recovery Assessment....6
2.4. Link between Recovery, Rehabilitation, Reconstruction, and Resilience....7
2.5. Recovery Assessment....8
2.6. Recovery Outcome....10
2.7. Stakeholders in the Recovery Process....10
2.8. Urban-rural Dynamics and Existing Literature....11
3. Test Area and data....14
3.1. Test Area and Datasets....14
4. Methodology....16
4.1. Conceptual Framework....16
4.2. Land Cover and Land Use Analysis....24
4.3. Develop a Practical Guide....29
5. Results and analysis....30
5.1. Land Cover and Land Use Analysis....30
5.2. Practical Guide....41
6. Discussion....45
6.1. Utility of the Conceptual Framework....45
6.2. Utility of SVM Relying on GLCM and LBP Features....45
6.3. Utility of LCLU and Recovery Maps....46
6.4. Utility of the Number of Imagery in Recovery Assessment....49
6.5. Utility of Practical Guide....49
6.6. Final Remarks....50
7. Conclusion....51
7.1. Recommendations and Future Works....53
List of references....54
ANNEX....63
Annex 1: A complete list of LC-based transition patterns in the study area....63
Annex 2: A complete list of LU-based transition patterns in the study area....65
Annex 3: LU plan of study area (CLP, 2016)....70

# LIST OF FIGURES

Figure 1-1 Disaster risk management cycle (Coppola, 2015) ........ 1
Figure 2-1 Different sectors in community recovery (CDEM, 2005) ........ 5
Figure 2-2 Recovery vs. Rehabilitation vs. Reconstruction (Ghaffarian, 2016) ........ 7
Figure 2-3 System trajectory (Fiksel, 2003) ........ 8
Figure 2-4 Relation between LC, LU and land function, and possible methods to collect spatial data (Verburg et al., 2009) ........ 11
Figure 3-1 (A) Track of typhoon Haiyan (Maly, 2017). (B) The location of study area ........ 15
Figure 3-2 three satellite images of the study area; red rectangles show the statuses of the slum areas which were heavily devastated by the typhoon Haiyan ........ 15
Figure 4-1 Interaction between post disaster recovery and LCLUC ........ 17
Figure 4-2 Relation between LC and LU recovery, and physical and functional recovery ........ 17
Figure 4-3 LCLU-based recovery conceptual framework ........ 19
Figure 4-4 Hierarchy definition of LCLU classes ........ 19
Figure 4-5 Damage classes for a single building, (Vertivel et al., 2016) ........ 21
Figure 4-6 Illustration of land cover classes ........ 22
Figure 4-7 Illustration of damage classes ........ 23
Figure 4-8 Illustration of land use classes; IBA: Informal Built-up Area, FBA: Formal Built-up Area, LSI: Large-Scale Industry ........ 23
Figure 4-9 Test area (500*500 pixel) ........ 25
Figure 4-10 Description of the recovery map ........ 29
Figure 5-1 A subset of WV2 imagery, (A) area of confusion between "crop" and "grass" in three time-span, (B) area of confusion between "palm tree" and "other tree" in three time-span and related multi spectral and panchromatic zooming window, (C) status of potential grass land ........ 33
Figure 5-2 Complex status of built-up-related classes in the three time-span ........ 33
Figure 5-3 Complexity of the palm tree and other tree classes; palm trees are shown with red circles; drone imagery ........ 34
Figure 5-4 LC Classification maps from SVM relying on GLCM features and NDVI2 for T0, T1, and T2 and corresponding pie charts ........ 36
Figure 5-5 LU Classification maps from SVM relying on LBP features and NDVI2 for T0, T1, and T2 and related pie charts, LSI: Large Scale Industry, IBA: Informal Built up Area, FBA: Formal Built up Area ........ 37
Figure 5-6 (A) LC-based recovery map; (B) LU-based recovery map; data source: WV2 images (T0, T1, and T2); recovery map approach: based on a code developed in R; main Observation: striking difference between A and B is mainly due to 2 issues:1) class slightly positive recovery (SP) in A, where the area is mostly covered by TP "building-rubble-building", which this TP is changed to other TPs in B such as IBA-rubble-IBA (N: negative recovery) 2) due to different TPs used in A and B.... 39
Figure 5-7 (A) A comparison between LC- and LU-based recovery map; (B) area per class for LC-based recovery map; (C) area per class for LU-based recovery map ........ 39
Figure 5-8 Visual examples of LC- LU-based recovery maps ........ 40
Figure 5-9 (A) Aggregated LC-based recovery map, (B) Aggregated LU-based recovery map ........ 41
Figure 6-1 Recovery vectors (A) concept of build back (B) concept of build back better ........ 45
Figure 6-2 Utility of LCLU in a holistic recovery, adopted from (CDEM) ........ 47

Figure 6-3 (A) Recovery projects after typhoon Haiyan at Santa Elena in the North part of Tacloban city; (B) project with high recovery rate; (C) project with low recovery rate; both projects are shown in 8-time-span ranging from; 2 months pre-typhoon (-02) to 40 months post-typhoon (+40). ................ 50
Figure 7-1 Proposed framework of combined information......................................................................... 53

# LIST OF TABLES

Table 4-1 LC class definition (H: high, M: medium, and L: low) ..... 20
Table 4-2 LU class definition (H: high, M: medium, and L: low) ..... 21
Table 4-3 Damage class definition (H: high, M: medium, and L: low) ..... 22
Table 4-4 LC- based conceptual framework for post- Haiyan recovery process in Tacloban city ..... 24
Table 4-5 LU- based conceptual framework for post- Haiyan recovery process in Tacloban city ..... 24
Table 4-6 Definition of parameters and related methods used in the experiment ..... 25
Table 4-7 Definition of grid search space for tuning the hyper-parameters SVM ..... 26
Table 4-8 Extracted features from multispectral image ..... 27
Table 4-9 Spectral index description ..... 27
Table 5-1 Selected GLCM features for LC classification ..... 31
Table 5-2 Selected GLCM features for LU classification ..... 31
Table 5-3 Comparison of LC classification accuracies of test area ..... 32
Table 5-4 Comparison of LU classification accuracies of test area ..... 32
Table 5-5 Comparison of LC classification accuracies for pre-, event, and post-disaster situation. Overall, user and producer accuracies and corresponding errors are computed across the whole study area by combining the confusion matrices of T0, T1, and T2 ..... 32
Table 5-6 Comparison of Land Use Classification Accuracies ..... 34
Table 5-7 Macro indicators with high utilities in the recovery assessment ..... 42
Table 5-8 Meso Indicators with medium to high utilities in the recovery assessment (list of acronyms is provided after Table 5-7 on the previous page) ..... 43
Table 5-9 Micro indicators with low to medium utilities in the recovery assessment ..... 44

# 1. INTRODUCTION

## 1.1. Background

A disaster is "a serious disruption of the functioning of a community or a society involving widespread human, material, economic or environmental losses and impacts, which exceeds the ability of the affected community or society to cope using its own resources" (UNISDR, 2009, p. 9). A disaster occurs when a hazardous event hits a vulnerable society or community, and the negative consequence of it surpasses the capacity of the society or community to cope with its own resources, including information and finance (UNISDR, 2015a). Disaster events, in Disaster Risk Management (DRM) perspective, are based on four distinct elements: mitigation, preparedness, response, and recovery (Figure 1-1). Post-disaster recovery - in short, "recovery" - can be seen from three different and in parallel interconnected aspects; goal, phase, and process. Recovery phase begins with the emergency response activities, and it is finished when recovery reaches its goals; i.e., restoring before disaster state. Recovery is the process by which societies rebuild what has been lost during a disaster and return to a functional condition (Coppola, 2015).

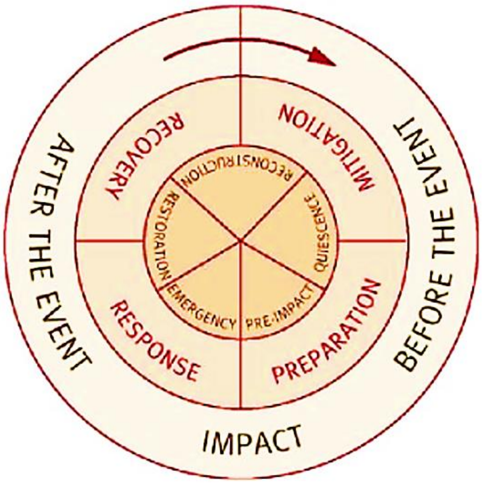


Figure 1-1 Disaster risk management cycle (Coppola, 2015)

After large disasters, a considerable amount of money from donors and governments tends to finance the recovery process (Brown et al., 2009) to reach the recovery goals (Lindell, 2013). Although it is important for all stakeholders to monitor and assess the recovery process towards its goals systematically, it has been described as the least understood phase of disaster management in natural hazards literature. There are no comprehensive models to measure the complexity of recovery over time ( Haas et al., 1977; Miles & Chang, 2006). Thus, recovery assessment is vital for policyholders and donors. Supporting their needs of obtaining reliable and useful indicators can ideally represent the entire recovery process. These indicators should be cost-effective, measurable, reproducible, sensitive to change over time, and helpful for decision making on a different dimension of recovery; i.e., policy, executing agency and research (Horney et al., 2016). In addition, they need a method that allows them to make quick and right decisions and to give the alarm when the recovery process does not work as planned (Brown et al., 2010). Current recovery assessment methods comprise of ground-based techniques such as household survey and social audit, which cannot cover all aspects of integrated recovery (physical and functional recovery), specifically over large areas, while also are time- and money-consuming (Platt et al., 2016). However, to monitor recovery, conventional methods such as ground survey and social audit can also be combined with satellite imagery analysis. Remote sensing (RS) allows to quantify and assess recovery over large areas, and the qualitative methods allow to get details from the ground for small areas.

In the RS-based recovery assessment, most of the developed methods have traditionally been focused on the reconstruction part of recovery. However, there have been changes in this trend towards a more holistic recovery process (sustainable recovery), taking other parts of recovery into account (Joyce et al., 2009b). Brown et al. (2010) used indicator-based methods based on very high resolution (VHR) imagery combined with the social audit for recovery assessment. However, this work uses a rather conventional method which has been criticized in recent publications of been not very suitable for VHR imagery (Lu & Weng, 2007a).

Disasters and their subsequent recovery processes influence land cover (LC) and land use (LU) (Banba & Shaw, 2017; Platt et al., 2016). Therefore, land cover and land use change (LCLUC) detection can be used as an important and reliable as well as practical indicator to monitor and assess the recovery process. It can reveal functional changes (land use) on the ground beside general physical changes (land cover). Furthermore, out of all possible LCLUCs, some specific changes tend to occur within the recovery, which can characterize the process. LCLUC, moreover, are two robust indicators with high explanatory power across the recovery process and over time, which also can be used to assess how well the affected area is recovered (Banba & Shaw, 2017). In addition, LCLUC can help stakeholders to shift from expensive recovery assessment to a more sensible one.

The increasing availability of VHR datasets before and after the event, allow the use of change detection (CD) in recovery assessment (Pitts & So, 2017). Change detection based on remotely sensed data is an established method in other domains (Joyce et al., 2009b). RS-based change detection is an ever-growing topic with the most focus on LC and less on LU classification. A large number of RS based CD methods have been established using conventional pixel-based and object-based approaches (Hussain et al., 2013).

Machine learning (ML) algorithms are popular in the field of RS where they have demonstrated their capability in different learning tasks with different data types and potentially are robust enough to handle high-dimension data (e.g., VHR and high-spectral data) (Hussain et al., 2013). Among ML methods, support vector machine (SVM) is a non-parametric classifier, which can handle complex learning task with the small amount of training datasets that produce competitive results (Mboga et al., 2017), while also is capable of handling high dimensional data (Persello & Bruzzone, 2016).

### 1.2. Research Motivation

Disaster events tend to receive huge financial and technological supports, which mostly flow from donors towards executing agencies, within the recovery process. Yet, there is no comprehensive model to assess and monitor the integrated recovery process, and as a result, the recovery output is not clear (quantifiable). For example, conventional recovery assessment methods are expensive, time-consuming, prone to subjectivity, and hard to communicate among stakeholders, while also lacking accuracy, transparency, and reliability (Brown et al., 2010). One of the motivations of this study is to help stakeholders involved in the recovery process to avoid an expensive recovery assessment and provide a more quantifiable recovery assessment, which also covers physical and functional recovery. This can be done with the help of a recovery (assessment) map based on tracking some trajectories of LCLU changes (transition patterns). For instance, a disaster and corresponding recovery process affect some special types of LCs and LUs - not all change patterns are related to the recovery - within the affected area. In the recovering community, moreover, there are some RS-based recovery assessment indicators (e.g., Brown et al., 2010) with different levels of practicality, which are also based on visual interpretation. For instance, local type indicators such as "clean and neat swimming pool" with low practicality to assess recovery. Thus, there is a need to group them and further link them with more advanced RS methods.

In a recent study, researchers from the recovering community highlighted RS-based recovery assessment "requires specialized software and trained staff" (Platt et al., 2016, p. 459), which clearly shows a gap of robust and advanced approaches in RS-based recovery assessment. For instance, the commonly employed RS methods for recovery assessment are rather dated, not suitable for VHR imagery and do not use latest developments of the RS community (e.g., machine learning). Besides, in the urban RS community, there are established methods using abovementioned ML methods coupled with feature texture for LCLU classification, which potentially can be adapted in this research. However, the use of LCLUC to understand/characterize recovery has not been sufficiently investigated in an urban-rural context using VHR satellite imagery. Therefore, there is a need to develop an RS-based methodology which suits the special properties of the recovery process and VHR data characteristics by a multi-step approach based on some trajectories of changes.

Moreover, although in studies on recovery assessment there are a few examples of using LC, they are either limited to a local area or applied to a subcategory of the recovery process (e.g., Khan et al., 2014). Therefore, this study aims to provide a more holistic understanding of the recovery process through investigating the value of LCLUC, considering physical and functional recovery, spatially over large areas.

## 1.3. Research Identification

The research focuses on investigating the utility of LCLUC with RS methods in the post-disaster recovery assessment, aiming to understand and characterize it over large areas (including rural and urban areas), using VHR satellite imagery. This study uses Worldview 2 images (3 time-span), acquired over the Tacloban city 8 months before (pre), 3 days after (event), and 4 years after typhoon Haiyan (post), in the Philippines. Considering the research problem, the study is broken down into main objective and three sub-objectives and related research questions.

## 1.4. Objectives and Research Questions

### 1.4.1. Main Objective

To investigate the value of land cover and land use changes (LCLUCs) in the post-disaster recovery assessment, using remote sensing.

### 1.4.2. Specific Objectives and Research Questions

Specific objectives and related research questions are:

- To develop a conceptual framework for the recovery assessment using land cover and land use changes.
    1. How to translate observable, theoretical and potential LCLUC in the post-disaster recovery process into a conceptual framework? How to implement such a framework in the study area?
    2. Which LCLU classes are the most meaningful to understand the recovery process and why?
    3. How far can recovery be understood by LC information? What is the contribution of LU information?
- To investigate the significance of land cover and land use change to understand the recovery.
    4. Which advanced urban RS based method is appropriate for LCLU classification for Tacloban city?
    5. Which image features are suitable for the LCLU classification?

6. How is Tacloban city recovering in terms of LCLU? How many images are appropriate to assess recovery process in Tacloban city and why?

- To develop a practical guide from existing recovery indicators.

7. How can the conceptualization in existing urban-recovery literature (e.g., Brown et al., 2010 indicators) be linked with RS methods?
8. How well can existing indicators be used in practice? Which indicators from this thesis or other disciplines can be used in the recovery assessment?

## 1.5. Thesis Structure

This study is organized into seven chapters. A concise outline explaining the content of each chapter is given below:

**Chapter1**

The general background and motivation of this study are provided. Then the research problem is introduced followed by objectives and research questions.

**Chapter 2**

In chapter 2, a deep literature review is conducted to understand the recovery aspects, land cover and land use and their relations with land functions, and methods used to assess recovery and LCLU, where the focus is given to RS-based methods.

**Chapter 3**

A brief background about study area and typhoon Haiyan is given together with an overview of the relevant data set for the purpose of the study.

**Chapter 4**

This chapter starts by introducing the conceptual framework followed by a class definition and implementation of the CF in the study area. Next, the methodology is described to carry out the experiments, to produce recovery maps. In the end, existing RS-based indicators in recovery field are investigated in terms of practicality and a guide is provided to link them with advanced RS methods.

**Chapter 5**

This chapter provides the results obtained through the applied methodology.

**Chapter 6**

A comprehensive discussion is presented in this chapter, including a critical analysis of the data used, results obtained, and limitations.

**Chapter 7**

Lastly, conclusions drawn from the study and recommendations for future research opportunities are presented in this Chapter.

# 2. UNDERSTANDING POST DISASTER RECOVERY

## 2.1. Post Disaster Recovery

Definitions of recovery vary in the literature. The term is generally used as the process of returning to a normal condition after a period of difficulty (Chang, 2010). Recently, recovery has been described as a complex and arduous process, which in minor cases can be evaluated in months, years and in extreme cases in decades (Lindell, 2013). That is mainly because recovery is a multi-layer process. Several researchers have portrayed different aspects of recovery. Early studies conceptualized long-term recovery as a foreseeable process which happens sequentially (Haas et al., 1977) with the focus on the reconstruction aspect of recovery (physical recovery). Subsequent criticisms have contested the logic claimed in this study (Rodríguez et al., 2007). Rather, recovery has later been described as an ambiguous process, which can be influenced by decision making, social disparities and available resources (Bolin, 1994). Along with this definition, Rodríguez et al. (2007) described the recovery as a complex and uncertain process which different factors such as race, class, past disaster experience, power, and access to resources, can influence the process, ranging from individual to community level.

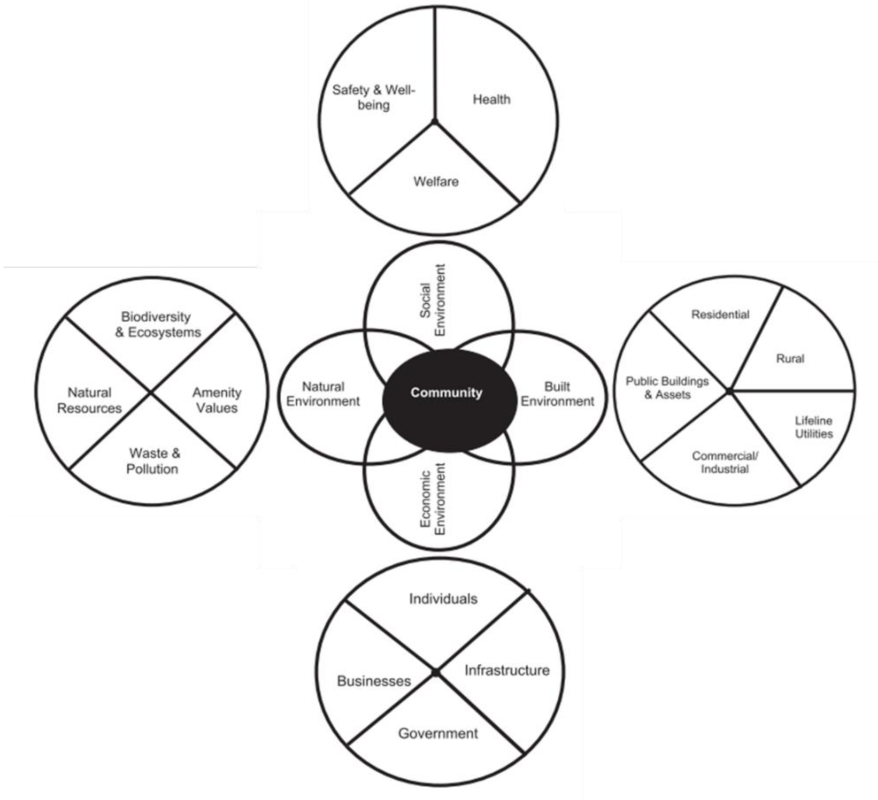


Figure 2-1 Different sectors in community recovery (CDEM, 2005)

A holistic view of the recovery is introduced by CDEM (2005) (Figure 2-1). In this framework, community recovery consists of four distinct aspects which partially overlap: *social*, *natural*, *economic*, and *built environment*, and they will be referred as recovery sector, which each sector contains some other subdomains. Lindell (2013) stresses temporal differentiation among different phases in the recovery process and divides it into four phases; *disaster assessment*, *short-term recovery*, *long-term recovery*, and *recovery management*, which can happen either sequentially or simultaneously. *Short-term recovery* focuses on starting the recovery process for businesses and households as well as immediate relief activities; i.e., providing shelters and debris removal among others. Among short-term recovery activities, providing temporary shelter is a challenge specifically after large disasters, in parallel with restoring critical infrastructure.

*Long-term recovery* or reconstruction phase includes the reconstruction of the affected area and manages social, psychological, demographic, economic and political impacts due to a disaster. Successful long-term recovery requires a good planning strategy, a substantial amount of coordination and employment of policies (Coppola, 2011). Nowadays, the recovery process is generally accepted beyond reconstruction. It is a multi-dimensional, nonlinear and complex process. It concerns changing from physical recovery to rebuilding of people's lives and livelihoods (functional recovery)(Brown et al., 2010). Thus, disaster recovery can be described as "the differential process of restoring, rebuilding, and reshaping the physical, social, economic, and natural environment through pre-event planning and post-event actions" (Rodríguez et al., 2007, p. 237). Moreover, Olshansky et al. (2012) argue that the fundamental difference between post-disaster situation and the normal condition is "time compression". The post-disaster environment consists of a compression of urban development activities in time and in a limited space (Olshansky et al., 2012).

## 2.2. Physical vs. Functional Recovery

The definition of urban functions varies depending on author and research goal (Foerstnow, 2017). The urban function can be characterized based on the land use type such as commercial, residential and industrial among others, which inherently are related to the corresponding land cover. While land cover represents physical aspect of the earth surface, land use signifies how the landscape is used and is "about the functional aspect of land" that differs by the level of human actions (Food and Agriculture Organization of the United Nations (FAO), 2009). Although urban function can be related to an operational aspect of land; i.e., if a barely damaged hospital is functioning after the disaster, it can also relate to the use of land (FAO, 2009). The focus of this study is more based on FAO definition of land use and functions. The relation between land cover, land use, and land functions is further discussed in section 2.8.1.

Disasters cause socio-economic and physical damages in urban systems. Accordingly, disaster recovery includes not only physical reconstruction (physical recovery) but also the more challenging re-establishment of the whole damaged socio-economic system (functional recovery) in the affected area. Functional recovery of the affected area may be much more complicated to be attained than physical recovery (Dong, 2012). Sustainable recovery requires not only to look at the physical recovery but also functional recovery and provides an opportunity to improve the pre-disaster vulnerability (Passerini, 2000).

## 2.3. Importance of Recovery Assessment

Many people and societies suffer from (large) natural disasters' impacts, such as social and physical impacts (for more background on disasters' impacts see Lindell, 2013). For example, between 2005 and 2014, 169 million people were affected on average by disasters on a yearly basis (CRED, 2014). Accordingly, the annual average damage (due to disaster) to economy and assets -in the past 50 years- jumped from US$10bn to US$100bn. Although large-scale natural disasters extremely damage the affected area, many researchers have also shown that disasters and subsequent recovery processes can bring specific opportunities for disaster-stricken communities. For example, to solve pre-existing vulnerabilities and to further advance remarkable changes and betterment which is well known as the "windows of opportunity that opens following a natural disaster" (Olshansky, 2006). When stakeholders are ambitious to restore the damage and disruption and further to maximize the benefits, it is vital to know how long would the process take for a society to recover (Platt et al., 2016). Moreover, how well it would be (Saito et al., 2009) or how much have been reached so far and what should be done next (Brown et al., 2008).

Post-disaster recovery creates the opportunity for mitigation to reshape the community in a way that can either improve or hinder sustainability. A careless recovery process can lead to numerous negative impacts on the community including losing jobs, shoddy reconstruction, missing mitigation opportunities, and losing people's trust among others (Johnson, 2012) as well as making unpractical decisions (Dong, 2012). Conversely, successful recovery introduces a significant window of opportunity for mitigation (Nakabayashi, 2014) and to rebuild a stronger structure compare to the pre-disaster situation, alter land-use plan with the focus on risk reduction and meaningfully reshape the current socio-political and economic landscape (Rodríguez et al., 2007). Moreover, the recovery process is important for people's safety, well-being and is the main subject of long-term planning for the affected area. Recovery assessment improves aid policy, transparency of the process, the capability of executing agency for on-going works and provides liability (Brown et al., 2009). Comprehensive knowledge of recovery (especially over large areas) helps stakeholders to act quicker, more efficient, and better for both short- and long-term recovery. A better understanding of recovery also helps post-disaster actions, increase societies resilience rather than regain pre-disaster stage (Miles & Chang, 2007).

## 2.4. Link between Recovery, Rehabilitation, Reconstruction, and Resilience

Terms recovery, rehabilitation, and reconstruction are often confused. Rehabilitation is a short-term process and refers to an elementary restoration of facilities and services in a way that the affected community can continue functioning (UNDP, 1993). The focus should be on helping victims to (temporarily) repair physical damages to prevent secondary damage in a disaster situation such as explosion due to gas leakage. Reconstruction, however, is a long-term process and refers to the rebuilding of all damaged physical structures and restoration of facilities, services, and livelihoods which are needed for the full functioning of an affected community in a timely and efficient manner (UNISDR, 2015a) (Figure 2-2). Moreover, in the reconstruction phase, it is important to take many issues into account: i.e., building codes and program standards (technical construction assistance to disaster-stricken community), regulations (land use control) as well as social policies (for more background see EPC, 2004), equity and relocation (EPC, 2004). However, displaced people mostly care about the availability of services to meet their basic needs, before returning to the before disaster place. Reconstruction can also be seen as a basis for functional recovery. Rehabilitation and reconstruction collectively are referred as recovery (Chang, 2010).

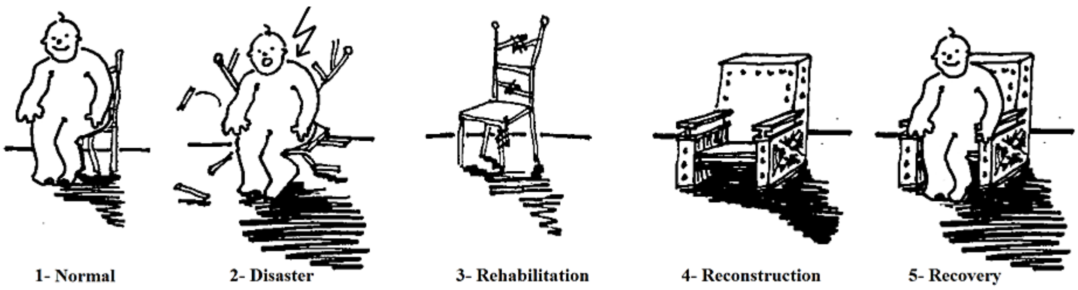


Figure 2-2 Recovery vs. Rehabilitation vs. Reconstruction (Ghaffarian, 2016)

The recovery process, moreover, is in a close relationship with the resiliency of a society. The concept of resilience has been imprecise in the disaster-related literature (Platt et al., 2016). According to UNISDR (2015), resilience is "the ability to "resile from" or "spring back from" a shock. Measuring resilience is a complex issue, or as Cutter (2016) has described "is messy and increasingly hard to navigate". Next to Cutter, Alexander (2013) in an etymological study described resilience comprises a community's capacity to bounce back after a disaster, its preparedness level, and capability to recover quickly. Additionally, the social aspect of resilience comprises of coping capacity (i.e., to cope with and overcome hardship), adaptive capacity (i.e., ability to transfer past experience), and transformative capacity (i.e., the ability to foster people) (Keck & Sakdapolrak 2013). Resilience is recently being used in the land use planning framework called 'resilience planning' which is often confused with sustainability (Saunders & Becker, 2015). To analyze resilience, Fiksel (2003) adopted a simple graphic from thermodynamic systems to describe different types of resilience. Cities can be seen as (complicated) systems which have their own stable state (i.e., normal state) and resources. While system 1 is resistant to a small shock but unable to cope with a larger event, system 2, shows a better resiliency to disturbances, and ultimately, system 3 offers even a greater resilience in the case of a significant disturbance (Figure 2-3).

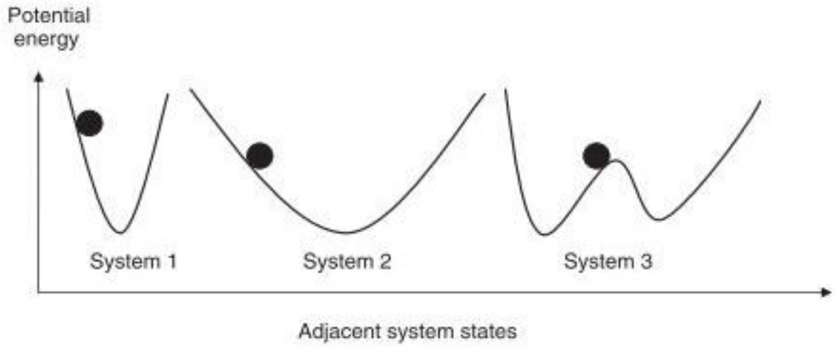


Figure 2-3 System trajectory (Fiksel, 2003)

The quality and the speed of the recovery process can be used as indicators of the resilience of an affected area (Platt et al., 2016). Lin & Wang (2017) argue that the resilience of a community can be assessed by its residual functionality after a disaster (robustness) and by the speed of functional recovery to a normal situation; i.e., pre-disaster norm or a new equilibrium.

## 2.5. Recovery Assessment

Post-disaster recovery assessment is an important issue in terms of providing accountability, enhancing aid policies, helping decision makers and executing agencies with reliable information from on-going work on the ground and to further check whether they are in the right track or not (Saito et al., 2009). This assessment requires valid data from different involved sectors in the process such as physical, social, economic and environmental sectors. In addition, the level of analysis (i.e., individual, households, neighborhoods, community, city or regions) plays an important role in the assessment. Besides, understanding the recovery is essential for assessing and reaching to community resilience (Lin & Wang, 2017).

Recovery assessment necessitates robust methods and reliable data (Brown et al., 2008). This requires a "comprehensive understanding of post-disaster circumstances and conditions, including damage and serviceability of buildings and lifelines, their interactions with social and economic systems, availability of human and financial resources for recovery activities, and decisions made by relevant stakeholders"(Lin & Wang, 2017, p. 96) at each stage of the recovery process. Many techniques and methods and data are available in the literature; satellite imagery analysis, volunteered geographic information (VGI), official publications and statistics, social audit (key informant interviews and focus groups), ground survey and observation, household surveys, and insurance data (Platt et al., 2016). These methods and data-types can be categorized into two main groups: direct observation; i.e., remote sensing, and social audit; i.e., ground-based surveys (Brown et al., 2010). Since the focus of these study is remote sensing based recovery, the recovery assessment is categorized into remote sensing based and in-situ based methods (here is called ground-based methods). The following sections provide examples from the literature on recovery assessment for both groups.

### 2.5.1. Ground-Based Methods

A growing body of literature from different disciplines has been directed towards assessing and monitoring recovery (Brown et al., 2009). Conventional studies in the post-disaster recovery assessment focus on built-up environment and short-term evaluation of damaged buildings. However, recovery assessment is vastly related to the *scale* (i.e. individual, household, business, and community) and *timespan* (i.e., different recovery output is possible for the same place but different timeframe) being studied, as well as the *perception* of the evaluator (i.e., the result may vary per individual, aiding agency, and local people) (Brown et al., 2008). Some researchers have assessed recovery considering household and housing unit (Bolin & Bolton, 1983), while others focused on business recovery (Webb et al., 2000). Assessing recovery, moreover, at a community level has captured the attention of the scientific community (Rubin et al., 1985), including various social audit methods (Brown et al., 2008) from ground survey (Dong, 2012), semi-structured interviews to household surveys (Yi et al., 2015). Social audit is mainly used to collect and combine the data regarding the timing and the quality of the process, as well as people's perception of the process. Additionally, published materials including official and statistical reports mainly from local governments, census data, and archived documents serve as sources of information for validating the extent and timing of different parts of the recovery process (Platt et al., 2016).

Recently, social media such as Twitter has been recognized by researchers and practitioners as a key to communicate and coordinate the recovery process, especially in its early stage. In a new research, for example, Yan et al. (2017) discussed how geo-tagged social media data in Flicker, as VGI, can contribute to monitor and assess tourism recovery. However, alternative ways of communication and awareness raising such as mass media campaigns, should not be neglected (Khan & Sayem, 2013). In 2015, Takahashi et al. used Twitter within and after typhoon Haiyan in the Philippines where results showed social media mostly used to disseminate second-hand information, in coordinate with relief and recovery efforts.

#### 2.5.2. Remote Sensing-Based Methods

Remote sensing has been proven as an ideal tool for spatial information and related utilities in case of natural disasters around the world (Kerle, 2016). However, there are different data types (e.g., radar, and optical) and techniques (i.e., different image processing techniques) regarding remote sensing, and different disaster types (e.g., volcanic activity, earthquake, and typhoon). In disaster risk management cycle perspective, disasters consist of four phases (Figure 1-1) where, the use of remote sensing to support or monitor recovery is the least developed application of this technology (Joyce et al., 2009). However, remote sensing can greatly contribute to monitor and assess the recovery process through facilitating time-series analysis over large areas and at short intervals.

In RS-based recovery assessment, most of the developed methods and data-types have traditionally been focused on the reconstruction part of recovery. However, there have been changes towards a more holistic recovery process (sustainable recovery), taking other parts of recovery into account (Joyce et al., 2009b). Curtis et al. (2010), for instance, used video dataset in recovery assessment analyzing accessibility problems of remote places. In an extensive study, Brown et al. (2010) used indicator-based methods based on VHR imagery combined with the social audit for recovery assessment. Their indicators were mostly local-types indicators, which were expensive and time-consuming to collect while also lacking practicality. For instance, they used "clean/dirty swimming pool" as an indication of the recovery. Although the indicator can be helpful to a limited extent, it does not reveal information about recovery on a practical scale, unless for one specific building which has a swimming pool. Besides, the image analysis technique used (maximum likelihood classification) is not appropriate for VHR imagery (Lu & Weng, 2007).

#### 2.5.3. Remote Sensing Based Indicators

In the recovering community, there are remote sensing based indicators for recovery assessment. Indicators, in general, are informative tools, which can efficiently help recovery assessment. However, to address the recovery assessment, the indicators require some systematic level of standardization (Chang, 2010). Some of the indicators include a range of environmental, physical, social and economic factors where together provide a more comprehensive view of the recovery process (Platt et al., 2016). Building and corresponding removal of medium to long-term emergency shelters, commencement, and completion of new infrastructures such as roads, bridges and buildings, and vegetation regrowth among others are examples of these indicators for recovery assessment (Joyce et al., 2009).

Built-up and infrastructure sectors and corresponding indicators are more physical recovery-related indicators which are normally visible from satellite imagery. For example, the spatial location of recovery and the development-stage of it, debris removal, and roads are of large-scale indicators (macro indicators). Change in building morphology is an important indicator of living condition, and debris removal is an indicator of the speed of the recovery process in a time-series analysis (Brown et al., 2010). Although there are few researches using indicators for functional recovery, e.g., infrastructure-related indicators (accessibility and vehicle counts) to assess functional recovery (Foerstnow, 2017).

Economic related indicators and related factors are different (Brown et al., 2010) in different contexts. For example, shops and mini scale businesses in the developing countries should reopen quickly. Some remote sensing-based indicators of economic recovery are; the presence of large-scale industries, cooling towers, the presence of heavy vehicles, railroads, pipelines, roof color and material, and warehouses. Post-disaster reconstruction, in addition, highlights opportunities for manufacturers to move to a safer area based on the recovery plan which also has direct and unavoidable impacts on the transportation system (Hagelman et al., 2012). Social-type recovery indicators can also be extracted by RS methods. Built-up related activities impact social recovery, and consequently physical related indicators can be employed to assess social recovery (Carpenter, 2012). Temporary transition camps, the longevity of camps and local amenities are examples of physical-based social indicators, which can be detected and monitored in a timely manner to assess social recovery.

## 2.6. Recovery Outcome

It is difficult to define a precise goal for recovery and further to check whether the process was successful or not (Platt et al., 2016). There are different states described as recovery goals in the recovering community, aiming at different angels and dimensions of recovery. However, in general, the recovery process should achieve two goals; to replace lost housing stock (Brown et al., 2008) and to return to the pre-disaster level of economic function and finish the physical reconstruction; like infrastructure, housing, and public facilities. The ultimate recovery goal is to reach to long-term reconstruction to make the new permanent city with regards to a sustainable development plan (Olshansky, 2006).

The UNDP describes the aim of disaster recovery as "restore the capacity of national institutions and communities to recover from conflict or a natural disaster, enter transition or 'build back better', and avoid relapses" (UNOCHA, 2008, p. 28). Achieving to a sustainable recovery goes beyond restoring and reconstruction of the physical landscape, but it contributes similarly to risk and vulnerability reduction (Rodríguez et al., 2007). Sustainable recovery confirms that future generation will not suffer from the recovery process. Besides, recovery process should leave room for technological advancement and increase of awareness. Recovery, moreover, should boost mobility, accessibility and ensure building liveability (UNDP, 2013). Recovery outcomes are different based on their contexts; for example, the US government aims to return buildings to their previous state and avoid people profiting from the disaster. In a way, the government makes sure that there is no need for repeated construction. Other countries like Japanese and EU administrations aims to return to normality over a regional-scale when assessing recovery (Zorn & Shamseldin, 2015). Moreover, the goal of a non-physical aspect of recovery is to promote security and safety, health care, wellbeing, and engage psychological support for the people affected (Chang, 2010). Resilience is also one of the outcomes of the recovery process from policymakers and experts perspectives (Woolf et al., 2016).

## 2.7. Stakeholders in the Recovery Process

One of the important challenges in coordinating the recovery process is the large number of stakeholders (Brown et al., 2012). The potential users of the recovery process differ by level and context of disaster. For example, scientists and researchers from universities, institutes and research companies, planners from government and coordinating agencies, and NGOs can benefit from recovery information. Planners are involved throughout all the phases of the recovery process and are in charge of the decision making and support within and after recovery phases, where they require to act quickly and get together to make recovery plans and fund necessary resources. Besides, scientists can use the outcome of the decision making to explain the event and to provide further insight on the event. Additionally, NGOs need to access information about the transport, infrastructure, residential, etc. in their areas of interest and to inform the community (Brown et al., 2010).

## 2.8. Urban-rural Dynamics and Existing Literature

An effective post-disaster disaster recovery requires taking complexity of urban-rural components into account. In the previous sections, an overview of the recovery process was given. This section covers physical and functional aspects of the recovery process in an urban-rural setting through land cover, land use, and land functions and tries to explore their relations.

### 2.8.1. Relation Between Land Cover, Land Use, and Land Functions

The urban-rural setting can be divided into separate land covers, and their associated land uses. For example, bare soil can represent a dirt road, fallow land (agricultural land), and recreational area. Each of abovementioned examples has its own function; road, for instance, functions as a network. Definition of LCLU varies in the literature, mostly by the purpose of studies. However, in a broad term, LC refers to physical characteristics of the Earth surface (e.g., vegetation and concrete), whereas LU is attributed to the purpose of those characteristics or how they transformed by human activities (e.g., agriculture for vegetation), including land management practice. LC and LU are tightly related, but the relations are complex (nonlinear). Their changes are driven by natural activities and by human developments motivated by economic goals. (Verburg et al., 2009).

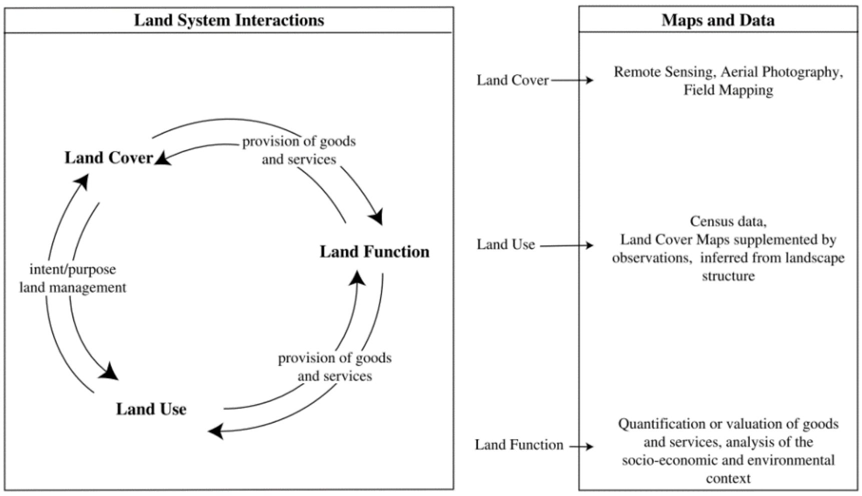


Figure 2-4 Relation between LC, LU and land function, and possible methods to collect spatial data (Verburg et al., 2009)

Land cover as a physical characteristic of the land surface is directly observable; either in the field or from remote sensing imagery. Land use, however, is more difficult to observe and may be inferred by observable activities; like grazing (Verburg et al., 2009), or by using appropriate image based features (Kuffer et al., 2016) in the remote sensing field. Monitoring and assessment of land function are often impossible based on LC data only (Pontius et al., 2008), and additional socio-economic data is needed.

Mapping land functions are complicated. Taking spatio-contextual and ability to provide goods and services of land into account, common approaches for land cover mapping may not be used for land functions analysis; i.e., land functions may frequently change while the land cover remains the same and vice versa. Verburg et al. (2009) asserted that there is no one-to-one relation between land cover and functionality. Thus, land cover is not a comprehensive indicator for land functions quantification. For instance, the non-linear relation between grassland and its function (e.g., grazing or natural grassland) exemplifies the limitation on information derived from land cover data provided by satellite imagery. However, land functions assessment is often restricted to land cover-based (change) map (Metzger et al., 2006) or an inconsistent mixture of LC and LU classes (Jansen & Gregorio, 2002). Alternative methods to map land functions could be using observable and/or modeled proxies (For more detail see Chan et al., 2006).

### 2.8.2. Urban Remote Sensing and Existing Literature

The availability of VHR datasets before and after the event in one hand, and a growing image records, on the other hand, allow the use of change detection in recovery assessment in a complex setting such as urban-rural areas. Change detection based on remotely sensed data is an established method in other domains (Joyce et al., 2009); however, it is mostly related to land cover change classification.

RS-based CD is an ever-growing topic with the most focus on LC and less on LU classification (Hussain et al., 2013). A large number of RS-based CD methods have been established, using pixel-based and object-based approaches. The pixel-based method compares corresponding pixels, while the object-based method compares related objects, both in time series images (Hussain et al., 2013). Both methods point to find different types of changes and associated locations, quantification, and accuracy. The conventional pixel-based change detection (PBCD) methods mostly focus on the spectral value of pixels and more recently exploit the spatial context of an image (Hussain et al., 2013). In contrast, the focus of object-based change detection (OBCD) is mostly on spatial correlation between neighboring pixels and tries to find changes within-objects (spectral changes) and in the objects (geometric changes) (Tewkesbury et al., 2015). Giving merit to one of the OBCD or PBCD is a controversial issue in the RS literature and demands considering many different aspects ranging from the purpose of the study to data types (Tewkesbury et al., 2015). In a comprehensive study, Duro et al. (2012) concluded there is no significant difference in statistical accuracy between these two approaches when the same machine learning methods are employed. Among many techniques for CD such as image differencing, image rationing, regression analysis, vegetation index analysis, multi-date direct analysis, and post-classification comparison, the latter is widely used due to reducing the need of image pre-processing. The accuracy of post classification image is dependent on the classification accuracy of the individual result (Hussain et al., 2013).

The result of OBIA is dependent to the accuracy of segmentation, and also it has problems with searching objects, which spatially correlated in time-series images as well as expert knowledge requirement for defining rule sets (Tewkesbury et al., 2015). On the other hand, image-pixels have been considered the basic unit of image processing and its spectral characteristics are used to provide thematic maps, mostly neglecting the spatial context of the image (Hussain et al., 2013). However, there have been changes in pixel-based approach to using texture features as an effective method in different image analysis disciplines to overcome context-related problems, ranging from urban disaster analysis (Tomowski et al., 2011) to land cover and land use change detection (Gevaert et al., 2016). These examples highlight the benefit of adding contextual information to pixel-based approaches. According to Clarke et al. (2014), pixel-based analysis works better for urban LCC, whereas in urban LUC it is recommended to use image context, pattern, and texture.

ML algorithms are a hot topic in the urban and other fields of RS. These algorithms have shown their robustness in different contexts and data types like, optical, radar, and UAV data (Ali et al., 2015). They are potentially capable of handling complex spectral measurement space, large volume data and high-dimensional data, while also they reduce computational time in comparison with conventional classifiers, such as maximum likelihood (Persello, 2017). Although these algorithms need many ground truth datasets, they are flexible and can be applied to any learning tasks, like image classification (Ali et al., 2015). Kuffer et al. (2016), in a review study ascertained among different approaches, machine learning methods obtained the "highest mean accuracy" and can handle learning tasks with very high-resolution imagery in complex urban, whereas "the variance of the performance of OBIA is rather large" and performs well for differentiating objects (e.g., roads) on neighbourhood scale.

In urban remote sensing discipline, non-parametric classifiers such as neural networks (Mboga et al., 2017), random forest (RF) (Stumpf & Kerle, 2011) and support vector machines (SVM) (Mathur & Foody, 2008) are of interest among machine learning methods. However, the methods are based on image-pixel and cannot exploit the potential of very high-resolution images (Kuffer et al., 2016), that might also be influenced by the impact of mixed pixel problem (Lu & Weng, 2007). Thus, contextual information of neighboring pixels is needed as well as image-based proxies; such as image-based features (Pelizari et al., 2017). However, the choice of image features is highly important, and sometimes a careless use of textural features reduce the overall accuracy (Vetrivel et al., 2016).

Artificial Neural Network (ANN) and more recent Convolutional Neural Network (CNN) has the ability to retrieve complex patterns from the data (Ali et al., 2015) and even "learning features" from the data. CNN has shown advantages over other ML methods (Vetrivel et al., 2016); however, its hidden layer is a "black box," and the overall accuracy is highly dependent on the amount of training data while also the user has no control on the process "except providing large input data" (Hussain et al., 2013). Moreover, CNN is not easy to use and computationally is extensive, that normally needs special hardware to handle the process. On the other hand, recent studies prove the classification result of the ML methods is highly dependent on the data characteristics (Foody & Mathur, 2004; Vetrivel et al., 2016). For instance, the performance of SVM is very well for complex datasets; such as urban-rural setting in developing countries, where the performance of random forest (RF) is highly data dependent and only performs well for "non-complex" datasets. Vertivel et al. (2016) concluded that "the SVM-based, supervised models were more reliable and mostly showed better generalization performance than RF, particularly for the complex datasets". Although SVM models have difficulty in kernel selection and computational time for optimization, they can handle learning tasks with a small amount of training dataset (unlike CNN), which show competitive results. Moreover, SVM has demonstrated to be very effective in solving nonlinear classification problems while also is capable of handling high dimensional data (Bruzzone & Persello, 2009). Comparative studies have shown more accurate results by an SVM in combination with texture features than conventional ML methods or comparable result with CNN (Gevaert et al., 2016b; Mathur & Foody, 2008; Mboga et al., 2017; Tewkesbury et al., 2015) Other advantages of SVM are; higher generalization capability and robustness to high dimensionality phenomenon and lower struggle needed for model selection in the learning stage as well as "optimality of the solution obtained by the learning algorithm" compare to conventional ML methods (Bruzzone & Persello, 2009).

To summarize, a deep literature review was conducted to develop an understanding of recovery process and the ways to assess it. The relation between LC and LU and land functions was discussed, and in the end, RS methods to measure LCLU were reviewed. There is a substantial amount of literature regarding image classification and CD in the remote sensing community under pixel and object-based categories. Numerous classification methods have been established, where post classification CD is a popular method. Moreover, ML methods provide more consistent results compared to other image analysis methods. ML methods are capable of dealing with very high-resolution imagery where more accurate and consistent results are achieved by CNN and SVM. SVM coupled with texture features approaches have the potential to solve the learning tasks especially when it comes to complex urban-rural setting. In next chapter concise information regarding study area, data used, and typhoon Haiyan will be given.

# 3. TEST AREA AND DATA

In this chapter, a description of typhoon Haiyan, the study area, and raw data used is provided.

## 3.1. Test Area and Datasets

Tacloban city in the Philippines has been chosen to test LCLUCs methods for post-disaster recovery assessment which in this case is post-Haiyan recovery. The city stretches from 11º15´- 11º12´N to 124º59´- 125º17´E. The total land area of Tacloban is about 200 km². The city was hit by super typhoon Haiyan on November 8, 2013. The eye of the typhoon passed through Tacloban city directly causing massive destruction. Based on official news, just in the city itself, 2678 people died (45% of the total number of fatalities in the country), and approximately 40,000 homes, representing 88% of all households, were demolished or damaged (Mejri et al., 2017) with the majority of informal coastal communities (Maly, 2017). While based on the unofficial news, number of fatalities is more than 15,000. Besides, in 2014, typhoon Rubi struck. It was less significant than typhoon Haiyan and “the worst affected areas from Rubi were outside of Typhoon Haiyan affected areas” (the Philippines, 2014). As a result of the typhoon and – short-term and long-term - recovery process a wide range of changes occurred in terms of LC and LU. For example, there were changes due to short-term recovery in reconstruction, trading, and agricultural sectors as well as changes in medium to long-term recovery in industrial development, tourism, economic, and infrastructure development (Tacloban Recovery and Sustainable Development Group, 2014). Besides, the rate of recovery has been diverse in different parts of the city (Evangelista, 2015). All above mentioned making this area suitable to study recovery assessment in terms of LCLUC. Below there is a list of available dataset and its description related to the study area:

| ID | Acquired Date | Timeline | Satellite | MS Resolution | Description |
|---|---|---|---|---|---|
| 1 | 3/17/2013 | 8 months before disaster (T0) | Worldview-2, 8bands {C, B, G, Y, R, RE, NIR1, NIR2} | 2 m | Tacloban city, in the Philippines, Area~26 sq.km |
| 2 | 11/11/2013 | 3 days after disaster (T1) | | | |
| 3 | 3/18/2017 | 4 years after disaster (T2) | | | |

The dataset for this study was consist of five multispectral WV2&3 imagery. Selection is made based on the time of imagery, cloud-free scenes, and coverage. Among selected images (Figure 3-2), some area in the event time is hazy. However, since haze reduction is not necessary for LCLU classification at the level of 2-meter image resolution, when also spectral information of all bands are normalized (which is the case in this study), haze reduction did not apply (Lin et al., 2015). Figure 3-1(A) shows the track of typhoon Haiyan across the Philippines and (B) shows the selected of the study area for this study. Moreover, Figure 3-2 shows the imagery used in this study (~25 km²), as T0 shows pre-Haiyan, T1 shows event time, and T2 shows post-Haiyan situations.

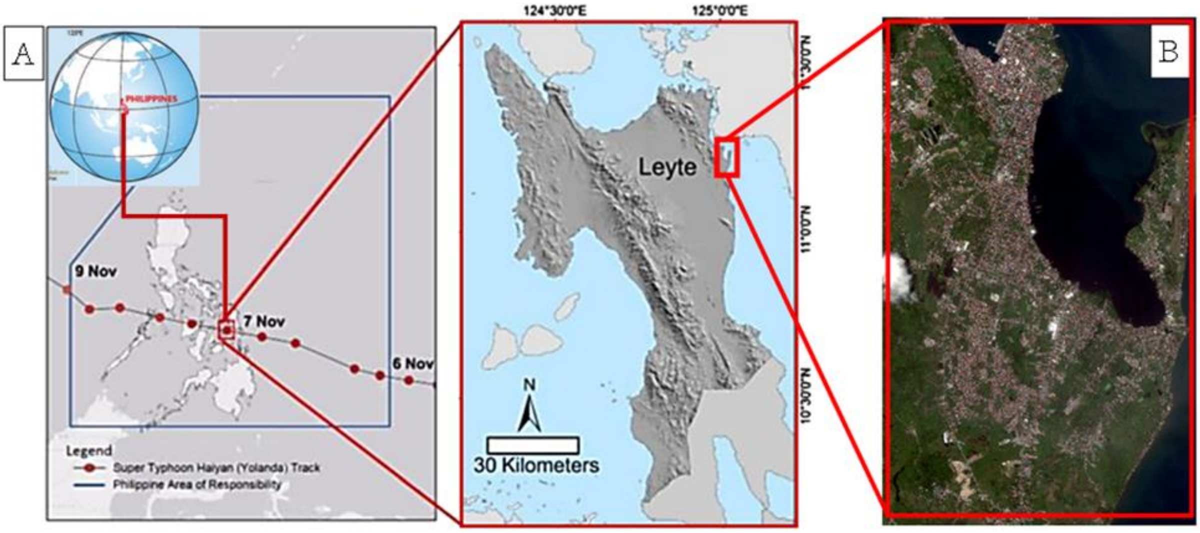


Figure 3-1 (A) Track of typhoon Haiyan (Maly, 2017). (B) The location of study area

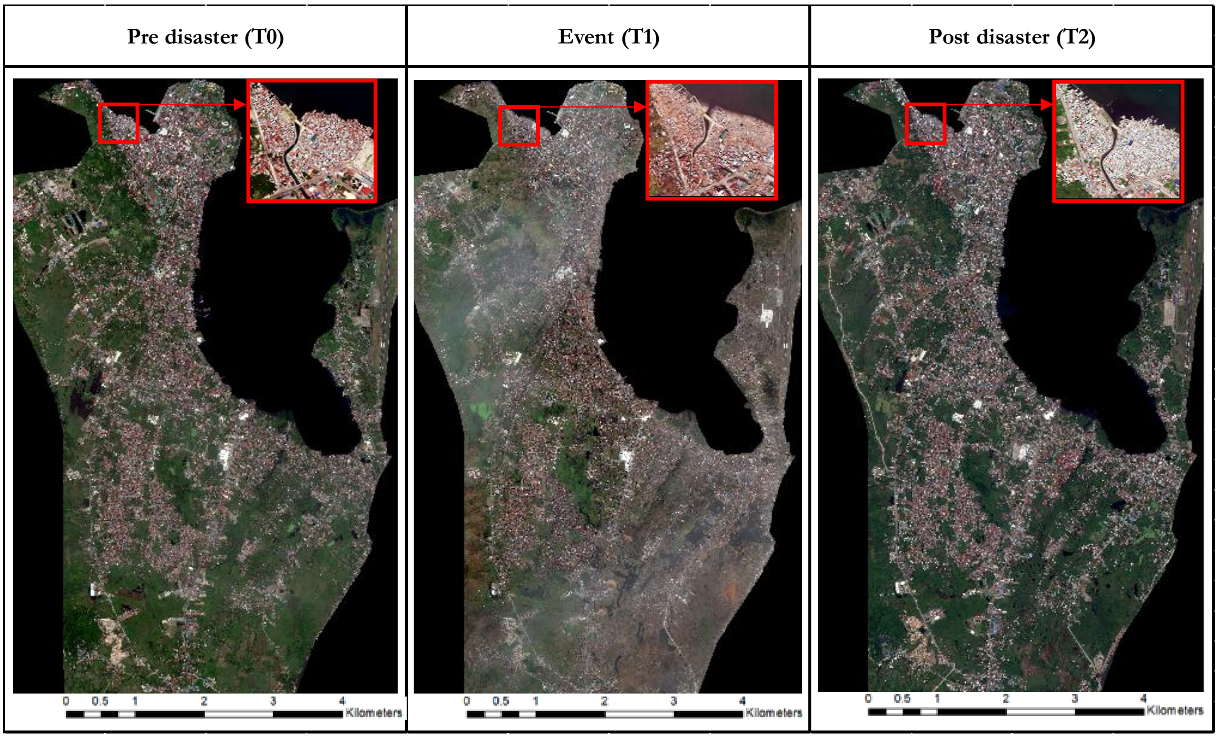


Figure 3-2 three satellite images of the study area; red rectangles show the statuses of the slum areas which were heavily devastated by the typhoon Haiyan

# 4. METHODOLOGY

The first section of this chapter describes the developed conceptual framework. It is constructed based on a comprehensive literature review and understanding gained from this study, which is an original contribution to recovery studies. It serves both as a result and methodology, as the remaining methodology is developed based on it. Therefore, the conceptual framework becomes the first output and necessary part of the methodology. In the second section, the classification method is selected based on both a deep literature review from remote sensing studies as well as preliminary experiments carried out within the study. Then, employed image features and spectral indices are described followed by the approach of creating recovery maps. The third section describes the development trajectory of a practical guide. Throughout this study, typhoon Haiyan in Tacloban city is referred to as "(the) typhoon".

## 4.1. Conceptual Framework

This section addresses the first research objective and the related research questions, as described in chapter one. It aims to demonstrate a comprehensive conceptual framework as a guide for the second objective. In the first part, a generic conceptual framework is developed, and the related transition patterns are defined. Then, to implement the conceptual framework in relation to the study area, different LCLU classes are identified. In the last part, the conceptual framework is implemented in the post-Haiyan recovery context considering the Comprehensive Land use Plan (CLP) of Tacloban city.

### 4.1.1. LCLU-based Conceptual Framework

The conceptual framework is based on the LCs and LUs and their inherent relation to physical and functional aspects of recovery, which potentially can cover an integrated recovery model. The CF is generic, meaning that it is neither disaster- nor country-specific. It is based on Transition Patterns (TP), which is grounded in multitemporal image analysis. TPs are the trajectories of change related to an identical pixel in an "n" time-span imagery (n is at least 3 and relates to the number of imagery, here is 3). These trajectories of change describe the state of identical pixels in each time; e.g., in T0, T1, and T2. It is evident that the state of pixels is defined by LCLU classes. Thus, TPs traces the state of pixels which implies a change; i.e., at least there are two different classes in a transition pattern.

TPs are restricted to the disaster-stricken area and normally happen within a certain time frame, with respect to recovery goals. These TPs are normally different from normal changes such as phenology. For example, one of the well-known TPs with respect to LC and conventional recovery definition, build back, is building (T0) - rubble (T1) - building (T2). Where, T0 corresponds to pre-disaster situation and imagery (here 8 months before disaster) which also serves as a basis for the concept of "Build Back (BB)" and "Build Back Better (BBB)" in the Sendai framework (UNISDR, 2015b), T1 corresponds to after the disaster situation (here an imagery 3 day after disaster), and T2 is related to the post-disaster recovery situation (here 4 years after disaster).

Figure 4-1 illustrates a simplified interaction between post-disaster recovery and LCLUC based on BB. The time-difference between satellite imageries T0 and T1 should be as low as possible, and it is better to be defined based on the resilience of the area and data availability. Post-disaster recovery happens between T1 and T2, here the red color represents short-term recovery, and the other colors represent a medium- to long-term recovery. The suitable timing between T1 and T2 imageries should be defined based on the purpose of the study, fund, policies, former experience of natural disasters in the affected area, and data availability among others. The higher the number of imagery is, the more detail information can be extracted from the recovery process. However, the number of imagery is a function of the purpose of the study, where each of post-disaster images can characterize different recovery outputs.

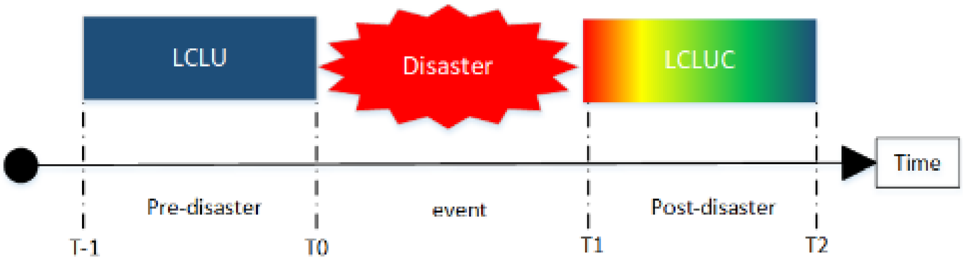


Figure 4-1 Interaction between post disaster recovery and LCLUC

Figure 4-2 provides detailed insights on the role of LC and LU separately in the post-disaster recovery process with respect to multi-temporal image analysis. The hypothesis here is that an LC-based recovery map; reveals physical aspects of recovery, while an LU-based recovery map reveals functional aspects of the recovery. In essence, the developed recovery maps are a special type of change maps providing meaningful recovery information.

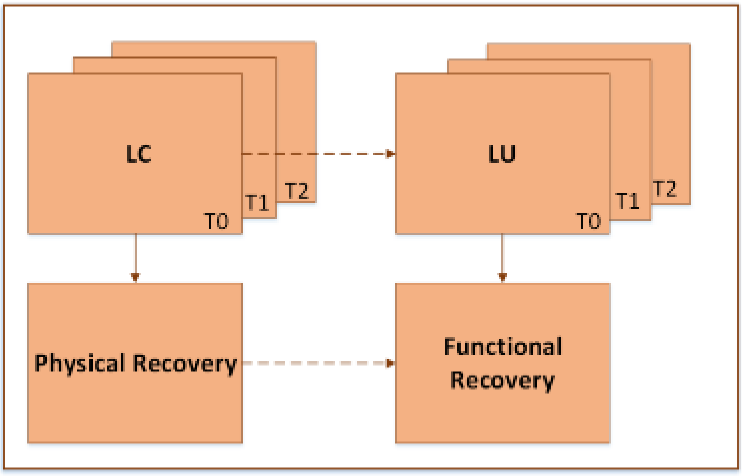


Figure 4-2 Relation between LC and LU recovery, and physical and functional recovery

There are two simplistic recovery statuses in the conventional perspective of recovery in literature; positive and negative recovery. Positive recovery is when the damaged class is rebuilt to the pre-disaster level, whereas negative recovery is when it does not. Nevertheless, as mentioned in chapter 2, the recovery process is more complicated than a simple positive or negative recovery. It needs a more comprehensive framework to cover the process. Therefore, this study provides a basis for a more nuanced interpretation of recovery by introducing six recovery classes:

1. Negative recovery (N)
2. Slightly negative recovery (SN)
3. Neutral recovery (NT)
4. Slightly positive recovery (SP)
5. Positive recovery (P)
6. Other transitions (OT)

The definition of these classes is based on the most relevant LC-based and LU-based TPs within three time-span; e.g., building-rubble-building and are based on the land use plan of the study area (Annex 3) and the BBB perspective. Class NT (Figure 4-3) refers to those TPs that are not informative enough, as the classes have the same parent class (Figure 4-4). For example, the TP "building-building-impervious surface" represents a change from building to impervious surface from T1 to T2 which both classes have the same parent class (built-up). Negative recovery (N) and positive recovery (P) refer to those TPs, where the state of the class at the time of the event (T1) remains the same as before the disaster (T0), while it faces changes in the post-disaster time (T2). These changes, therefore, determine if the pattern is negative or positive based on the land use plan of the study area (CLP, 2016). Moreover, this definition is based on an assumption that if a class can retain its state at the time of event; i.e., T1 is the same as T0, and survive the disaster, it will not be vulnerable to that specific disaster; meaning that the class is either located in the safe zone or is well-adapted to that specific disaster. For example, in this study, patterns "building-building-bare land" and "grassland-grassland-impervious surface" represent N and P respectively. Classes SN and SP are the middle-level classes between negative and positive recovery with inherent uncertainty. More information such as additional satellite images, (multi)hazard map of the area, and in-situ data is required for SN and SP to be further precisely defined as N and or S. However, in the absence of such information, class SN tends to be negative, and SP tends to be positive. For instance, patterns "building-rubble-bare land" and "building-rubble-building" exemplify the SN and SP respectively. The last class, "other transition" (OT) comprises of either minor and/or rare TPs (e.g., "building-building-open water") or no change TPs (e.g., "building-building-building"). However, one exception exists in this class such as slum-slum-slum. This TP is always considered as negative recovery. The reason is that from BBB perspective, the rebuilding of IBA always weakens urban resilience (Ahmed, 2014).

One of the potential uncertainties with this framework that might arise is that how to characterize those patterns which are difficult to interpret. For instance, pattern "tree-flattened tree-non-tree vegetation" could be NT (same root), SP (rebuild), and P (alternative crop instead of palm tree). The uncertainty will be mitigated by introducing more relevant and detailed information; i.e., LU information of the area. For LC level, such TP is characterized as NT, and further, in LU level, they will be assigned to the correct class. This is one of the limitations of LC-based recovery assessment, which will be solved by LU information. Figure 4-3 illustrates the TPs in a color scheme which has been chosen to depict TP variation.

#### 4.1.2. Class Definition

Defining relevant classes is the basis for implementing the conceptual framework and further classification and producing recovery maps. Based on the main objective of this study and image data characteristics, the most relevant classes are selected and categorized into three parent groups; built-up, vegetation, and water. Land cover and land use classes are defined based on the parent groups hierarchically (Figure 4-4).

Although class definition should signify the whole thematic structures in the scene of interest, there should be a balance between the generalized and detailed definition of classes in a specific study. While the former may result in a "too homogeneous" representation of landscape (may fail to detect important features), the latter may lead to a loss of relevant features in heterogeneous data (Herold et al., 2014). In terms of the number of classes, it is reported (Herold et al., 2014) that the overall accuracy usually decreases as the number of classes increase. Besides, a successful class definition should take into account the thematic definition of classes according to the objective of the study, and spectral and spatial resolution of the mapping sensor (Herold et al., 2003) as well as number of images for multi-temporal analysis. Furthermore, in a taxonomic class definition, a large similarity among classes would predict vague classes that will be more prone to confusion and hence, image misclassification (Giri, 2012). Mixed classes do not follow standard principles and very often increase the ambiguity of classification tasks (Giri, 2012).

However, some urban-related classes such as slum areas, need an abstract semantic class definition, making it hard to be automatically discriminated from the image (Mboga, 2017).

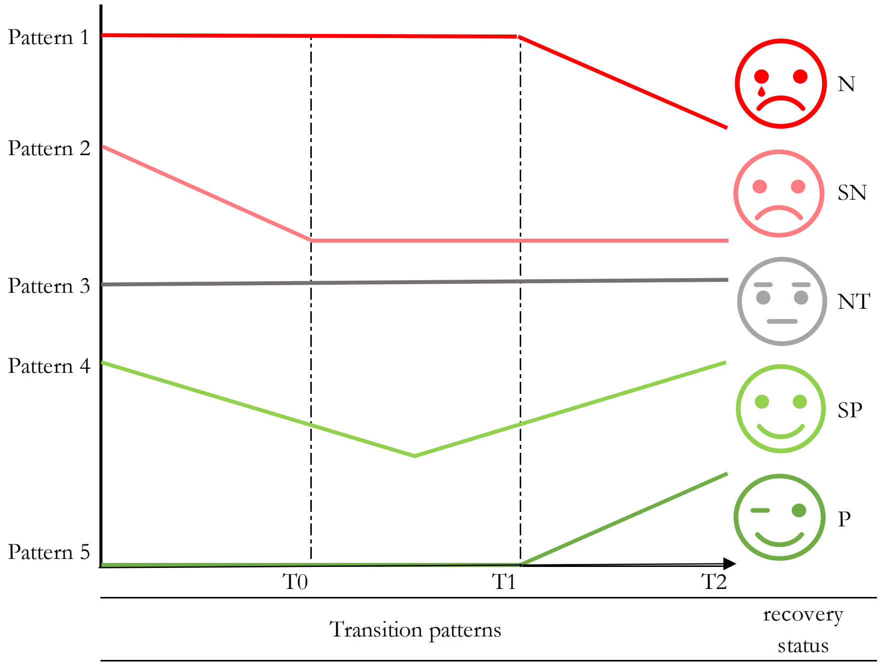


Figure 4-3 LCLU-based recovery conceptual framework

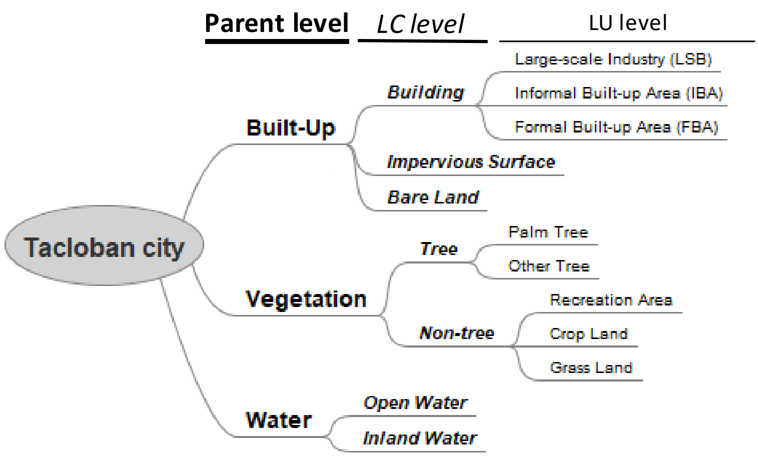


Figure 4-4 Hierarchy definition of LCLU classes

Based on the literature and comprehensive visual observation (multi-source data; e.g., Google Earth, OSM, etc.) of Tacloban city as well as field data gathered by the supervision team, among many potential classes the following seven LC classes are selected: building, impervious surface, bare land (built-up category), tree and non-tree (vegetation category), inland water and open water (water category). However, not all classes are equally important. A detailed description of the LC classes and their importance in this study is given in Table 4-1. Generally, the importance of LCLU and damage classes are ranked in a qualitative manner and range from high (H) to medium (M) and low (L). In the next paragraph, the importance of the classes for LC and LU and damage is explained which addresses research question 2.

Class building and its states across the time frame is one of the important indicators of long-term recovery. A big portion of the money is normally invested in rebuilding by aid agencies, which as a result runs many businesses. The permeability of surfaces is an important indication of the degree of urbanization and environmental quality. Impervious surfaces can both positively and/or negatively contribute to the long-term recovery process and its goals (for more detail see: Weng, 2012). Bare land can represent a temporary transition stage of development (i.e., plantation, re-vegetation, and building development) or a permanent stage (i.e., abandoned area and no-build zone). Furthermore, the class tree represents natural and economic sectors in the holistic recovery view and includes palm, banana, fruit and natural trees (Mas et al., 2015). The class non-tree vegetation represents all vegetation types of the study area except the class tree. However, vegetation related classes in LC level are not highly informative regarding the recovery process. The class inland water comprises of lakes, aquacultures, and rivers while the class open water represents the ocean.

Table 4-1 LC class definition (H: high, M: medium, and L: low)

| **Class name** | **Importance** | **ID** | **Class description** |
|---|---|---|---|
| Building | H | 1 | Land covered by building |
| Impervious surface | H | 2 | Pavements that are covered by impenetrable materials such as asphalt, concrete, and compacted soil (not building) |
| Bare Land | M | 3 | Urban fabric, discontinuous urban areas, bare rocks, bare soil |
| Inland Water | M | 4 | Any of the inland waters such as lakes, aquacultures, rivers, and swamps |
| Tree | M | 5 | Mixed trees (i.e. palm, banana, fruit tree) |
| Non-Tree Vegetation | M | 6 | Mixed group of (non-tree) vegetation such as crop, pasture, grass |
| Open Water | L | 7 | Sea/ocean water |

Although LC classes can represent some aspects of recovery, there are other aspects to be explored. For example, the class building is a general class that can directly reveal physical recovery but is unable to reveal the functional recovery directly, thus, LU classes are defined towards the main objective of this study (Table 4-2). Based on Figure 4-4, the "building" category is divided into 3 finer classes namely; large-scale industry (LSI), informal built-up area (IBA), and formal built-up area (FBA) in the land use level. The class LSI represents the economic activity of the area comprising of institutional, light-industries and commercial buildings (Journal of Philippine Statistics, 2012). Although IBA is not included in the CLP, the majority of 30,000 destroyed houses were from IBA. Based on Maly (2017), most vulnerable residents live in IBA, which are located mostly along the coastline. Accordingly, the status of IBA and FBA are informative to understand the post-Haiyan recovery. The region is the top national producer of coconut where the palm tree is the main source of income and economic activity for the majority of people. Around 60% of the population is directly engaged in palm production or indirectly in palm processing, which makes the palm production and processing the main industry in the area (Mayans, 2014; Yi et al., 2015b). Therefore, it is vital to differentiate palm trees from other trees. In addition, typhoon Haiyan destroyed almost all recreational facilities (CLP, 2016). Creating new green spaces such as recreational areas in high-risk zones can reduce the risk of the disaster (Coppola, 2011; Mader et al., 1980) and improve social recovery by the involvement of people in sports or recreation activities (Townshend et al., 2015). Besides, grassland is an important class for this study as it can potentially be targeted for reconstruction purposes within the recovery process. Agricultural crop and related cropland are also important to this study as they are other sources of income in addition to palm plantation. Moreover, it is relevant to mention that typhoon Haiyan destroyed almost all palm trees in Tacloban city, either uproot or make it fruitless. This resulted in a very low yield in the succeeding year (CLP, 2016) of the disaster. Therefore, coconut owners need to access innovative livelihood alternatives such as rice (Mayans, 2014).

Table 4-2 LU class definition (H: high, M: medium, and L: low)

| **Class name** | **Importance** | **ID** | **Class description** |
|---|---|---|---|
| Large-scale Industry (LSI) | H | 1 | Land covered by large building (size>1000$m^2$ ) |
| Informal built-up area (IBA) | H | 2 | Area covered by small, clustered buildings with no or little vegetation mostly located in hazardous zones |
| Formal built-up area (FBA) | H | 3 | Land covered by larger building, arranged in a regular spatial pattern and vegetation |
| Palm tree | H | 4 | Palm tree |
| Other tree | M | 5 | Mixed trees (i.e. banana, mangroves) |
| Recreation area | M | 6 | Green public spacess in the city such as parks, soccer fields |
| Crop land | H | 7 | Agricultural crop such as rice, irrigated lands |
| Grass land | M | 8 | Areas covered mainly by low vegetation, mainly different types of grass |
| Inland water | M | 9 | Any of the waters such as lakes, canals, rivers, and swamps |
| Bare land | M | 10 | Urban fabric, discontinuous urban areas, bare rocks, bare soil |
| Impervious surface | H | 11 | Pavements that are covered by impenetrable materials such as asphalt, concrete, and compacted soil |
| Open water | L | 12 | Sea/ocean water |

In addition to LCLU classes, it is necessary to study damage classes for the situation right after the typhoon. If the LCLU classes from pre- and post-typhoon (T0 and T2) are considered as "normal" situations, the classes for typhoon situation (T1) are not considered as "normal". That is because natural forces; i.e., heavy wind and storm surge, heavily destroyed existing urban elements (almost all structures were washed away along the coastline). Therefore, there is a need to characterize the damage classes related to the typhoon (Table 4-3). Regarding buildings, mainly two damage classes can be assigned; rubble and debris as shown in Figure 4-5. However, at the city scale and with the spatial resolution of 2m, it is not possible to distinguish debris from the rubble, both spatially and spectrally, specifically in the typhoon Haiyan setting. Therefore, these two classes were merged into one class as rubble. There are two other damage classes: inundated land and flattened trees (Figure 4-7).

Figure 4-5 Damage classes for a single building, (Vertivel et al., 2016)

Table 4-3 Damage class definition (H: high, M: medium, and L: low)

| Class name | Importance | Class description |
|---|---|---|
| Rubble | H | Damage patterns corresponding to a mix wind- water-borne objects (rubble, debris, cars, building fragments) |
| Inundated land | H | Rising of a body of water and its overflowing onto normally dry land |
| Flattened tree | H | Lnad covered by fallen or toppled tree branches, uprooting of smaller trees |

Figures 4-6, 4-7 and 4-8 show land cover, damage, and land use classes, respectively. These photos have been taken from the study area and provide an insight of the classes showing ground- and satellite-based views.

To better understand recovery, there is a need to go from a coarse to a finer level (e.g., LC to LU) in a hierarchical manner as shown in Figure 4-4. However, the hierarchical division should be fit with respect to the recovery goals and the characteristics of the study area. In addition, except built-up related classes, LC information is not informative enough to understand the recovery process. However, LC information, as it is easier to extract from RS imagery, gives a general and quick overview of the area in the immediate aftermath of a disaster and further in other phases of recovery. The reason is that in large natural disasters and a short-term recovery a general overview of the process is required and can be used as an auxiliary tool in order to effectively enhance other recovery-related activities in the ground (which can be represented by LC information). On the other hand, LU can be used to understand medium- to long-term recovery, especially for large natural disasters, where mostly land use plan is defined in relation to the recovery process. In long-term recovery, more detailed information is needed to characterize the process and to further check with LU plan to see if it is on track or not. Although LCLU collectively can help to characterize different parts of recovery, it cannot characterize all aspects of the recovery process such as accessibility analysis. However, in the recovery literature there are many local indicators which together with LCLU information can help to cover this gap.

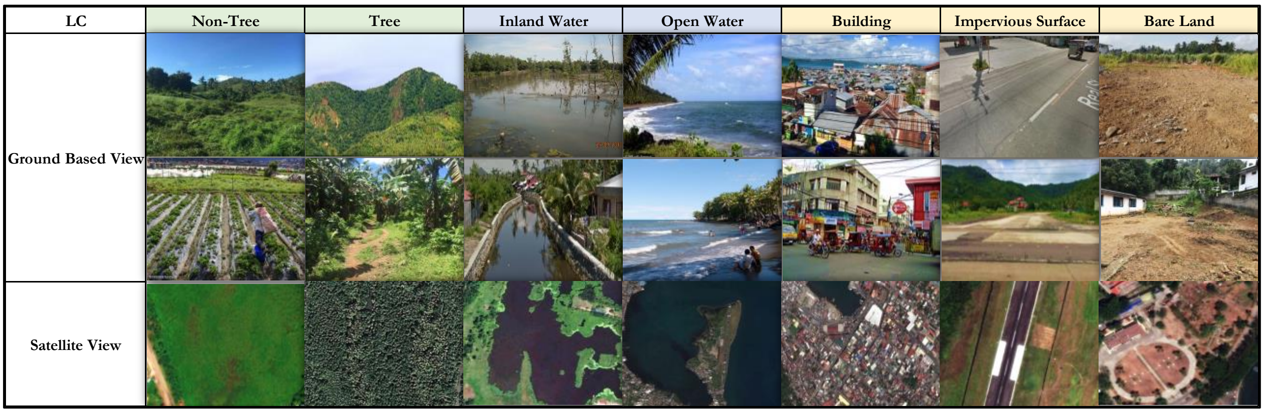


Figure 4-6 Illustration of land cover classes

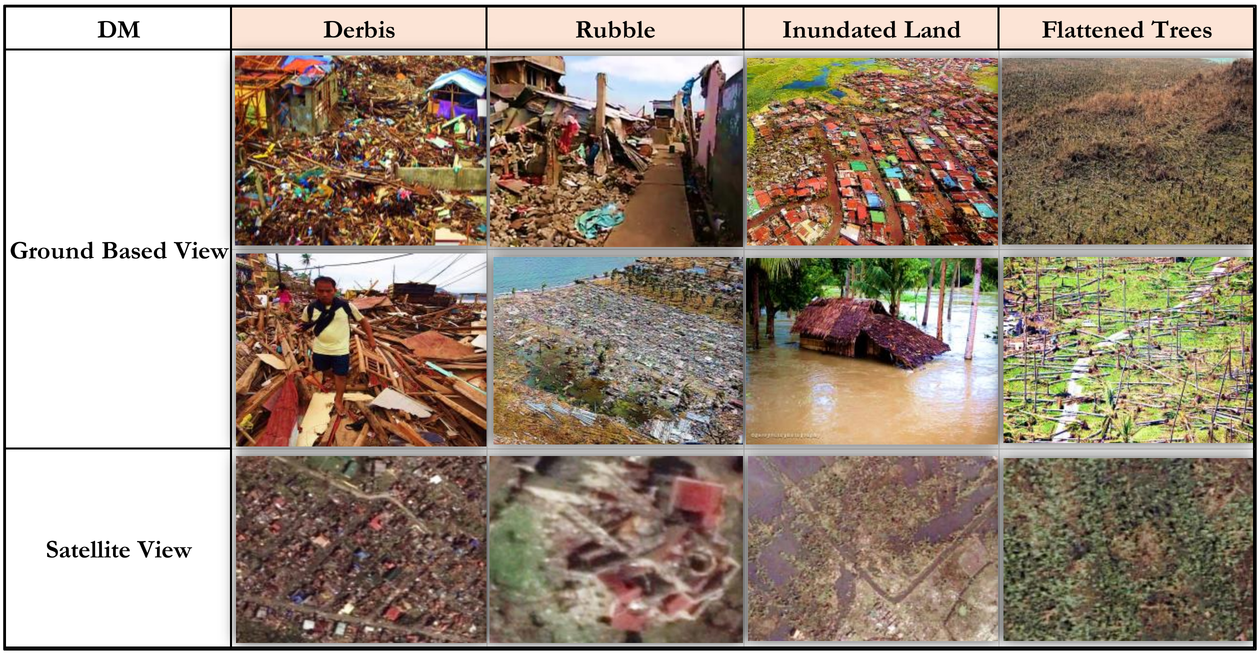


Figure 4-7 Illustration of damage classes


Figure 4-8 Illustration of land use classes; IBA: Informal Built-up Area, FBA: Formal Built-up Area, LSI: Large-Scale Industry

### 4.1.3. Framework Implementation

To implement the CF in the Tacloban city, first, complete TPs for LC and LU, which might occur in the post-Haiyan recovery in the Tacloban city are listed (Annexes 1 and 2). The most relevant TPs are selected and illustrated in Table 4-4 (LC) and Table 4-5 (LU). The characterization of the TPs is based on the conceptual framework (section 4.1.1).

Table 4-4 LC- based conceptual framework for post- Haiyan recovery process in Tacloban city

| Transition ID | T0 | T1 | T2 | Recovery Status |
|---|---|---|---|---|
| 644 | Non-tree vegetation | Non-tree vegetation | Inland water | N |
| 554 | Tree | Flattened tree | Inland water | |
| 285 | Impervious surface | Rubble | Tree | SN |
| 185 | Building | Rubble | Tree | |
| 556 | Tree | Flattened tree | Non-tree vegetation | NT |
| 221 | Impervious surface | Impervious surface | Building | |
| 181 | Building | Rubble | Building | SP |
| 281 | Impervious surface | Rubble | Building | |
| 282 | Impervious surface | Rubble | Impervious surface | P |
| 552 | Non-tree vegetation | Non-tree vegetation | Impervious surface | |

Table 4-5 LU- based conceptual framework for post- Haiyan recovery process in Tacloban city

| Transition ID | T0 | T1 | T2 | Recovery Status |
|---|---|---|---|---|
| 252 | Informal built-up area | Rubble | Informal built-up area | |
| 222 | Informal built-up area | Informal built-up area | Informal built-up area | N |
| 844 | Grass land | Flattened tree | Palm tree | |
| 444 | Palm tree | Flattened tree | Palm tree | |
| 747 | Crop land | Flattened tree | Crop land | SN |
| 3510 | Formal built-up area | Rubble | Bare land | |
| 3511 | Formal built-up area | Rubble | Impervious surface | |
| 3311 | Formal built-up area | Formal built-up area | Impervious surface | NT |
| 544 | Other tree | Flattened tree | Palm tree | |
| 353 | Formal built-up area | Rubble | Formal built-up area | |
| 1153 | Impervious surface | Rubble | Formal built-up area | SP |
| 393 | Formal built-up area | Inundated land | Formal built-up area | |
| 756 | Crop land | Rubble | Recreation area | |
| 253 | Informal built-up area | Rubble | Formal built-up area | P |
| 2511 | Large-Scale industry | Rubble | Large-Scale industry | |

## 4.2. Land Cover and Land Use Analysis

In this section to investigate the utility of LCLU in recovery assessment, image analysis is performed based on objective 2. This section addresses the research questions 4, 5, and 6.

### 4.2.1. A Brief Review of SVM

Based on the preliminary experiment carried out for a small subset of the area (Figure 4-9) and the literature review (2.8.2), SVM classifier is used for the classification task. SVM is a very effective technique, and it relies on both classification procedure and the elegance of the theoretical advances (Bruzzone & Persello, 2009). The classification strategy of SVMs exploits a margin-based "geometrical" principle rather than a purely "statistical" principle, meaning that it does not require an estimation of the statistical distribution of the classes for the classification task (non-parametric classifier). Rather, the classification is based on the concept of margin maximization and structural risk minimization, minimizing the misclassification error on the training set. SVM seeks an optimal hyperplane as a decision function in high-dimensional space which maximizes the margin between classes via a small number of training samples (support vectors) in feature space, which makes the SVM a suitable method to exploit the VHR imagery potential (Volpi et al., 2013).

Figure 4-9 Test area (500*500 pixel)

When classes are linearly separable (the simplest scenario), SVM finds the separating hyperplane in away the distance between the classes to the hyperplane (margin) is maximized. For linearly non-separable classes a "slack variable" is introduced. In this case, SVM seeks for the hyperplane that maximizes the margin, while minimizing a quantity proportional to the number of misclassification errors. The trade-off mentioned above is controlled by a positive regularization parameter C.

Moreover, for nonlinear decision surfaces a kernel function is introduced by Vapnik (1995) where among different kernels, RBF is widely used in the RS literature. The RBF kernel maps sample into a higher dimensional space in a nonlinear way. The accuracy of SVM-based RBF kernel is dependent on parameters C and $\gamma$. The constant parameter C controls the magnitude related to training data where lies in the wrong side of hyperplane and $\gamma$ controls the width of the kernel. A large value of $\gamma$ and/or C tends to over-fit the training data which may yield a low level of generalization ability which is unfavourable (Pal & Foody, 2010). There are some situations where the linear kernel performs better than RBF kernel; i.e., when the number of features is very large (Hsu et al., 2016). A detailed discussion on SVM and its mathematical background can be found in Bruzzone & Persello (2009).

To make the best use of the performance of SVM, the RBF parameters (C and γ) should be optimized and tuned (Foody & Mathur, 2004). It is suggested a grid-search using a cross-validation approach as the most effective method to optimize RBF parameters (Hamedianfar & Shafri, 2015). The goal is to identify the best parameter(s) so that the classifier can effectively predict previously unseen data (i.e., test data). The best value of parameters (C and γ) will differ in a different dataset. Hence the parameters need to be determined for each dataset (Richards & Jia, 2006) (Table 4-6).

Table 4-6 Definition of parameters and related methods used in the experiment

| Parameters Values | Method Description |
|---|---|
| 10-fold cross validation | Cross validation to tune the hyper-parameters for a learning model and based on the grid-search technique |
| The data set is seperated into 75% and 25% for tarining and testing, respectively | Training set is used for cross-validation for tuning the hyper-parameters and to train the model. Testing set is employed for assessing the trained model. |

For the SVM, both linear and RBF kernel is adopted, and the one with higher accuracy is picked and presented. The best values for penalty (C) and kernel (γ) parameters of SVM are determined via grid search algorithm and 10-fold cross-validation (Hsu et al., 2016). With the help of a training set, the approach provides many learning models for a number of hyper-parameters. Each model is assessed using the cross-validation procedure. The best model then is selected as the final model with tuned parameters and further the performance is evaluated using a test set. To facilitate the procedure, R package 'e1071', which was implemented in LIBSVM library by Chang & Lin (2011) is employed. Exponentially growing sequences of C and γ are used to identify best parameters, which is a one- and two-dimensional parameter for linear and RBF kernel along $2^d$, where d= {-5, -4, …} for γ and d= {5, 6, …} for C (Table 4-7).

Table 4-7 Definition of grid search space for tuning the hyper-parameters SVM

| Classifier | Parameters | Grid-search space | Description |
|---|---|---|---|
| SVM | C | $2^5$ $to$ $2^{10}$ logarithmically spaced | Regularization parameter which has a significant impact on the generalization performance of the classifier. |
| | $\gamma$ | $2^{-5}$ $to$ $2^0$ logarithmically spaced | Regularization parameter in RBF kernel with a great impact on the performance of the kernel. |

#### 4.2.2. Utilization of Image Features and Spectral Indices

Since in this study, some of the LU classes need a high semantic definition (e.g., informal built-up area) and also to decrease the spectral complexities of some similar classes (e.g., different types of impervious surface and bare land), texture feature and spectral indices are used to help the classification task. An example of the complexity is different road types in the study area: 1) concrete, 2) asphalt and 3) compact bare soil, which together with other classes such as building, bare land, and rubble create a highly complex scene.

Pixels, in very high (spatial) resolution imagery, are commonly smaller than the object of interest and holds a small amount of contextual information to identify a class of interest accurately. The contextual information describes the information derived from a neighborhood (image features). Image features are hidden representation in data that help the learning and classification task by providing supplementary information about image properties (Mboga et al., 2017). They are used to characterize the tonal or grey-level variations in an image. Many image feature extractions are used in the urban remote sensing literature. Image features such as those based on the calculation of the grey-level co-occurrence matrix (GLCM) and local binary pattern (LBP). The GLCM and LBP, due to their discriminative power and computational plainness are reported as the most useful for analyzing the content of VHR imagery for urban studies (Gevaert et al., 2016; Kuffer et al., 2016; Mboga et al., 2017).

GLCM method computes the occurrence of pairs of grey-level value pixels in an image. The maximum grey value of a pixel determines the size of the GLCM. The association between the pixels in GLCM is determined by varying lag and direction (Rao et al., 2002). LBP features (Ojala et al., 2002) are rotationally-invariant (image-based) texture features, which identify uniform features, such as corners and edges, based on a well-defined number of neighboring pixels (P) at a distance (R) from the pixel located in the center. For more information about LBP, see Ojala et al. (2002).

In this study, a code (in python) is used for LBP extraction using a variety combination of R= {2~4} and P= {6~12}. Moreover, ENVI software is used to extract texture features with different lag distances and windows sizes (e.g., 3*3, 5*5, 7*7, 9*9 and 3*3, 5*5, 7*7,15*15 for LC and LU tasks, respectively) (Table 4-8). Although there are eight types of GLCM features (mean, contrast, angular second moment, variance, dissimilarity, correlation, homogeneity, and entropy) which can be extracted from the image, not all of them are helpful, and some are highly correlated, resulting in redundancy (Graesser et al., 2012). In addition, 18 different types of spectral indices (Table 4-9) from the most recent literature (mostly using Worldview 2 imagery) are used in order to help classification task.

Table 4-8 Extracted features from multispectral image

| Type of Feature | Features count | Description |
|---|---|---|
| Original bands | 8 | (b1:b8) reflectance values of multispectral image |
| Spectral indicies | 18 | spectral indices calculated based on the table … |
| Local Binary Pattern | 186 | $LBP_{R=\{2:4\},\, P=\{6:12\}}$ |
| GLCM | 256 | GLCM textural measures calculated for multispectral bands |

Literature suggest that accuracy increases when combining textural and spectral features (Dhumal et al., 2015). To prevent redundancy and to increase the effectiveness of classification task a feature selection is employed. The feature selection reduces computational costs and avoids over-fitting the classifier. Hilbert – Schmidt independence criterion (HSIC) is one of the popular methods in the RS community (Song et al., 2012). HSIC is a nonparametric dependence measure, which takes not only into account linear correlation, but also all modes of dependence between the features.

Table 4-9 Spectral index description

| ID | Spectral index | Equation | Reference |
|---|---|---|---|
| 1 | NDNB | Blue - NIR 1 / Blue + NIR 1 | (Hamedianfar & Shafri, 2015) |
| 2 | NDVI 2 | NIR 2 - Red / NIR + Red | |
| 3 | NDRR | Rededge - Red / Rededge + Red | |
| 4 | NDGR | Green - Rededge / Green + Rededge | |
| 5 | NDBC | Blue - Coastal / Blue + Coastal | |
| 6 | NDN2C | NIR 2 - Coastal / NIR 2 + Coastal | |
| 7 | BAI | Blue - NIR 2 / Blue + NIR 2 | (Shahi et al., 2015) |
| 8 | REI | NIR 2 - Blue / (NIR 2 + (Blue * NIR 2)) | |
| 9 | R1 | Red - NIR 1 / Red + NIR 1 | (Elsharkawy et al., 2012) |
| 10 | R2 | Coastal - Red / Coastal + Red | |
| 11 | R3 | NIR 1 - Yellow / NIR 1 + Yellow | |
| 12 | BSI | Yellow - (2*NIR 1) / Yellow + (2*NIR 1) | (Sameen & Pradhan, 2016) |
| 13 | NDWI | Green - NIR 2 / Green + NIR 2 | (Aguilar et al., 2016) |
| 14 | NDVI | NIR 1 - Red / NIR 1 + Red | |
| 15 | NDWI 1 | Coastal - NIR 2 / Coastal + NIR 2 | (Wolf, 2012) |
| 16 | NDVI 1 | Red - NIR 2 / Red + NIR 2 | |
| 17 | NDSI | Green - Yellow / Green + Yellow | |
| 18 | NHFD | Rededge - Coastal / Rededge + Coastal | |

#### 4.2.3. Experiment Setup

The main focus of the classification section is to employ the methodology that works well for both LC and LU classification in order to either achieve the acceptable accuracy or improve the classification accuracy for creating corresponding recovery maps. It is proposed that acceptable accuracy limits to LC classification are when OA is higher than 80% (Manandhar et al., 2009). Since the experiments are computationally intensive and due to hardware limitation, they are first applied in a small but representative area (Figure 4-9), and once the best setting of features is defined, they will be applied for the whole study area in order to produce the final results. The experiment setup is summarized as follow:

1) Using only the spectral bands of the WorldView-2 images for LC and LU classification (test area).

2) Extract relevant spectral indices, then select the most informative ones and add them into spectral bands for LC and LU classification (test area).
3) Calculate the GLCM measures (varying windows size with respect to LC and LU classes), then select the most informative ones and add them into spectral bands for LC and LU classification (test area).
4) Calculate the LBP features (varying P and R for LU classification), then select the most informative ones and add them into spectral bands for LU classification (test area).
5) Combine the relevant spectral and textural features, then select the most informative ones and add them into spectral bands for LC and LU classification (test area).
6) Perform final LC and LU classification based on the most useful setting of spectral and textural features and produce the final LCLU maps (whole study area).

#### 4.2.4. Accuracy Assessment

Accuracy assessment of classified map helps assign credibility to a map. The overall accuracy of the classification is calculated from the confusion matrix, which is widely accepted in the remote sensing works. As a derivative of confusion matrix, the global accuracy gives the proportion of correctly classified pixels, by comparing the classified pixel to the reference data. The user's and producer's accuracies (UA and PA rescpecitvely) of each class are calculated in order to show the error contribution of each class. User's accuracy refers to the error of assigning an incorrect label to a specific class, and it is measured by dividing the total number of correct pixels in a category by the total number of pixels classified into that class. On the other hand, producer's accuracy is the error of failing to assign a correct label to a specific class (Foody & Mathur, 2004). While the user's accuracy is the degree of reliability of a classification, producer's accuracy is the degree of the ability to classify a particular class (Congalton, 1991). Moreover, visual quality evaluation of the classified maps is carried out.

A common strategy for sampling method is used; the dataset is separated into two parts, one part for training the classifier, and one (previously unseen) part of the study area for testing the accuracy of the classifier, using stratified random sampling method. Reference data is obtained using visual interpretation (Sliuzas, 2004). The prediction accuracy obtained from the previously unseen set more accurately reflects the performance on classifying an independent data set (Hsu et al., 2016). Seven LC and twelve LU classes were considered for accuracy assessment with the minimum of 500 sample pixels of each considered classes, which provide a representative basis for accuracy assessment (Foody, 2002). In the absence of fieldwork data, visual interpretation is used based on multi-source data such as Google Earth Pro (GE), Open Street Maps (OSM), Google street view, and panchromatic bands of WV2 imagery.

#### 4.2.5. Recovery Map

In order to address the research question 6, there is a need to define a methodology to assess the recovery process after typhoon Haiyan. The recovery map is basically based on the implemented conceptual framework and LCLU classified maps. It is pertinent to mention that, like the classification approach, recovery maps are also pixel-based. To develop the recovery maps, first LC maps from three time-spans (T0, T1, and T2) are stacked and then, for each map, the state of identical pixels is investigated. For example, pixels "a", "b" and "c" in Figure 4-10, represent the state of the identical pixels in LC classification maps in three time-spans, which collectively represent a TP (e.g., a-b-c). The same is done for all pixels in the maps, and all possible TPs are identified. In this study, a code in "R" is developed to identify all possible TPs and to further select TPs based on the implemented conceptual framework in section 4.1.1. The TPs are then illustrated in the output map. This map is referred as LC-based recovery map. The same procedure is done for LU maps to create LU-based recovery map.

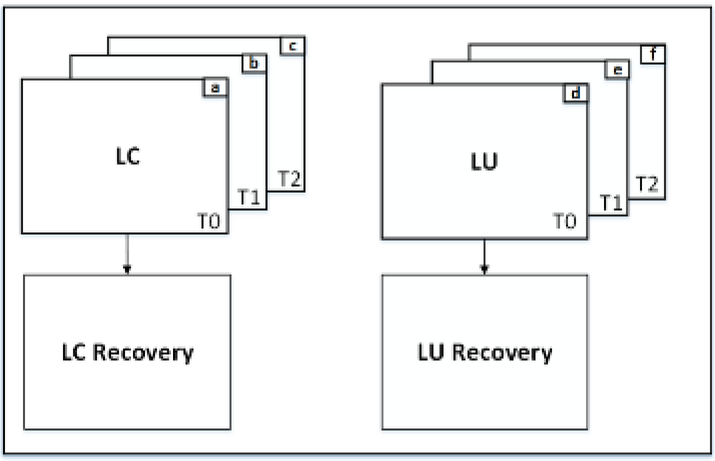


Figure 4-10 Description of the recovery map

## 4.3. Develop a Practical Guide

There are many RS-based indicators in the recovery literature. Although these indicators are helpful for ground-based recovery analysis, their exploratory power and practicality in the RS perspective are not investigated so far. Moreover, as mentioned earlier in chapter 2 there are some concerns about the indicators; i.e., they are: expensive to collect, mostly local-type indicators and prone to subjectivity which also are difficult to collect in a disastrous situation. Remote sensing data and methods are appropriate alternatives to address those concerns. This section aims to address research questions 7 and 8, by categorizing the indicators in relation to the recovery understanding gained from this study.

The practical guide is more a summary of an evaluation of existing recovery indicators. The guide checks which ancillary data might help to detect the indicators by advance RS methods better, as currently, they are not operationally usable. In order to address user needs, besides, the indicators categorized based on their utility in the recovery assessment; i.e., macro, meso, micro indicators. The categorization method is described in next paragraphs.

Among recovery indicators, there are some standards and well-established indicators in the recovery discipline, which have already been used with conventional RS methods, such as visual interpretation, and NDVI analysis (Brown et al., 2010). These indicators have high utilities in the recovery process. Meaning that they extract recovery information spatially over large areas such as city scale. These indicators are grouped under “macro indicators”. Moreover, there are indicators with medium to high utilities in the recovery community. Although these indicators have the potential to reveal the recovery process spatially within the city level, they are not frequently used in practice. Moreover, some indicators have been used in other RS domains and have not yet been applied in recovery studies. Collectively, these indicators are gathered as “meso indicators.” Thirdly, there are other types of indicators, which are local-types and represent elementary units such as individual buildings within the recovery process. These indicators are hardly visible and/or not visible by RS means. These indicators have low utility in the recovery assessment and are grouped in “micro indicators.” In this study, a practical guide is developed in order to link meso and micro indicators to remote sensing. In addition, these indicators are analyzed with respect to the recovery process.

Overall, this chapter introduced the methods used in this study in three main sections. It was started by introducing a generic LCLU-based CF which succeeded by LCLU analysis in the study area leading to create recovery maps. However, the CF was described in the methodology part (as one of the results of this study) which was needed for the remaining parts of this chapter, which is also mentioned in (Parsons et al., 2016). The last section introduced the logic behind the practical guide. The next chapter will show and analyze the result of methods employed.

# 5. RESULTS AND ANALYSIS

This chapter provides the result of this study. The first section represents the results of experiments (method selection and parameter tuning) and their interpretations, and two recovery maps (LC- and LU-based) are shown and interpreted. In the second section, a practical guide for existing indicators is developed.

## 5.1. Land Cover and Land Use Analysis

This study used SVM classifier for a multi-temporal classification task; i.e., pre-disaster (T0), event time (T1), and post-disaster (T2). In total, seven and twelve classes were identified (section 4.1.2) for LC and LU analysis, respectively. Since the LCLU classification maps are highly important for creating recovery maps, different experiments were conducted (section 4.2.3). A combined set of SVM, SVM+GLCM, and SVM+GLCM+indicies were used, and the one with the highest accuracy was selected, using both linear and RBF kernel. Feature selection was carried out based on HSIC method. Due to hardware limitation, feature selection was applied for a small but representative subset of the study area (Figure 4-9), and then the selected features in combination with original WV2 bands of the whole study area were used to create the final classified maps.

### 5.1.1. Selected Features for Classification Task

From 18 different spectral indices (Table 4-9), based on the HSIC, NDVI2 was selected as the most important spectral index. An experiment was carried out to select the most important GLCM measures while varying the window size. Here, the GLCM variance and contrast measures of the first five bands of WV2 imagery were selected as the most informative features for LC classification task (Table 5-1). Similarly, the GLCM experiment was carried out for the LU task, where the different setting of features - compare to LC features- were selected (Table 5-2). GLCM contrast is a suitable measure to differentiate built-up areas such as building and impervious surface from the other classes. GLCM variance mainly represents building structures in formally developed areas which help to differentiate between buildings and impervious surface (Kuffer et al., 2016).

An experiment to explore the effect of varying the window size of the extracted GLCM features on the LC and LU classification result was conducted. For the LC task, increasing the window size results in a corresponding decrease in the overall accuracy. For the LU task, some of the larger window sizes are selected in combination with 3*3 window size (Table 5-2). For LC classification a large window size such as 9*9 (324 $m^2$ on the ground) implies that features extracted from a larger context are less informative than those extracted from a smaller context. This is sensible, as detection of simple LC classes does not require abstract definition like informal built-up area (Mboga et al., 2017). To differentiate non-built up areas from vegetation areas NDVI2 shows a good discriminative power which also helps to improve the classification accuracy as also mentioned in the Kuffer et al. (2016) study.

Table 5-1 Selected GLCM features for LC classification

| band | feature | window size |
|---|---|---|
| Coastal | variance | 3*3 |
| | contrast | |
| Blue | variance | |
| | contrast | |
| Green | variance | |
| | contrast | |
| Yellow | variance | |
| | contrast | |
| Red | variance | |
| | contrast | |

Table 5-2 Selected GLCM features for LU classification

| band | feature | window size |
|---|---|---|
| NIR1 | variance | 3*3 |
| | contrast | 3*3 |
| | variance | 7*7 |
| | variance | 15*15 |
| Red | variance | 3*3 |
| | contrast | 3*3 |
| | variance | 7*7 |
| | variance | 15*15 |
| Blue | variance | 3*3 |
| | contrast | 3*3 |
| Rededge | variance | 3*3 |
| | contrast | 3*3 |
| NIR2 | contrast | 3*3 |

#### 5.1.1.1. Utility Analysis of Image-Features in LC Classification

The LC classification results from SVM, SVM+NDVI2, SVM+GLCM, SVM+GLCM+NDVI2 are compared in Table 5-3. The combination of SVM+GLCM+NDVI2, achieved the highest classification accuracy with an RBF kernel. Classifications relying on spectral bands alone result in lower classification accuracies. Addition of image-features causes an increase in the classification accuracy as shown for SVM+NDVI2, SVM+GLCM, and SVM+GLCM+NDVI2. As the SVM+GLCM+NDVI2 setting performs slightly better than (only 0.4%) SVM+GLCM using RBF kernel, this setting is selected to be applied to the whole study area in order to produce the final LC classification maps.

Several insights can be drawn by comparing the performance of the different experiment setups. First, linear-based SVM consistently shown lower performances than RBF-based SVM for LC classifications. The classification accuracy of linear-based SVM, are 76.3%, 79.6.2%, 81.2%, and 83.4%, whereas the classification accuracy of RBF-based SVM, are 81.2%, 83.7%, 94.3%, and 94.7% for SVM, SVM+NDVI2, SVM+GLCM, SVM+GLCM+NDVI2 respectively. Moreover, Table 5-3 shows spectral information alone is insufficient to discriminate the land cover classes. However, adding image-features improve the classification accuracy. For example, by adding GLCM, there is an increase of 10.6%.

#### 5.1.1.2. Utility Analysis of Image-Features in LU Classification

The LU classification results from SVM, SVM+GLCM, SVM+GLCM+NDVI2, SVM+LBP, SVM+LBP+GLCM, SVM+LBP+NDVI2 are compared in Table 5-4. The SVM+LBP+NDVI2 and SVM+LBP show the highest classification accuracies with RBF kernel. However, as the SVM+LBP+NDVI2 setting performs slightly better than (only 0.5%) SVM+LBP, this setting is selected to be applied to the whole study area in order to produce the final LU classification maps. Classification relying on spectral bands alone results in low classification accuracy. Addition of image features leads to an increase in the classification accuracy as shown in SVM+GLCM and SVM+LBP. For example, by adding GLCM, there is an increase of 20.1%. This value increased by 8.7% when LBP is added. The linear-based SVM shows a lower performance than the RBF-based SVM. Moreover, SVM+LBP performs better as compared to SVM+GLCM. Surprisingly, SVM+LBP+GLCM has led to a lower accuracy as compared to SVM+LBP.

Table 5-3 Comparison of LC classification accuracies of test area

| Experiment setup | OA% | |
|---|---|---|
| | Linear | RBF |
| SVM | 76.3 | 81.2 |
| SVM+NDVI_2 | 79.6 | 83.7 |
| SVM+GLCM | 81.2 | 94.3 |
| SVM+GLCM+NDVI_2 | 83.4 | 94.7 |

Table 5-4 Comparison of LU classification accuracies of test area

| Experiment setup | OA% | |
|---|---|---|
| | Linear | RBF |
| SVM | 45.6 | 46.3 |
| SVM+GLCM | 62.6 | 66.4 |
| SVM+GLCM+NDVI_2 | 61.1 | 68.3 |
| SVM+LBP | 71.3 | 75.1 |
| SVM+LBP+GLCM | 69.8 | 72.4 |
| SVM+LBP+NDVI_2 | 72.2 | 75.6 |

### 5.1.2. Accuracy Assessment

The classification result of both LCLU maps is analyzed and discussed in this section.

#### 5.1.2.1. LC Accuracy Assessment

For creating the LC classification maps, SVM+GLCM+NDVI2 was applied to the whole study area for the three-time span. In Table 5-5, UA and PA for three time-span (T0, T1, and T2) are presented.

Table 5-5 Comparison of LC classification accuracies for pre-, event, and post-disaster situation. Overall, user and producer accuracies and corresponding errors are computed across the whole study area by combining the confusion matrices of T0, T1, and T2.

| Class | Pre Disaster (T0) | | | | | Event (T1) | | | | | Post Disaster (T2) | | | | |
|---|---|---|---|---|---|---|---|---|---|---|---|---|---|---|---|
| | Accuracy | | | Error | | Accuracy | | | Error | | Accuracy | | | Error | |
| | UA% | PA% | OA% | Commission | Omission | UA% | PA% | OA% | Commission | Omission | UA% | PA% | OA% | Commission | Omission |
| Building | 95.5 | 83.8 | **89.4** | 4.5 | 16.2 | 68.0 | 55.0 | **82.2** | 32.0 | 45.0 | 82.2 | 94.2 | **90.8** | 17.8 | 5.8 |
| Impervious Surface | 83.8 | 96.3 | | 16.2 | 3.7 | 82.0 | 68.8 | | 18.0 | 31.2 | 84.3 | 99.5 | | 15.7 | 0.5 |
| Bare | 88.0 | 83.4 | | 12.0 | 16.6 | 76.9 | 50.2 | | 23.1 | 49.8 | 98.0 | 62.3 | | 2.0 | 37.7 |
| Inland Water | 87.3 | 90.3 | | 12.7 | 9.7 | 95.2 | 94.2 | | 4.8 | 5.8 | 98.8 | 99.9 | | 1.2 | 0.1 |
| (Flattened) Tree | 77.9 | 88.9 | | 22.1 | 11.1 | 83.1 | 96.1 | | 16.9 | 3.9 | 96.5 | 92.9 | | 3.5 | 7.1 |
| Non_tree vegetation | 93.5 | 85.2 | | 6.5 | 14.8 | 89.5 | 61.0 | | 10.5 | 39.0 | 92.7 | 90.9 | | 7.3 | 9.1 |
| Rubble | *** | *** | | *** | *** | 64.4 | 87.7 | | 35.6 | 12.3 | *** | *** | | *** | *** |
| Open Water | 99.8 | 96.5 | | 0.2 | 3.5 | 98.5 | 100.0 | | 1.5 | 0.0 | 98.3 | 98.9 | | 1.7 | 1.1 |

In general, SVM set has higher values for pre- and post-disaster as compared to the event time. The Overall Accuracy (OA) for T0 and T2 are 89.4% and 90.8% respectively, while the OA for T1 is 82.2%. This is sensible because of the disaster in the area, a new setting of spectral reflectance of the classes exist as compared to spectral reflectance of the classes in the normal situation. For instance, bare land in a normal situation does not hold water, whereas in the disaster situation (although visually the class in the imagery seems the same) bare land contains a higher amount of water, which leads to a variation in its spectral reflectance (Figure 5-1 (A1)). This is also exemplified in the high value of omission error in the bare land class (49.8%). One possible solution for this is using another imagery from a time when holding water is evaporated. However, this could potentially lead to losing damage class information. The other reason for a lower OA for T1 is due to low PA and UA of the building, impervious surface, and rubble classes, see Figure 5-2 (T1). The UA of the classes building and rubble are 68.0% and 64.4%, respectively, which highlights the error of commission in these two classes and related uncertainty. This is sensible as they are spectrally similar, and the classifier confused these two classes, leading to the high amount of commission error. The problem potentially can be solved by introducing more useful information (data fusion) to classifier such as LIDAR data and or using pan-sharpened data. The former would differentiate the building from rubble due to the inherent height difference of these two classes, while the latter would potentially help to enhance the spatial discriminative power of the classifier. There is also confusion and relatively high amount of commission error for building and impervious class, ranging from 4.5% and 16.2% in T0, and 32.0% and 18% in T1, to 17.8% and 15.7% in T2, respectively. This confusion is unavoidable due to the presence of concrete and asphalt roads, making it difficult to differentiate between asphalt roads, concrete roads, and other built-up classes.

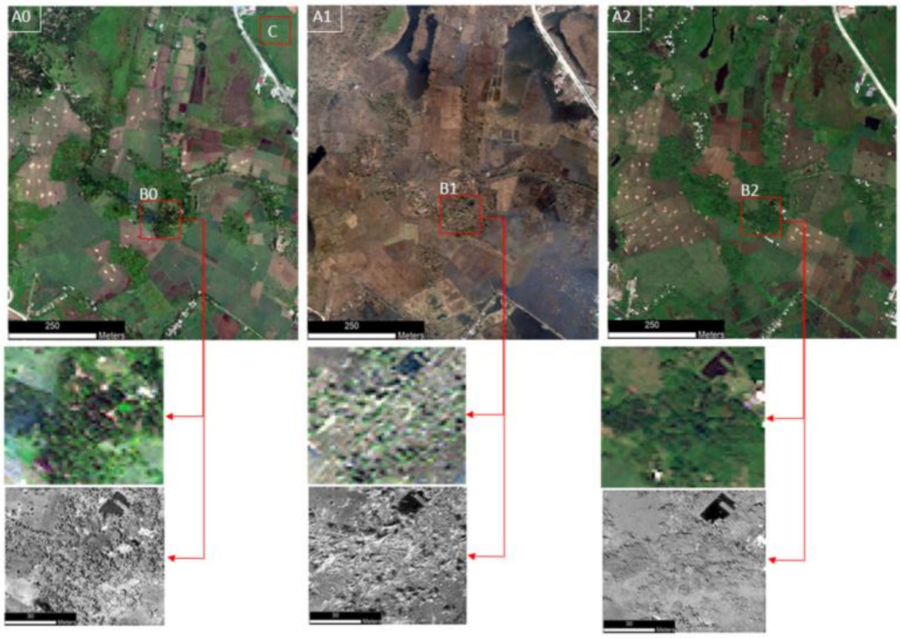


Figure 5-1 A subset of WV2 imagery, (A) area of confusion between "crop" and "grass" in three time-span, (B) area of confusion between "palm tree" and "other tree" in three time-span and related multi spectral and panchromatic zooming window, (C) status of potential grass land


Figure 5-2 Complex status of built-up-related classes in the three time-span

#### 5.1.2.2. LU Accuracy Assessment

SVM+LBP+NDVI2 is applied to the whole study area for a three-time span in order to create LU classification maps. Table 5-6 presents the UA and PA for three time-span.

Table 5-6 Comparison of Land Use Classification Accuracies

| T0, T2 Class | Pre Disaster (T0) | | | | | Post Disaster (T2) | | | | | Event (T1) | | | | | T1 Class |
|---|---|---|---|---|---|---|---|---|---|---|---|---|---|---|---|---|
| | Accuracy | | | Error | | Accuracy | | | Error | | Accuracy | | | Error | | |
| | UA% | PA% | OA% | Commission | Omission | UA% | PA% | OA% | Commission | Omission | UA% | PA% | OA% | Commission | Omission | |
| Large Scale Industry | 88.3 | 59.7 | | 11.7 | 40.3 | 84.2 | 86.6 | | 15.8 | 13.4 | 77.7 | 77.2 | | 22.3 | 22.8 | Large Scale Industry |
| Informal Built up Area | 76.7 | 81 | | 23.3 | 19.0 | 93.7 | 59.7 | | 6.3 | 40.3 | 97.6 | 37.0 | | 2.4 | 63.0 | Informal Built up Area |
| Formal Built up Area | 53.7 | 90.8 | | 46.3 | 9.2 | 69.8 | 72.7 | | 30.2 | 27.3 | 68.3 | 39.1 | | 31.7 | 60.9 | Formal Built up Area |
| Palm Tree | 66.1 | 93.4 | | 33.9 | 6.6 | 58 | 56.6 | | 42.0 | 43.4 | 84.6 | 83.5 | | 15.4 | 16.5 | Flattened Tree |
| Other Tree | 64.4 | 42.1 | 76.3 | 35.6 | 57.9 | 75.3 | 82.8 | 77.8 | 24.7 | 17.2 | 38.3 | 86.5 | 69.9 | 61.7 | 13.5 | Rubble |
| Recreation Area | 91.8 | 68.8 | | 8.2 | 31.2 | 97.2 | 73.8 | | 2.8 | 26.2 | 64.4 | 19.1 | | 35.6 | 80.9 | Recreation Area |
| Crop Land | 72.8 | 73.2 | | 27.2 | 26.8 | 80.7 | 43.2 | | 19.3 | 56.8 | 50.1 | 85.0 | | 49.9 | 15.0 | Crop Land |
| Grass Land | 66.7 | 65.6 | | 33.3 | 34.4 | 58.2 | 86.2 | | 41.8 | 13.8 | 40.5 | 33.4 | | 59.5 | 66.6 | Grass Land |
| Inland Water | 97.2 | 92.3 | | 2.8 | 7.7 | 96.2 | 99.1 | | 3.8 | 0.9 | 84.4 | 94.5 | | 15.6 | 5.5 | Inundated Land |
| Bare Land | 95 | 75.1 | | 5.0 | 24.9 | 94.5 | 73.7 | | 5.5 | 26.3 | 87.4 | 45.9 | | 12.6 | 54.1 | Bare Land |
| Impervious Surface | 79.5 | 82.7 | | 20.5 | 17.3 | 62.6 | 95.7 | | 37.4 | 4.3 | 74.5 | 69.6 | | 25.5 | 30.4 | Impervious Surface |
| Open Water | 100 | 98.9 | | 0.0 | 1.1 | 99.3 | 98.5 | | 0.7 | 1.5 | 98.6 | 99.1 | | 1.4 | 0.9 | Open Water |

The accuracies are computed for T0, T1, and T2. In general, higher accuracies are achieved for the pre- and post-disaster as compared to the event time. This highlights the complexity of the scene in the event time, as it is reflected in the LC result as well. Moreover, the OA of the LC classification consistently is higher than the OA of the LU classification. LU classes are rather heterogeneous and are more classes as compared to LC classification, as also mentioned in Herold et al. (2014, 2003). For example, LU classes range from palm tree to large-scale industry and informal settlements; from a very fine and simple class to a very large and abstract class in terms of the size and definition. Although such classes are needed from the recovery perspective, they make the image classification more complex as they cannot rely only on spectral information. Moreover, there is a confusion between the class "palm tree" and "other tree" (Figure 5-3), which is rooted in the high spectral similarity of the classes coupled with the low spatial resolution of WV2 imagery (2m) for such discrimination as shown in Figure 5-1 (B). The potential solution could be using higher spectral and spatial resolution imagery, including pan-sharpening images (Santoso et al., 2016), where due to the inherent variation of the class "other tree" (like crop) range of subclasses can also be defined to solve the ambiguity. However, introducing subclasses can restrict the study to a local context, and would demand more data; e.g., hyperspectral and radar (Dhumal et al., 2015; Ozdogan et al., 2010). For instance, radar data allow detecting rice fields, especially where it is characterized by wide inter-field variability in addition to being fragmented by other LUs as mentioned in the work of Mansaray et al. (2017). Another uncertainty is the confusion within classes "crop", "grass", and "recreational area". If

Figure 5-3 Complexity of the palm tree and other tree classes; palm trees are shown with red circles; drone imagery

"crop" is considered as an irrigated land, then a multi-temporal (phenology) analysis has a great potential to define cropland from the other two classes (Ozdogan et al., 2010). For instance, by adding images from the time when a specific crop-type is matured and, adding another from the time when the crop-type is harvested (2 images of pre-disaster and other 2 of post-disaster), which can also solve the confusion related to bare land and harvested land.

#### 5.1.3. Visualization of Classified Maps

From LC classified maps (Figure 5-4), it is observed that the boundary is much smoother in T0 and T2 over T1. Furthermore, T0 and T2 have less noisy classified maps than T1 map. For T1, there is a misclassification in the built-up area among the "bare land, "impervious surface, "building", and "rubble" which is also reflected in the confusion matrix. This confusion is worse in the LU classification, (Figure 5-5 and Figure 5-2), where the presence of the classes LSI, IBA, and FBA inherently add more confusion as they are spectrally similar. However, this misclassification is reduced in both T0 and T2 for both LC and LU maps. Zooming in at the raw image, it is clear that there is an open field in the South-East part of the area, which covered by "crops", "grass", "other trees", and "palm tree" see Figure 5-1 (A). This could be an example of existential uncertainty, whereby there is some doubt on the presence of the grass class in a given area. The classification results show the SVM with data of a spatial resolution of 2m perform well in LC level, while it faces difficulty in LU level, as mentioned earlier. GLCM features work well in LC classification, while more information could improve the accuracy of LC classification.

Figure 5-4 also shows the LC-related pie charts. The class building covers 15%, 8%, and 15% of the area in T0, T1, and T2 respectively. This implies that almost all buildings are reconstructed within 4 years after the typhoon, which also can be seen by visual interpretation of raw imagery. The above-mentioned rebuilding can be considered a positive sign of recovery. However, more information is needed to characterize that recovery status. Impervious surface shows an increase of 3% in T2 compared with T0. This also can be visually seen in the raw image, where, for instance, a national road that is constructed in T2 in the West part of the city (Figure 5-8 (F)). For the vegetation category, the area covered by tree decreased by 2% in T2 as opposed to T0, while conversely, the area of non-tree vegetation increased by 2% in T2 against T0. Considering the damage classes in the disaster situation (T1), 37% of the area is occupied by rubble, while 8% of the land is inundated and 27% of the land is covered by flattened tree. The damage classes show huge destruction in Tacloban city leading to a massive human and property loss (Adriano et al., 2015; Yi et al., 2015).

Figure 5-5, on the other hand, shows the LU related pie charts. In the sub-building category, the size of LSI is remained the same in T2 as like T0 (3%), though it shows a very slight decrease of about a mere 1% to 2% in T1, which in general indicates a good sign of business recovery. The area covered by IBA cut half in the event time from 4% (T0) to 2% (T1). This is sensible as typhoon heavily destroyed the slum areas in Tacloban city (Mas et al., 2015). Although the IBA class increased by 1%, from 2% to 3% in 2017 (T2), it is not a good sign of the recovery process. The FBA class showed a decrease of 5% in T2 as compared to T0. This is not very sensible and is mainly due to uncertainty in the classification of FBA in T2 as discussed earlier. The size of covered land by palm tree shows a decrease by 7%, from 18% in T0 to 11% in T2, which is sensible due to both CLP and required time for growing of a palm tree (Yi et al., 2015). With regards to subclasses of non-tree in LC level, in the recreational area increased by 1%, from 3% in 2013 to 4% in 2017. Moreover, there is an approximate 3% growth in cropland in 2017, compared to T0 in 2013. The increase in recreational area is a good sign of recovery, as the size of the recreational area also planned to be increased in the CLP (2016). However, the growth of the size of cropland is not necessarily a good sign of recovery as the CLP (2016) planned to reduce the size of cropland. On the other hand, the palm farmers need to replace flattened palm trees by another crop type in order to live (cash crop). However, more information would be required to investigate the role of cropland change in the recovery process.

Overall, in both T0 and T2, the most significant changes in LC is the increase in the area covered by the impervious surface in T2, while the building is reconstructed almost to the size of the pre-disaster situation which initially can be seen as a good sign of recovery. However, LU information revealed that the rebuilding is a negative sign of recovery, where slum areas (IBA) are reconstructed in the same area in T2.

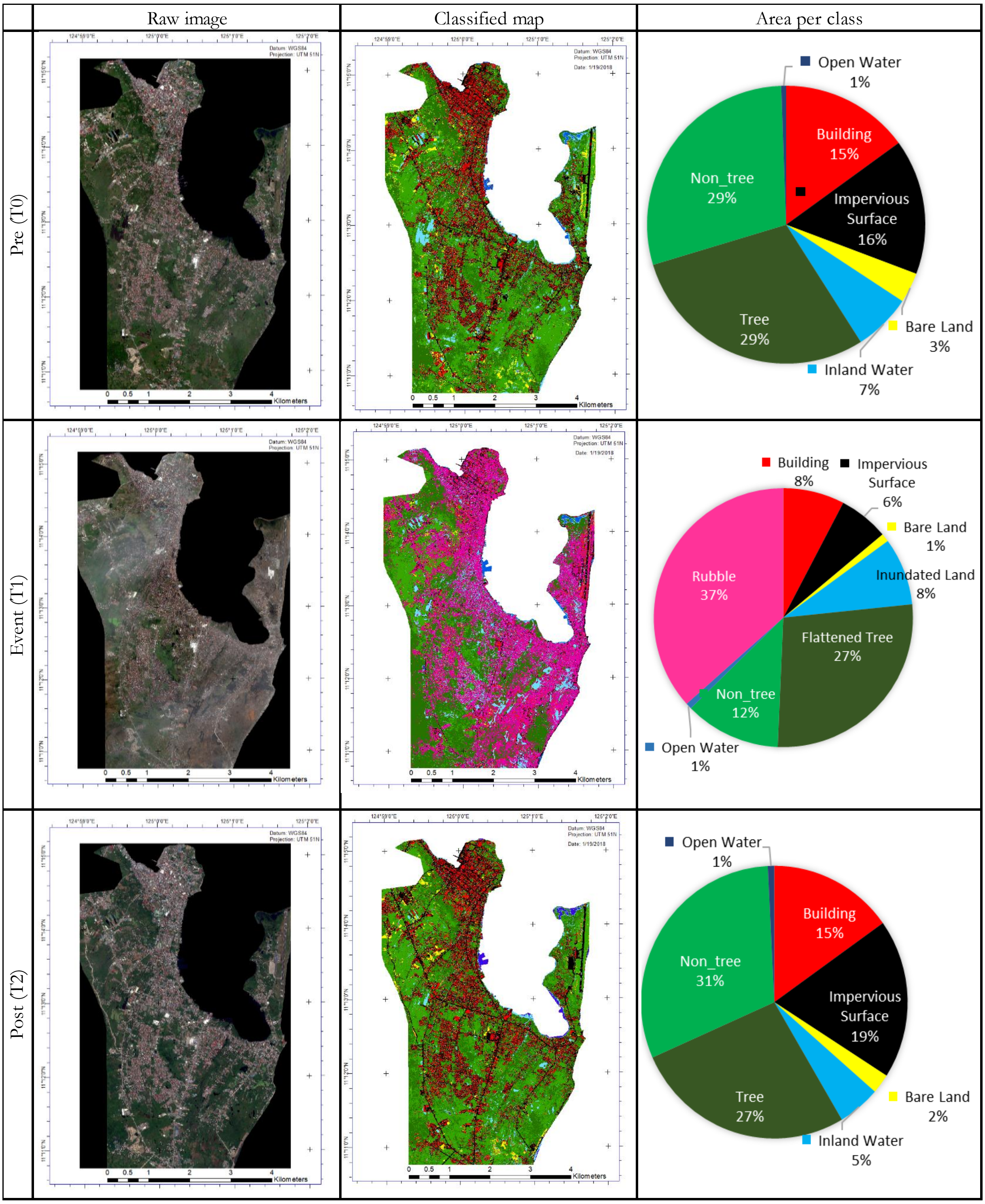


Figure 5-4 LC Classification maps from SVM relying on GLCM features and NDVI2 for T0, T1, and T2 and corresponding pie charts

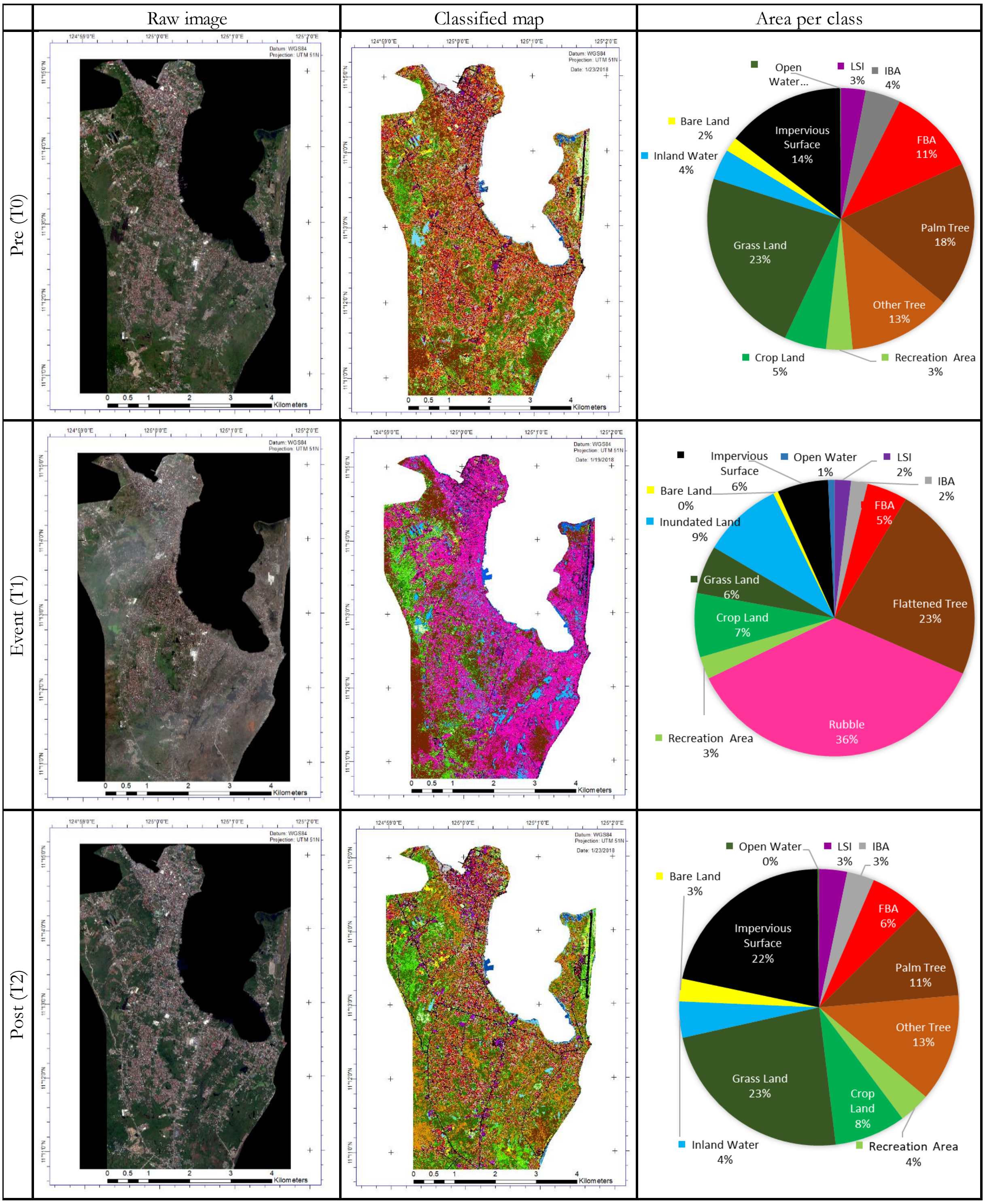


Figure 5-5 LU Classification maps from SVM relying on LBP features and NDVI2 for T0, T1, and T2 and related pie charts, LSI: Large Scale Industry, IBA: Informal Built up Area, FBA: Formal Built up Area

### 5.1.4. Errors Due to Uncertainty

Existential and extensional uncertainties are two factors of accuracy assessment. Existential uncertainty relates to whether an object is existing in the geographical location it is said to be, while extensional uncertainty is related to lack of an exact definition of the boundary of a phenomenon (Kohli, 2015). In the context of understanding the recovery process through LC and LU from VHR, these concepts are important. First, in the absence of fieldwork, normally important for the creation of reference data, visual interpretation of Google Earth imagery (same time of the satellite images) was used to digitize the requisite classes. In this process, instances were encountered whether an area was the class supposed to be or not. For instance, the most doubtful classes were grass, crop, palm tree, other tree, and bare land, such as the presence of green space (potentially grassland) next to an open cropland (Figure 5-1 (C)). Examples of existential uncertainties for palm tree and other tree are shown in Figure 5-1 (B), and for bare land in Figure 5-1 (A1). Second, defining the exact delineation between an area that is IFA, FBA, and rubble was a source of uncertainty (Figure 5-2). Uncertainty in the location and boundary of a phenomenon such as slum, probably will affect the accuracy of the reference data and the quality of the metrics calculated using it (Kohli, 2015).

However, this study was aware of the above-mentioned uncertainties and tried to mitigate them by using a multi-source data ranging from Google Earth at the same time of the satellite images, open street maps data, panchromatic band of WV2, street view of GE, to LC map from Tacloban as the first input to the visual interpretation process. In addition, morphological characteristics based on literature and described in Kuffer et al. (2014) were used to identify FBA and IBA. It would be favorable to measure these uncertainties in future research.

#### 5.1.5. Recovery Maps

Based on the developed conceptual framework for Tacloban city and LCLU classified maps, two recovery maps are developed (Figure 5-6). With regards to the LC-based recovery map (Figure 5-6 (A)), it is observed that the recovery class "slightly positive" (SP) is the dominant class (226 ha.), followed by classes "positive" (P) and "neutral" (NT), where the class "negative" (N) has the lowest portion by 12 ha as shown in Figure 5-7 (B). The reason why SP class is dominant is that the LC classes are mostly broad categories which can be divided into many subclasses. Therefore, most of the transition patterns need more information to be precisely characterized. For instance, slum areas are part of the "building" class in LC level, while it is "IBA" in the LU level. The transition pattern (TP) "building-rubble-building" in the LC-based recovery map, is the most responsible TP and is characterized as the class SP recovery. However, the TP mentioned above can be "IBA-rubble-IBA" in LU-based recovery map and is categorized as negative (N) recovery, see Figure 5-8 (A). Thereby, LU provides more effective information in some transitions, compared to LC information. Moreover, it seems LC information is enough to characterize some classes and related TPs. For instance, a new national road in the West part of the area is well-captured by LC-based recovery map, see Figure 5-8 (F). This is also exemplified in the Figure 5-8 (E), where a parking lot is added to a commercial building. Thereby, there is no need for more information to characterize P recovery in LC-based recovery map; i.e., land use information. A negative example of recovery, in LC level, is also shown in Figure 5-8 (C), where "non-tree" is turned to "inland water". The NT recovery also covers a large area in LC-based recovery map. This is related to the broad definition of the LC classes, where there are more chances for TPs to be categorized as NT compared to LU-based recovery map. Figure 5-8 (D), moreover, shows a potential positive recovery TP which has not been captured by both recovery maps. This can highlight lack of image data from other times to track some specific TPs which cannot be grasped by only a 3-time based recovery map. Considering LU-based recovery map (Figure 5-6 (B)), it can be seen that the recovery classes are almost equally distributed in terms of area covered in ha. The class SN is the dominant class (area covered is 87 ha.), which closely followed by SP (74 ha.), see Figure 5-7 (C). This is sensible as in LU regulation after Haiyan it was decided to reduce the amount of crop and increase the amount of FBA by CLP (2016). However, since the geographic location of the place where this reduction should be implemented is not defined in CLP (2016), it is characterized as SN.

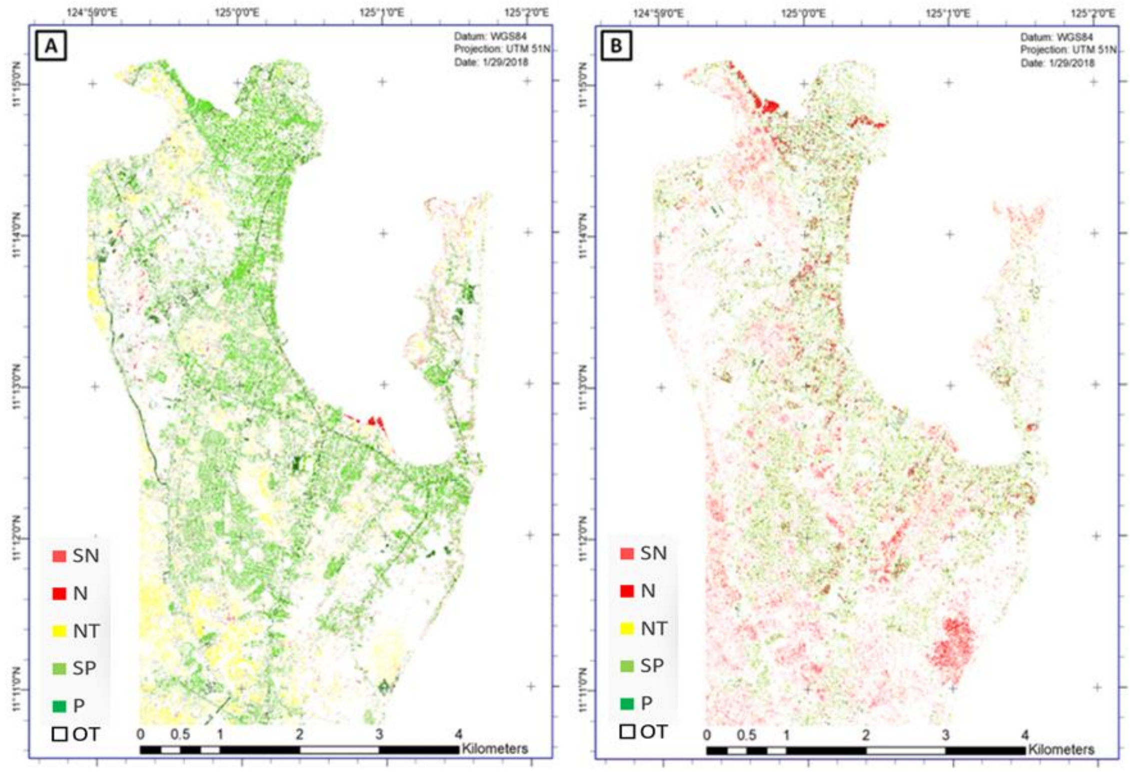


Figure 5-6 (A) LC-based recovery map; (B) LU-based recovery map; data source: WV2 images (T0, T1, and T2); recovery map approach: based on a code developed in R; main Observation: striking difference between A and B is mainly due to 2 issues:1) class slightly positive recovery (SP) in A, where the area is mostly covered by TP "building-rubble-building", which this TP is changed to other TPs in B such as IBA-rubble-IBA (N: negative recovery) 2) due to different TPs used in A and B

Moreover, in the Figure 5-7 (A), it is illustrated that the area covered by class "other transition" (OT), is almost equal for both LC- and LU-based recovery maps. More area is classified as SN and N in the LU-based recovery map compared to the LC-based recovery map. Conversely, classes NT, SP, and P are more dominant in the LC-based recovery map as compared to LU-based recovery map.

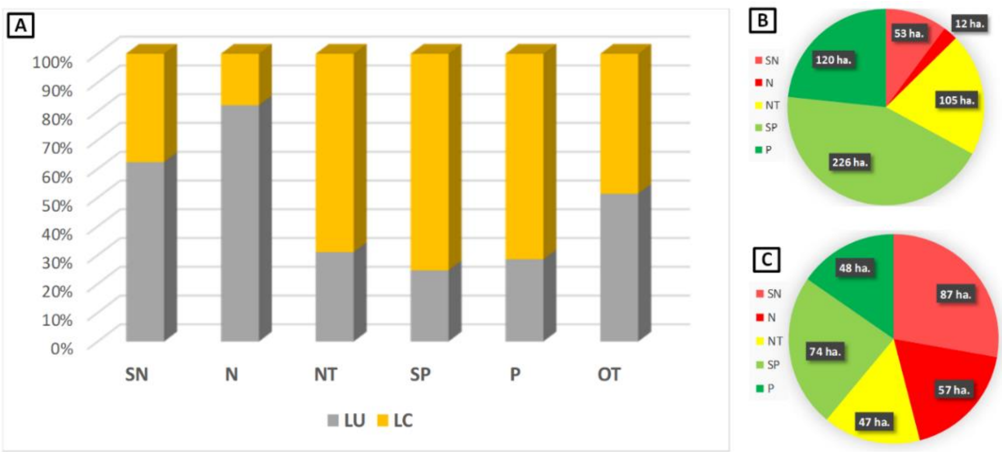


Figure 5-7 (A) A comparison between LC- and LU-based recovery map; (B) area per class for LC-based recovery map; (C) area per class for LU-based recovery map

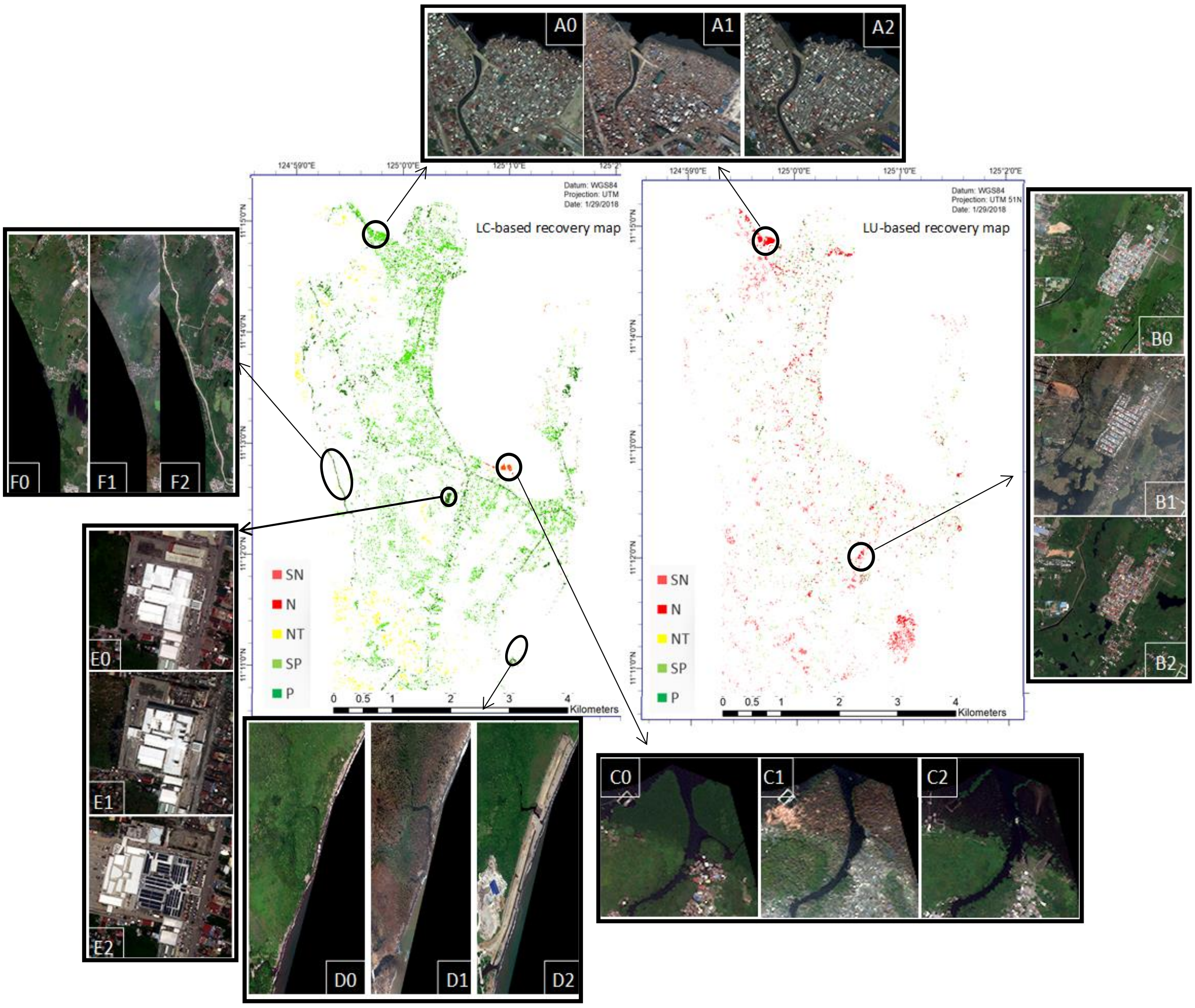


Figure 5-8 Visual examples of LC- LU-based recovery maps

In order to avoid noise introduced by isolated pixels a majority filter with the kernel size of 5*5 is applied to both recovery maps, see Figure 5-9. It is evident that more area in both maps are accounted for the class OT, and those which are not in the OT class are resilient enough to this aggregation. Although up-scaling of the map removes some information, the maps with majority filtering provide more efficient information for policymakers at city level. The reason for that is policymakers need more concise information than a detailed map full of information, while also an aggregate map is easier to communicate. A detailed map is appropriate for stakeholders at the neighbourhood level, where they can benefit from detailed recovery information for their needs at a local scale. Overall, an aggregated map is potentially useful in a city level while for a neighborhood level a detailed recovery map is more desirable.

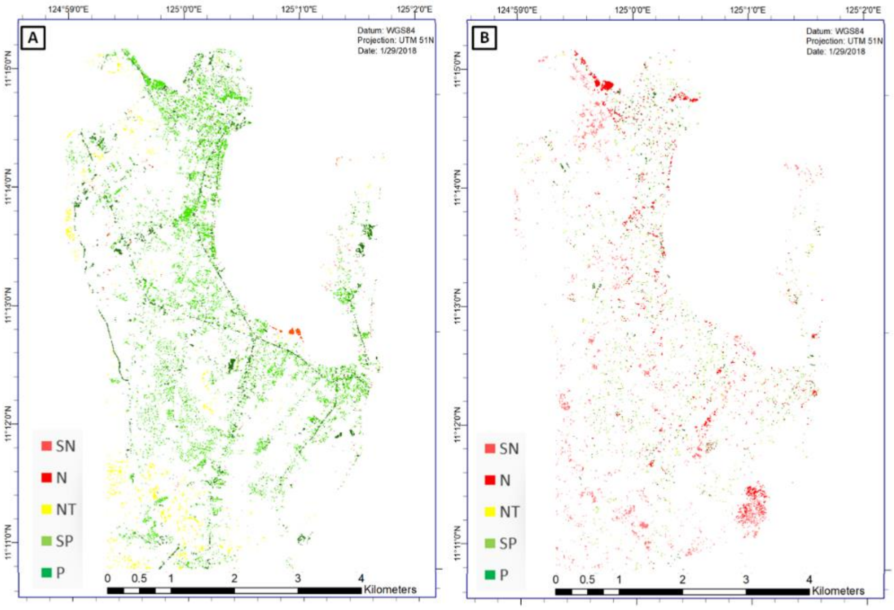

Figure 5-9 (A) Aggregated LC-based recovery map, (B) Aggregated LU-based recovery map

### 5.2. Practical Guide

An effective way to assess the recovery process and or to compare different events and related recovery processes is using indicators (Chang, 2010). In the recovery literature, there are some indicators with different levels of practicality. These indicators are categorized into 3 groups based on definitions given in section 4.3. Moreover, some indicators from other disciplines are included (with the potential to provide recovery information). Indicators are grouped as macro, meso, and micro indicators (Table 5-7, Table 5-8, and Table 5-9).

The first group of the indicators "macro indicators" are those with a high utility in the recovery context, where already well-established RS method(s) exist. For example, nighttime lights can be well captured by visible infrared imaging radiometer suite (VIIRS). These indicators can easily reveal important information about the recovery process over a large scale; i.e., city scale, see Table 5-7.

The second group of indicators are "meso indicators", which in comparison with macro indicators are less practical and mostly are applicable within the city scale. Although these indicators have the potential to be used in the recovery context, they have not frequently been used so far. Thereby, there is a need for a guide to distinguish them in RS data and proposed which kind of data processing can be employed for their recognition. By using the provided practical guide, they can be used more frequently and effectively in the recovery context. The practical guide aims to best link these indicators to RS methods. Moreover, a short recovery analysis for these indicators is done in Table 5-8. This table first, checks which spatial resolution is suitable for the specific indicator for both visual interpretation and semi-automatic analysis. Then, lists, which auxiliary data type, time of the day (ToD), unit of analysis, RS method, field of view, and number of images, is required. Auxiliary data type provides a list of potential auxiliary data in addition to optical RS to help to best detect and analyze a specific indicator. The indicators are checked whether they are related to physical and or functional recovery and also if they are more useful in the short- or long-term recovery.

As already mentioned earlier in chapter 2, there are some local type indicators with a low utility in the recovery, which are hard or impossible to detect by RS. These indicators are categorized in "micro indicator" as they have low utility in the recovery context; i.e., they can be used at the neighbourhood level (Table 5-9). They either can be visually detected with spatial resolution of 1-10 cm by super resolution visible (SRV), or there is no existing RS method to detect them. Moreover, for those that visually are detectable, there is no existing semi-automatic method allowing for monitoring.

Table 5-7 Macro indicators with high utilities in the recovery assessment

| Indicator | Methods | Reference |
|---|---|---|
| Change in urban morphology | landscape metrics | (Hagelman et al., 2012) |
| Night time light | Visible Infrared Imaging Radiometer Suite (VIIRS) | (Deville et al., 2014; Sutton et al., 2007) |
| Deforestation | NDVI analysis | (Brown et al., 2010; Curtis et al., 2010) |
| Impervious surface | visual interpretation, maximum likelihood | |
| Reconstruction of bridges and public transportation facilities | standard CD methods | |
| Proportion of built up and vegetated area | NDVI analysis, standard CD methods combined with GIS | (Ebert et al., 2009) |
| Debris removal | visual interpretation, standard CD methods | (Hill et al., 2011) |
| Vegetation recovery | NDVI analysis, visual interpretation, standards CD methods | (Wagner et al., 2012) |
| Reservoirs | visual interpretation, NDVI analysis, maximum likelihood | (Harb et al., 2015) |
| Roads | visual interpretation, maximum likelihood | (Weng, 2012) |

**Key for Tables 5-8 and 5-9**

Optical RS: *MRV*, moderate resolution visible (spatial resolution >10–30 m); *HRV*, high resolution visible (spatial resolution >2–10 m); *VHRV*, very high resolution visible (spatial resolution better than 2 m); *SRV*, super resolution visible (spatial resolution >1–10 cm);

Auxiliary data type: *Hyp*, hyperspectral imagery; *IR*, infrared (typically a NIR band in optical sensors); *VIIRS*, Visible Infrared Imaging Radiometer Suite; *Vin*, vegetation index; *BuI*, built-up index; *TF*, texture feature; *DF*, data fusion;

Unit of analysis: *PB*, pixel based; *OB*, object based; *RB*, region based;

RS Method: *ML*, machine learning; *DL*, deep learning; *LM*, landscape metrics;

FoV (field of view): *V*, vertical; *Obl*, oblique;

Recovery analysis Type: *Phs*, physical; *Fnc*, functional;

Recovery analysis Time: *STR*, short term recovery; *LTR*, long term recovery

*EM*, existing method

⊗: from ecology discipline

Table 5-8 Meso Indicators with medium to high utilities in the recovery assessment (list of acronyms is provided after Table 5-7 on the previous page)

| Indicator | Optical RS | | | | Practical guide | | | | | | | | | | | | | | | | | | | | | | | Recovery analysis | | | | | Reference |
|---|---|---|---|---|---|---|---|---|---|---|---|---|---|---|---|---|---|---|---|---|---|---|---|---|---|---|---|---|---|---|---|---|---|
| | | | | | Auxiliary data type | | | | | | | | | ToD | | | | Unit of analysis | | | RS Method | | | FoV | | # image | | type | | | Time | | |
| | MRV | HRV | VHRV | SRV | Hyp | IR | VIIRS | Radar | VIn | BuI | TF | LiDAR | DF | Mor | Noo | Eve | Nig | PB | OB | RB | ML | DL | LM | V | Obl | 1 | >1 | Phs | Fnc | Mix | STR | LTR | |
| Building height and area | | | * | | | | | * | | * | | * | * | na | | | | * | | | * | | * | * | | * | | * | | | | * | (Brunner et al., 2010; Shaker et al., 2011; Xie et al., 2017) |
| Parking lots | | | * | | | | | | | * | * | | | | * | | | * | * | * | * | | | * | | * | | | | * | | * | (Wei et al., 2013; Xiao et al., & Paparoditis, 2016) |
| Presence of boats (fishery industry) | | | * | * | | * | * | | | | | | | * | | | * | * | | | * | | | * | | * | | | * | | * | * | (Elvidge et al., 2015; Xu et al., 2014) |
| Arable land (different crop type) | | * | * | | * | | | * | * | | * | | * | na | | | | * | * | * | * | | | * | | * | * | | | * | * | * | (Dhumal et al., 2014; Ozdogan et al., 2010) |
| Reconstruction of government buildings | | | * | | | | | | | * | * | * | * | na | | | | * | | * | | * | | * | | * | | | | * | | * | (Xie & Zhou, 2017) |
| Warehouses | | | * | * | | | | | | * | * | * | * | * | | | | * | * | * | * | | | * | | * | | | | * | | * | (Huifeng & Aigong, 2008) |
| rail roads | * | * | * | | | | | | | | | * | | na | | | | | * | | * | | | * | | * | | * | | | | * | (Arastounia, 2015; Gedrange et al., 2011) |
| Structure unchanged since disaster event | | | * | * | | | | | | * | * | | * | na | | | | * | | | * | | | * | * | | * | * | | | | * | |
| Structure rebuilt in same footprint | | | * | * | | | | | | * | * | | * | na | | | | * | | | * | | | * | * | | * | * | | | | * | (Rathfon et al., 2013) |
| Structure rebuilt different footprint | | | * | * | | | | | | * | * | | * | na | | | | * | | | * | | | * | * | | * | * | | | | * | |
| Stage of development (identification of land clearance and foundations) | | | * | * | | | | | | * | * | | * | na | | | | * | | | * | * | | * | * | | * | | | * | * | * | (Brown et al., 2010) |
| Traffic activity (presence of vehicle) | | | * | * | | | | | | * | * | * | | * | | * | | * | | | | * | | * | | * | * | | * | * | * | * | (Wei et al., 2013; Xiao et al., 2016) |
| Camp longevity | | | * | | | | | | | * | * | | * | na | | | | | * | | * | | | * | | | * | | | * | * | | (Pelizari et al., 2017; Spröhnle et al., 2014; Tiede et al., 2017) |
| Accessibility/ Road access (condition) | | | | * | * | | | | | | | * | * | na | | | | * | | | * | | | * | | | * | | * | | | * | (Andreou et al., 2011; Herold & Roberts, 2005) |
| Bridge condition | | | * | * | | * | | * | | | | * | * | na | | | | | * | | | * | | * | * | | * | | | * | * | * | (Ahlborn et al., 2010; Chaudhuri & Samal, 2008; Endsley et al., 2012) |
| Number of street intersection | | | * | | | | | | | * | * | * | * | na | | | | * | * | | * | * | | * | | | * | | | * | | * | (Schnebele et al., 2015; Wang et al., 2016) |
| Slop position | | | * | * | | | | | | | | * | | na | | | | * | | | * | | | * | * | * | | | | * | | * | (Vanneschi et al., 2017) |
| Turbidity, Suspended sediment ⊗ | | * | * | | | * | | * | | | | | | na | | | | * | | | * | * | | * | | | * | | * | | * | | (Pettorelli et al., 2017) |
| Presence of waste products in the soil ⊗ | | * | | | | | | | * | | | | | na | | | | * | | | * | | | * | | | * | | * | | * | * | (Peng et al., 2016) |
| Presence of ships in harbor | | | * | * | | | | * | | | | | | na | | | | * | * | | | * | | * | | | * | | | * | * | * | (Elvidge et al., 2015; Margarit et al., 2009; Xu et al., 2014) |
| presence of air plane in the airport | | | * | * | | | | | | | | | | na | | | | * | | | | * | | * | | | * | | * | | * | * | (Chen et al., 2014; Qinhan Luo, 2016) |
| Presence of coconut tree | | | * | * | * | | | * | * | | * | * | * | na | | | | * | * | * | * | * | | | | | * | | | * | | * | (Santoso et al., 2016; Srestasathiern & Rakwatin, 2014) |

Table 5-9 Micro indicators with low to medium utilities in the recovery assessment

| Indicator | EM | FoV | | Recovery analysis | | | | | Reference |
|---|---|---|---|---|---|---|---|---|---|
| | | | | Type | | | Time | | |
| | VI | V | Obl | Phs | Fnc | Mix | STR | LTR | |
| Clean/dirty swimming pools | * | * | | | * | | * | | (Brown et al., 2010) |
| Indoor parking place | * | | * | | * | | * | | |
| Proximity to services | na | | | | | | | * | |
| Distribution and connectivity of water points | na | | | | | | | * | |
| Tanks and towers (water towers) | * | * | * | | * | | * | * | |
| Playground | * | * | * | | * | | * | | |
| Chimneys | * | | * | | * | | * | | |
| State of garden | * | * | | | * | | * | | |
| Window flower pot | na | na | | | * | | * | | |
| Construction of stable housing | na | na | | | | * | | * | |
| Presence of trash bins | * | * | * | | * | | * | | (Curtis et al.,2010) |
| Neat front yards | * | * | | | * | | * | | |
| Pedestrian access | * | * | * | | * | | * | * | (Song & Knaap, 2004) |
| Lifeline utility | na | na | | | * | | * | * | (Ruiter, 2009) |

Overall, this chapter provided and analyzed the result of LCLU analysis and practical guide. In LCLU analysis the selected image features were illustrated and succeeded by accuracy assessment of LC and LU maps. Two recovery maps based on LC and LU were showed, and the results were analyzed. Moreover, in the practical guide, three tables regarding macro, meso, and micro indicators were showed and analyzed. In the coming chapter, the results will be discussed.

# 6. DISCUSSION

This chapter discusses main findings of this research, considering and reflecting upon limitation of methods applied and experimental results. A comparison with existing research is made where applicable and, in some cases, possible future research items are mentioned. The main objective of this study was to understand and conceptualize post-disaster recovery through LCLU assessment using RS, and also investigate the value of LCLU information in the recovery assessment.

## 6.1. Utility of the Conceptual Framework

The developed conceptual framework was both a philosophical justification of recovery process within three time-span and one of the important outputs of this study which remainder outputs were sensitive to it. The conceptual framework is helpful to understand the recovery processes involved in each TP and to classify mapping approaches and further providing recovery maps. Thus, as Parsons et al. (2016) mentioned, the CF should be published before results. In the light of the CF, both physical and functional recovery were explored, leading to a more holistic understanding of recovery process. However, in order to increase the generalization capacity and to make a deeper understanding of recovery process, the conceptual framework could be refined from a theoretical viewpoint. One possibility would be to bring the population information of the affected area corresponds to each image which would improve the functional understanding of recovery.

There is an uncertainty in the developed CF regarding TPs, specifically on the event (T1) and post-disaster (T2) times. In the developed CF degree of damage and rebuilding are assumed to be discrete. Nevertheless, in reality, different levels of damage exist, ranging from complete collapse to cracks on the building roof or façades (Vetrivel et al., 2016) as well as different degrees of rebuilding (Coppola, 2011). If TPs are considered as "recovery vectors" (see Figure 6-1), disaster damage will imply a negative change (between T0 and T1), while rebuilding (between T1 and T2) will imply a positive change. Therefore, from conventional recovery perspective, at least three recovery vectors V1, V2, V3 can be anticipated which have corresponding damage depths; i.e., moderate, high, and total damaged d1, d2, and d3 respectively (Figure 6-1 (A)). Moreover, with respect to the concept of BBB, other 3 recovery vectors can be expected with different degrees of positive and negative changes as, e.g., V1, V2, and V3 as shown in Figure 6-1 (B). Clearly, such enhancements would claim substantially greater data than what is currently required. However, this new insight would provide valuable opportunities for deeper understanding regarding recovery.

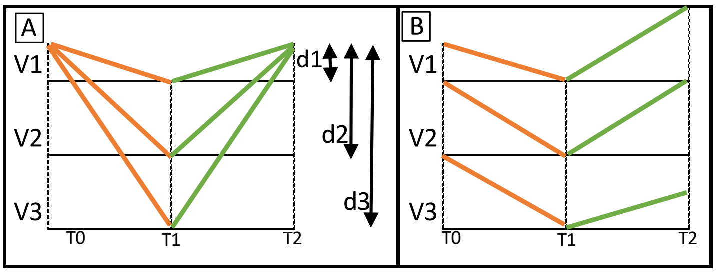


Figure 6-1 Recovery vectors (A) concept of build back (B) concept of build back better

## 6.2. Utility of SVM Relying on GLCM and LBP Features

The study area was a complex setting of both urban and rural, which makes the scene very heterogeneous. A low inter-class spectral variation and intra-class separability of the LCLU classes led to an inaccurate result when SVM performed solely on spectral bands of the WV2 images, and especially for the event time (T1). Utilizing image feature, inherent in the image, in the classification leads to an increase of class separability and accordingly improves the classification accuracy (Kuffer et al., 2016). In this study, several spectral and textural measures were extracted from the WV2 images and then employed in SVM. Results showed that such measures increase the overall classification accuracy. In LC classification, SVM relying on GLCM and NDVI2 improved the classification accuracy which corresponds with the finding of Kuffer et al., (2016) and Salehi et al., (2011). In LU classification, SVM relying on LBP and NDVI2 provided the highest accuracy among different settings of SVM and image features which showed an agreement with the result of Mboga et al., (2017) and Ella & Wyk, (2008). Besides, the resulting LCLU classified maps were of good visual quality, meaning that hand-crafted features can give a competitive performance when carefully considered, although it is time-consuming.

Some inaccuracies (uncertainty) in the classified maps were shown in Table 5-5 and Table 5-6. There are different reasons for incorrect classification. For instance, an area having spectral characteristics of grassland, which occurring within a cropland, an area with morphological appearance of informal built-up area (IBA) yet occurring within a formal built-up area (FBA), and low spatial resolution and high spectral similarity to differentiate palm from other trees make classification difficult. Some work on uncertainty analyzing for image interpretation of informal settlements has been done in Kohli et al. (2016). Nevertheless, the quantification of the extent and nature of these uncertainties could be assessed in future studies, where CNN-learned features from the image (especially over event image) can be used as an input into SVM as suggested in the work of Razavian et al., (2014). Overall, the utility of SVM combined with image features provide a good result in built-up related classes which agreed with the result of Mboga et al. (2017). Regarding vegetation-related classes, the result of SVM was correlated with the result of Ozdogan et al. (2010) over a large area, while it was not corresponding to the result of Mathur et al. (2008) over the local scale. Uncertainty due to mixed-unit classes in LU level is conditional upon the temporal and spatial variability of the spectral signature of the classes in question. Thus, a careful definition of mixed-unit classes in LU level would improve mapping of the heterogeneous scene as mentioned in the work of Herold et al. (2008). Moreover, appropriate images (pre-disaster) must be available for the temporal approach to providing a complete inventory of all irrigated fields in a study area (Ozdogan et al., 2010). Therefore, understanding vegetation-related classes change after a disaster requires an understanding of corresponding vegetation changes before the disaster. Meaning that a five time-span framework would be more informative than a three time-span framework in vegetation-related recovery assessment.

## 6.3. Utility of LCLU and Recovery Maps

In this study, the utility of LCLU and related changes were examined in Tacloban city with regards to the post-Haiyan recovery process. From LC maps (Figure 5-4), it is evident that there is an increase in the size of impervious surface within recovery process in 2017, which can be considered as a good sign of recovery (Brown et al., 2010). Moreover, in 2017, the area related to non-tree is increased, while the class "tree" is decreased as the same size. This is sensible and can be considered as a good sign of recovery due to huge damage in tree class and the required time for growing of a palm tree (4-7 years), which leads people to adjust their source of income from palm tree to other cash crops that is in an agreement with the work of Mayans (2014). However, the recovery status is different if the reduction in tree means that the area got abandoned. With regards to LU maps (Figure 5-5), it is observed that class large-scale industry remained the same which is a positive sign of recovery, as the CLP (2016) decided not to relocate large scale industries. Regarding the state of activity of LSI, a visual interpretation based on indicators was made in the image of 2017 for 10 samples. The indicator used were presence of truck, car, and storage containers in combination with Google street view. The result showed that the LSI samples were active in

2017. Decreasing in the size of IBA in 2017, moreover, is considered a good sign of recovery. However, the remaining part of IBA is still relatively high and is related to a region along the coastline. Thus, there is a need that the policymakers modify the comprehensive CLP and consider the situation of IBA to improve the area and become more disaster resilient. As mentioned earlier growth in cropland is clearly due to decrease in palm tree, while the overall increase in non-tree is attributed to both anthropogenic activities and typhoon Haiyan (Mayans, 2014). Furthermore, some uncertainties were related to the quality of data; for instance, uncertainties related to the damage classes and palm tree are functions of the spatial resolution of the image. Moreover, recreational area proved to be a meaningful class to assess social recovery (EPC, 2004).

As mentioned earlier in chapter 2, CDEM (2005) is a well-accepted holistic recovery framework. The utility of LCLU, from the evolving understanding of recovery within this study, is investigated in different aspects of recovery process formed by CDEM (Figure 6-2). Utility of LCLU in each aspects of recovery in a colour-coded manner is shown in Figure 6-2, where LCLU has a low to high utility in CDEM recovery framework (almost seventy percent of different aspects of recovery) except health (social), biodiversity (natural), individual, infrastructure, government (economic), and lifeline (built-up).

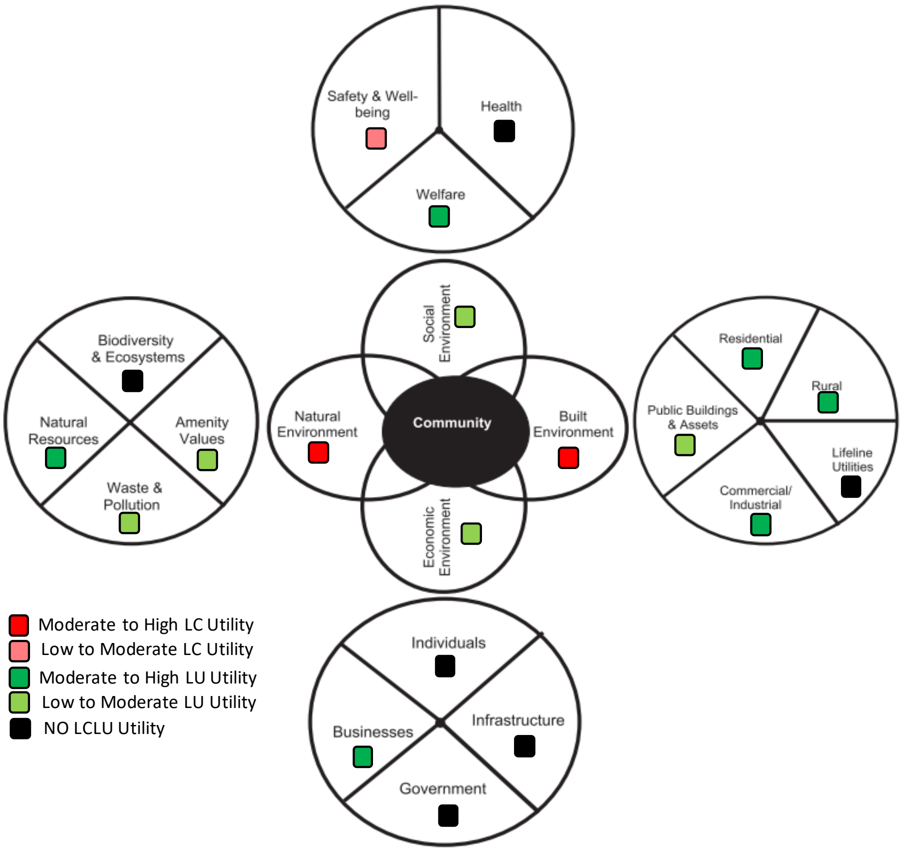


Figure 6-2 Utility of LCLU in a holistic recovery, adopted from (CDEM)

In this study, 7 LC and 12 LU classes were selected based on the context of Tacloban city and typhoon Haiyan. In LC level, classes building, and impervious surface proved to be important. In LU level, however, classes LSI, IBA, FBA, palm tree, and cropland were the most informative ones. LU classes showed high exploratory power more on a local scale, while LC classes were informative over a larger area. The other insight is that LCLU information can complement the recovery insight and smart use of LCLU information can produce a robust recovery map and consequently, provide a deeper understanding of recovery process. Meaning that, as providing LC information is easier and probably cheaper than LU, LC can serve as a basis layer which can give sufficient vision as well as an accurate result over large areas. While LU-derived information can be effectively used in the area of uncertainty in "cover" level, where more detailed information is required within a city level.

The "balancing point" for using different levels of information is a trade-off of the purpose of the study, data availability, and scale of study. However, from this study can be perceived that the LC-derived information can be sufficient to talk about built-up and vegetation recovery and specifically about the status of the impervious surface over city level. This study, moreover, proved the initial hypothesis and showed LC-derived information largely reveal physical aspects of recovery and LU information can expose functional recovery. Overall, LC information is helpful in a blanket classification over large areas, and LU information is more helpful in a focused target classification for some aspects of recovery such as economy recovery, while also LU can be best employed to detect long-term recovery activities.

With regards to recovery maps developed in this study and related TPs, it is evident that some TPs can characterize short-term recovery such as impervious surface-rubble-impervious surface, while some characterize specifically long-term recovery such as grass-grass-impervious surface. Regarding LC-based recovery map, it is observed that the area belongs to the classes SP and SN are the areas of extensional uncertainty, where they ultimately need to be defined as N and or P by providing more relevant data. There was, moreover, a striking difference between LC- and LU-based recovery maps, where the former mostly was covered by class SP (green) and the latter was mostly covered by classes SN and N (red). This was sensible as in LC-based recovery map class SP was the dominant class (226 ha.), which mostly characterized by TP "building-rubble-building". However, in LU-based recovery map, this TP was divided into other detailed TPs. These new TPs necessarily did not hold the same class-value as LC level due to a detailed level of information. Accordingly, these new TPs changed their class-values mostly from SP to SN and N from LC to LU level respectively. For instance, IBA-rubble-IBA (N: negative recovery). Thus LC-based recovery map is more useful for initial assessment of recovery over large areas, and LU-based recovery map is more useful to assess specific recovery activities, a certain process, and certain LU on a local scale. The aggregation level used in this study might not be applicable in other studies as the context of disasters and cities varies and could be a potential area of further research. However, it is observed that the bigger and the more consistent the classes are (in terms of size and connectedness), the more resilient to the aggregation (based on a majority filter) they are.

Recovery information is specifically for a disaster-stricken area and is related to a certain period. From GIS perspective, thus, the recovery information is a geographic phenomenon that is made up of transition patterns (geographic objects) (Tolpekin & Stein, 2013), which potentially come in different "flavors". Perhaps the most desirable recovery information comes in a "region-based" manner, where noises can also be avoided. This means that recovery information is not "everywhere" in the area of question. Thus, not all pixels hold recovery information. Thereby, those which hold relevant (recovery) information should be unified meaningfully. Transition patterns (geographic objects) should not be studied in isolation, but instead investigated in a collection of TPs. It is important to highlight that transition patterns -based on the law of "mutual non-overlap" of geographic objects- do not occupy the same location in the scene (Tolpkein & Stein, 2013). It is sometimes useful to present TPs at a more aggregated level, where "pixel" is not the best unit for analyzing recovery map, and pixel-based recovery map is, thereby, perhaps somewhat difficult to grasp. For example, those moments that policymakers need approximate information (spatial analysis) to answer the questions like which part of the city is positively recovered? What is the shortest route of two area assigned as negative recovery? Thus, when the recovery information about coverage, capacity, and connectedness is needed in a city level, the recovery information can be aggregated.

It is also worthwhile to mention that, as there are many TPs which can be selected to create recovery maps, it potentially could be misused and be manipulated. For example, by emphasizing just on the positive side of recovery for larger areas, while highlighting negative recovery for a small subset of the area which potentially can be eliminated in an aggregated map. This misuse of information can also be happened in LC-based recovery map in classes SP and SN (the area of uncertainty), which may give a false insight of recovery status.

Lastly, to portrait the whole procedure of producing the aggregated recovery map, this study reminds the aggregated recovery map is a function of majority filter applied on pixel-based recovery map, and recovery map is a function of post-classification change analysis of the classified map (based on the CF). Each classified map, moreover, is a function of SVM (and related parameters, reference, and trained data, etc.) applied on raw imagery, and each raw imagery is a function of factors defined by image provider. The study is provided an extensive discussion in chapters 5 and 6 about uncertainty in each steps mentioned above and possible solutions for each. However, developing the LCLU-based recovery maps is providing a deeper insight into this complicated process.

## 6.4. Utility of the Number of Imagery in Recovery Assessment

The number of imagery is highly important in RS-based recovery assessment. The optimum number of imagery used in a CF is a trade-off between the purpose of the study, dynamic activity of the area, and analysis practicality. A 3-time-based framework provides a basic recovery insight of the region. An interesting area to illustrate different "recovery rate" (dynamic of the recovery process) is Santa Elena (Figure 6-3 (A)) in the North part of Tacloban city. TP grass-grass-FBA (2 months pre-disaster, disaster time, 40 months post-disaster; -02, 00, +40, respectively) (Figure 6-3 B), can exemplify a 3-time-based framework. However, this TP shows a very steep change 40 months after the typhoon where the recovery progression is neglected. Thus, the area with a high recovery rate requires more than 3-time-based framework to cover the recovery evolution which in this example could be an 8-time-based framework ranging from 2 months before the disaster (T0) to 40 months after the disaster (T7) (Figure 6-3 B). The recovery rate varies project by project due to many issues such as policy and finance. An interesting example of this is the different recovery rates of project C compare to project B (Figure 6-3), which are only 500 meters apart from each other. Although images were taken at the same time, clearly the recovery rate is totally different, suggesting a 4-time based framework for project C (-02, 00, +21, +40).

In the vegetation related recovery analysis, to understand the change in post-disaster situation, it is better first to understand the change in pre-disaster situation, where "grass" can be differentiated from "crop". The greenness (amount of biomass) in grassland varies gently throughout the year, whereas the changes of greenness in the crop are sinusoidal (Homolová et al., 2013). Ideally, acquiring 2 images from the start and the end of the dry season (for pre- and post-disaster situation) would help to differentiate grass from the crop, when at the end of the dry season crops are cultivated, and lands are being prepared for next crop. In this way, crops can be differentiated from grass which is still green. Therefore, ideally, a 5-time-based framework is suggested in a way that images were taken from the start and the end of the dry season which is correlated to the harvesting pattern of the crop (pre-event1, pre-event2, event, post-event1, post-event2).

## 6.5. Utility of Practical Guide

A set of indicators were categorized based on their practicalities and utiliti in the RS-based recovery assessment under "macro", "meso", and "micro" indicators. The relationship between the set of indicators and the aggregation method was inspected via the related tables usiesng a practical guide. The extracted information would then be used for detecting and analyzing meso and macro indicators. Meso indicators would support RS-based recovery assessment methodologies, while still holding rooms for improvement in terms of completeness and quality assessment of the indicators. For example, one can comprehensively investigate the utility of indicators from a wider range of disciplines in the recovery context. Most important is that the key reference is provided for each indicator which can help researchers to explore the capability of them.

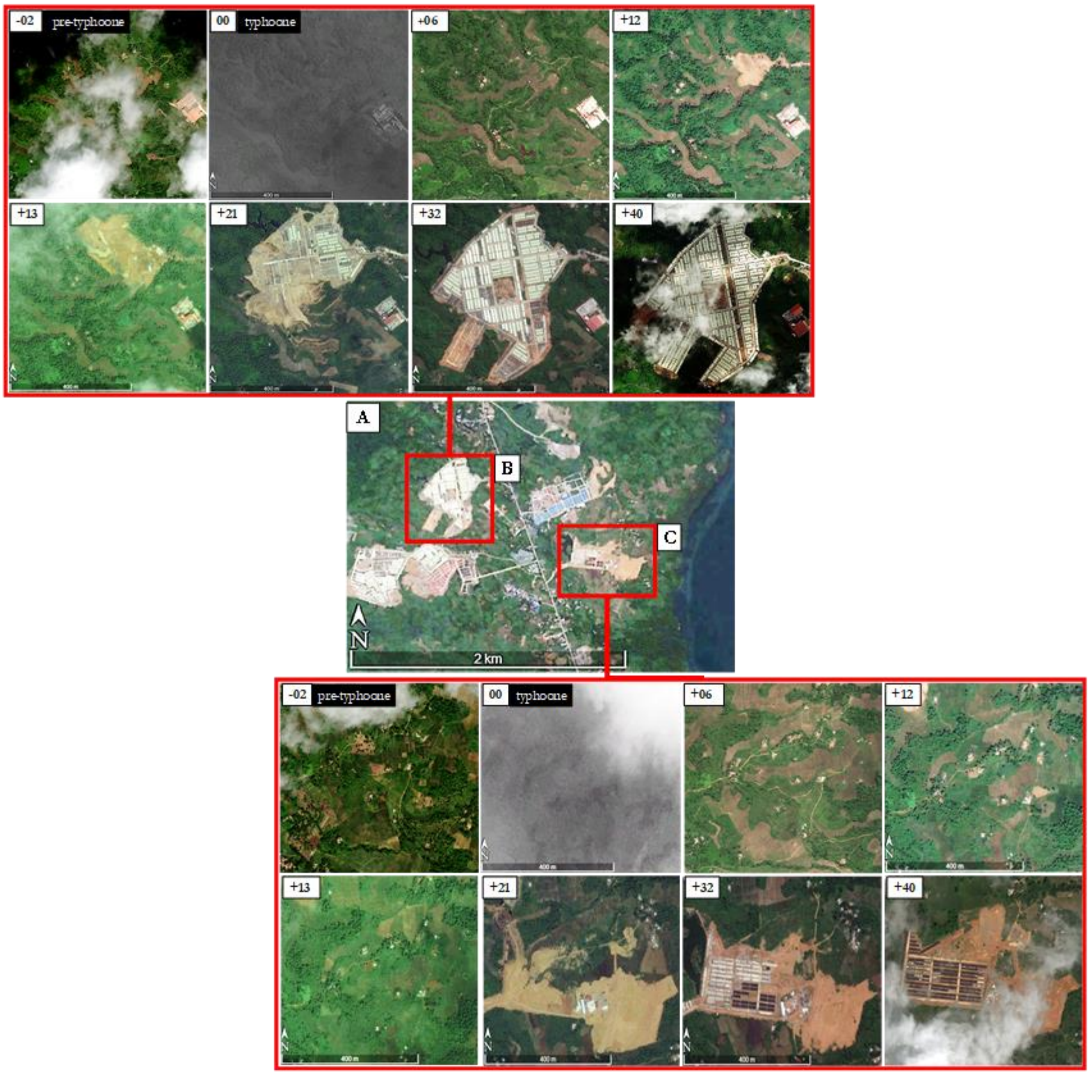


Figure 6-3 (A) Recovery projects after typhoon Haiyan at Santa Elena in the North part of Tacloban city; (B) project with high recovery rate; (C) project with low recovery rate; both projects are shown in 8-time-span ranging from; 2 months pre-typhoon (-02) to 40 months post-typhoon (+40).

## 6.6. Final Remarks

Key insights that were evident in the course of this research are discussed. LCLU information is very promising evidence, especially in the analysis of satellite imagery. Several limitations were identified which mainly were concerned with efficiency and probable solutions suggested. In addition to this, strategies to advance the accuracy of the classification and quality of the maps need to be explored. In next chapter, the conclusion will be drawn, and some suggestions will be given.

# 7. CONCLUSION

LCLU information extracted from satellite imagery is widely used in the RS disciplines. However, the value of this information in the recovery context has not yet been explored. The principal purpose of this study was to understand post-disaster recovery through LCLUC specifically through RS over large areas and to understand the value and utility of LCLU-derived information from RS in post-disaster recovery assessment (urban-rural setting). The available data were 3 WV2 images from 8 months before, right after, and 4 years after typhoon Haiyan in Tacloban city in the Philippines. A methodology was developed based on a generic conceptual framework, comprised of transition patterns to characterize different recovery statuses. Moreover, for classification purposes, SVM was employed, and a detailed comparison of the performance of linear- and RBF-based SVM relying on the various setting of hand crafted features (GLCM, LBP, spectral indices) was conducted. The best combination of SVM with image features (SVM+GLCM+NDVI2, SVM+LBP+NDVI2) was applied in 3 time-span images in order to produce LCLU maps. The LCLU maps were stacked and, based on the developed CF different TPs from the stacked LC and LU maps were extracted. The final products were referred as LC- and LU-based recovery maps which further were up-scaled to a region level.

The developed CF introduces a nuanced definition of recovery statuses based on TPs, which were categorized into five groups: positive, slightly positive, neutral, slightly negative, and negative recovery. Based on the definition and evolving understanding of this study, it is understood that recovery information is a geographic phenomenon and related transition patterns are geographic objects. Moreover, it is found that some TPs can specifically characterize short- and some long-term recovery.

Furthermore, the conducted experiments showed that SVM relying on GLCM+NDVI2 features resulted in high LC classification accuracy with an overall accuracy of 89.4%, 82.2%, 90.8% for T0, T1, and T2 respectively. SVM relying on LBP+NDVI2, moreover, resulted in an acceptable LU classification accuracy with an overall accuracy of 76.3%, 69.9%, 77.8% for T0, T1, and T2 respectively. In both LCLU maps, the least accuracies were belonged to the event time. In general, the quality of the LC maps was better than LU maps. The main uncertainty in LU maps was due to the misclassification in the vegetation related classes. Overall, results showed that well designed hand-crafted features could show competitive performance in a complex task involving classes from simple and small to abstract and big in terms of complexity and size, respectively. However, more investigation is needed when it comes to vegetation related classes in "use" level.

In this thesis, it was found that the characteristic of the post-Haiyan recovery in Tacloban city can be explained through the LCLUC information. By the result of this study, in both LC- and LU-based recovery maps, it was observed that 168 ha of the area was positively recovered, while 69 ha was assigned as negative recovery. Positive recovery was mainly related to the recovery projects were in part effective to build back the damaged area and build impervious surfaces back better. However, the recovery project fails where IBA has rebuilt again along the coastline and crop types was increased (as they had to be decreased in CLP). Thereby the study suggests reviewing land use policy and considering slum area in the planning and land readjustment projects in order to strengthen the resilience of Tacloban city. However, to achieve successful readjustment projects such as slum relocation, the location of the new settlement and award of compensation in the presence of strong leadership and active participation of community members (Hong & Brain, 2012; Viratkapan & Perera, 2006) should be considered in the CLP. Thus, resilience should be used in the land use planning where bottom-up participation of affected people should be well-adjusted with regards to the top down regularization.

Additionally, it was understood that the general understanding of the recovery could be provided by LC-based recovery map and LC information, which are easier to produces and normally have high accuracy. LC-based recovery map can give planners the basic idea of how recovery and reconstruction planning could entirely consider the pre-disaster situation and deal with the dramatically changed situation after the event, however the area of uncertainty in the LC-based recovery map (SN, SP) require more information to be further precisely characterized. LU information and LU-based recovery map are not necessarily effective in the early stage of the recovery process. However, smart use of LU information can effectively improve the understanding of the recovery in medium- to the long-term recovery phase. It is recommended that not to use LU information in the whole study area, but only in the area of uncertainty (which is a derivative of LC-based recovery map) as creating it, is also expensive and less accurate specifically over large areas. With doing so, a robust recovery map can be created. Moreover, the impact of the level of aggregation was investigated. The result suggested that stakeholders can use a pixel-based recovery map within a neighborhood level, while policymakers need a more summary of information where isolated pixels can be avoided, thus a region-based recovery map is more desirable for them.

The other finding was regard to the optimum number of imagery used in a CF, which is a trade-off between the purpose of the study, dynamic activity of the area, and analysis practicality. A 3-time-based framework provides an initial recovery (assessment) insight of the region. However, it can potentially neglect recovery progression for the region with high recovery rate or recovery for specific LU, function, and neighborhood. Thus, a 5-time-based framework is suggested when an overall assessment of the area (for instance Tacloban city) is required. The timing of these 5 imagery should be adjusted with regards to the recovery rate. However, as recovery rate for the different area is different, an adaptive approach can be employed to cover different recovery activities. Meaning that, a region with high recovery rate should employ more than 5-time-based and region with low recovery rate should employ 3-time-based framework, which in the former it should be less than 10-time-based due to practically issues (operational, time, and cost). The other added value of a 5-time-based framework is that for hazard-prone areas such as the Philippines, it can, cover not only large natural disasters but also the minor ones which happen frequently. This study recommends, in order to understand the changes in vegetation recovery in a post-disaster situation, it is better first to understand the change in pre-disaster situation. Thus a 5-time-based framework is suggested for vegetation recovery assessment in a way that two images relate to the pre-disaster situation and two for post-disaster (in the start and the end of dry season) and one for the event time. The other added value of this timing is that for tropical countries such as the Philippines there are more chances to acquire cloud-free images which are highly important.

The other important objective of this study was to investigate how existing indicators previously proposed by the recovery community can be linked with RS data and techniques. The study provides 3 tables, where all relevant indicators grouped based their utilities in the recovering community ranging from low and medium to high; micro, meso, and macro indicators respectively.

Overall, LCLU information is two of the indicators to understand recovery (among many). It is shown that they are capable of providing from a basic (LC) understanding to a more deeper insight (LU) of the recovery process, while also LC and LU could reveal physical and functional recovery, respectively. However, this information cannot cover whole aspects of the recovery process (Figure 6-2). Therefore, LCLU can be combined with other data to provide a full view of the recovery process. This can be achieved by the proposed CF in Figure 7-1.

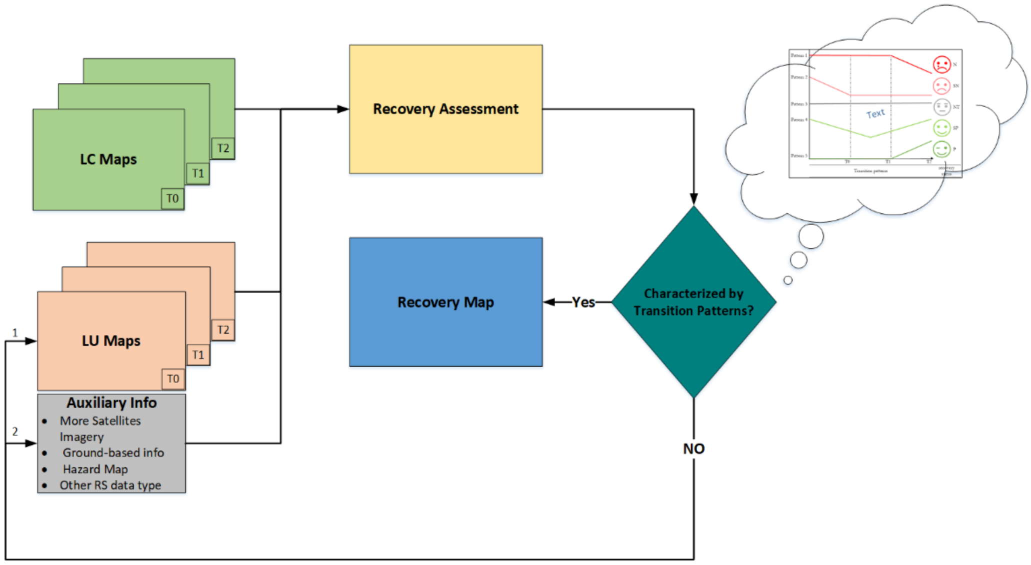


Figure 7-1 Proposed framework of combined information

## 7.1. Recommendations and Future Works

The recommended future works are following:

- Investigate the capacity of crowd sourced information to validate LCLU maps as well as recovery maps in the absence of fieldwork data which is time-money consuming.
- Investigate the value of transfer learning to directly train a classifier for automatic recovery characterization.
- Investigate the optimal number of imagery can be used in the recovery assessment and to characterize the situation which that optimal number of imagery is based on.
- Investigating transferability of the developed conceptual framework in other geographical regions.
- Investigate the potential of a region-based recovery map based on a region-based classification approach.
- Examine the value of providing a 3-D recovery map in order to get a full view of the recovery process, where 2-D recovery map can be LCLUC information (X, Y), and Z value would be in-situ based information (could be potentially provided by citizen-powered information).
- To improve the understanding of transitions patterns and their related recovery statuses developed in this study in order to enhance the concept of BBB mentioned in the Sendai framework (UNISDR, 2015b).

# LIST OF REFERENCES

Adriano, B., Mas, E., & Koshimura, S. (2015). Buildings damage due to the 2013 Haiyan Typhoon inferred from SAR intensity images. *Proceedings of the 2015 IEEE 5th Asia-Pacific Conference on Synthetic Aperture Radar, APSAR 2015*, 667–671. https://doi.org/10.1109/APSAR.2015.7306294

Ahlqvist, O., & Gahegan, M. (2005). Probing the Relationship Between Classification Error and Class Similarity. *Photogrammetric Engineering & Remote Sensing*, *71*(12), 1365–1373. https://doi.org/10.14358/PERS.71.12.1365

Ahmed, I. (2014). Factors in building resilience in urban slums of Dhaka, Bangladesh. *Procedia Economics and Finance*, *18*(September), 745–753. https://doi.org/10.1016/S2212-5671(14)00998-8

Alexander, D. (2013). Resilience and disaster risk reduction: An etymological journey. *Natural Hazards and Earth System Sciences*, *13*(11), 2707–2716. https://doi.org/10.5194/nhess-13-2707-2013

Ali, I., Greifeneder, F., Stamenkovic, J., Neumann, M., & Notarnicola, C. (2015). Review of machine learning approaches for biomass and soil moisture retrievals from remote sensing data. *Remote Sensing*, *7*(12), 16398–16421. https://doi.org/10.3390/rs71215841

Arastounia, M. (2015). Automated recognition of railroad infrastructure in rural areas from LIDAR data. *Remote Sensing*, *7*(11), 14916–14938. https://doi.org/10.3390/rs71114916

Banba, M., & Shaw, R. (2017). *Land Use Management in Disaster Risk Reduction*. *Land Use Management in Disaster Risk Reduction Practice and Cases from a Global Prespective*. Kobe , Japan: Springer Japan 2017. https://doi.org/10.1007/978-4-431-56442-3 ISSN

Berke, P. R., Kartz, J., & Wenger, D. (1993). Recovery after Disaster: Achieving Sustainable Development, Mitigation and Equity. *Disasters*. https://doi.org/10.1111/j.1467-7717.1993.tb01137.x

Bolin, R. C. (1994). *Household and community recovery after earthquakes*. Colorado: Institute of Behavioral Science, University of Colorado.

Bolin, R. C., & Bolton, P. A. (1983). *Recovery in Nicaragua and the USA*. International Journal of Mass Emergencies and Disasters.

Brown, D., Platt, S., & Bevington, J. (2010). *Disaster Recovery Indicators* (First edit). CURBE, Cambridge University Centre for Risk in the Built Environment. Retrieved from http://www.pacificdisaster.net/pdnadmin/data/original/Disaser_Recovery_Indicators.pdf

Brown, D., Platt, S., Bevington, J., Saito, K., Adams, B., Chenvidyakarn, T., … Spence, R. (2009). Monitoring and Evaluating Post-Disaster Recovery Using High-Resolution Satellite Imagery – Towards Standardised Indicators for Post-Disaster Recovery Reference :, (March).

Brown, D., Saito, K., Liu, M., Spence, R., So, E., & Ramage, M. (2012). The use of remotely sensed data and ground survey tools to assess damage and monitor early recovery following the 12.5.2008 Wenchuan earthquake in China. *Bulletin of Earthquake Engineering*, *10*(3), 741–764. https://doi.org/10.1007/s10518-011-9318-7

Brown, D., Saito, K., Spence, R., Chenvidyakarn, T., Adams, B., Mcmillan, A., & Platt, S. (2008). Indicators for Measuring, Monitoring and Evaluating Post-Disaster Recovery. *6th International Workshop on Remote Sensing for Disaster Applications*, (4), 1–8.

Brown, M., Gunn, S. R., & Lewis, H. G. (1999). Support vector machines for optimal classification and spectral unmixing. *Ecological Modelling*, *120*(2–3), 167–179. https://doi.org/10.1016/S0304-3800(99)00100-3

Brunner, D., Lemoine, G., Bruzzone, L., & Greidanus, H. (2010). Building height retrieval from VHR SAR imagery based on an iterative simulation and matching technique. *IEEE Transactions on Geoscience and Remote Sensing*, *48*(3 PART2), 1487–1504. https://doi.org/10.1109/TGRS.2009.2031910

Bruzzone, L., & Persello, C. (2009). Approaches based on support vector machines to classification of remote sensing data. In *Handbook of Pattern Recognition and Computer Vision* (pp. 329–352). Trento: Dept. of Information Engineering and Computer Science,.

Burby, R. J., Beatley, T., Berke, P. R., Deyle, R. E., French, S. P., Godschalk, D. R., … Platt, R. H. (1999). Unleashing the power of planning to create Disaster-Resistant communities. *Journal of the American Planning Association*, *65*(3), 247–258. https://doi.org/10.1080/01944369908976055

Carpenter, A. (2012). A safe haven from the storm? Disaster recovery and space. *Eighth International Space Syntax Symphosium*.

CDEM. (2005). *A Holistic Framework for Recovery in New Zealand*. Wellington. Retrieved from

www.civildefence.govt.nz
Chan, K. M. A., Shaw, M. R., Cameron, D. R., Underwood, E. C., & Daily, G. C. (2006). Conservation planning for ecosystem services. *PLoS Biology*, *4*(11), 2138–2152. https://doi.org/10.1371/journal.pbio.0040379
Chang, C., & Lin, C. (2011). LIBSVM -- A Library for Support Vector Machines. Retrieved January 8, 2018, from https://www.csie.ntu.edu.tw/~cjlin/libsvm/
Chang, S. E. (2010). Urban disaster recovery: A measurement framework and its application to the 1995 Kobe earthquake. *Disasters*, *34*(2), 303–327. https://doi.org/10.1111/j.1467-7717.2009.01130.x
Chang, S. E., & Falit-Baiamonte, A. (2002). Disaster vulnerability of businesses in the 2001 Nisqually earthquake. *Environmental Hazards*, *4*(2–3), 59–71. https://doi.org/10.1016/S1464-2867(03)00007-X
Chang, S. E., & Miles, S. B. (2004). The Dynamics of Recovery: A Framework. In Y. Okuyama & S. E. Chang (Eds.), *Modeling Spatial and Economic Impacts of Disasters* (pp. 181–204). Berlin, Heidelberg: Springer Berlin Heidelberg. https://doi.org/10.1007/978-3-540-24787-6_10
CLP. (2016a). *Tacloban City Comprehensive Land Use Plan*. Tacloban.
CLP. (2016b). *Volume 1 -The Comprehensive Land Use Plan of the City of Tacloban*. *Semikron* (Vol. I). https://doi.org/10.1002/ejoc.201200111
Congalton, R. G. (1991). A review of assessing the accuracy of classifications of remotely sensed data. *Remote Sensing of Environment*, *37*(1), 35–46. https://doi.org/10.1016/0034-4257(91)90048-B
Coppola, D. P. (2011). Recovery. *Introduction to International Disaster Management*, 377–423. https://doi.org/10.1016/B978-0-12-382174-4.00007-0
Coppola, D. P. (2015). The Management of Disasters. In A. Chester (Ed.), *Introduction to International Disaster Management* (2nd ed., pp. 1–39). Burlington: 2011 Elsevier Inc. https://doi.org/10.1016/B978-0-12-801477-6.00001-0
CRED. (2014). *Centre for Research on Epidemiology of Disasters (CRED) for the Period: 2005– 2014*. Retrieved from http://www.cred.be/
Curtis, A., Duval-Diop, D., & Novak, J. (2010). Identifying Spatial Patterns of Recovery and Abandonment in the Post-Katrina Holy Cross Neighborhood of New Orleans. *Cartography and Geographic Information Science*, *37*(January 2015), 45–56. https://doi.org/10.1559/152304010790588043
Cutter, S. L. (2016). The landscape of disaster resilience indicators in the USA. *Natural Hazards*, *80*(2), 741–758. https://doi.org/10.1007/s11069-015-1993-2
Deville, P., Linard, C., Martin, S., Gilbert, M., Stevens, F. R., Gaughan, A. E., … Nordhaus, W. D. (2014). Using luminosity data as a proxy for economic statistics. *Proceedings of the National Academy of Sciences*, *108*(45), 8589–8594. https://doi.org/10.1073/pnas.1408439111
Dhumal, R. K., Vibhute, A. D., Nagne, A. D., Rajendra, Y. D., Kale, K. V, & Suresh, C. (2015). Advances in Classification of Crops using Remote Sensing Data. *International Journal of Advanced Remote Sensing and GIS*, *4*(1), 1410–1418. https://doi.org/10.23953/cloud.ijarsg.130
Dong, X. (2012). *Post-disaster recovery planning and sustainable development – a lesson from the Wenchuan earthquake, China, 2008*. University of Illinois, MSc thesis.
Duro, D. C., Franklin, S. E., & Dubé, M. G. (2012). A comparison of pixel-based and object-based image analysis with selected machine learning algorithms for the classification of agricultural landscapes using SPOT-5 HRG imagery. *Remote Sensing of Environment*, *118*, 259–272. https://doi.org/10.1016/j.rse.2011.11.020
Ebert, A., Kerle, N., & Stein, A. (2009). Urban social vulnerability assessment with physical proxies and spatial metrics derived from air- and spaceborne imagery and GIS data. *Natural Hazards*, *48*(2), 275–294. https://doi.org/10.1007/s11069-008-9264-0
Ella, L. P. A., & Wyk, B. J. Van. (2008). A COMPARISON OF TEXTURE FEATURE ALGORITHMS FOR URBAN SETTLEMENT French South African Technical Institute in Electronics Tshwane University of Technology Pretoria , South Africa Remote Sensing Research Unit Meraka Institute Pretoria , South Africa. *Building*, *1*(c), 1308–1311.
Elvidge, C. D., Zhizhin, M., Baugh, K., & Hsu, F. C. (2015). Automatic boat identification system for VIIRS low light imaging data. *Remote Sensing*, *7*(3), 3020–3036. https://doi.org/10.3390/rs70303020
EPC. (2004). Participatory Planning Guide for Post-Disaster Reconstruction. *EPC-Environmental Planning Collaborative, TCG International, LLC*, (January), 1–22. https://doi.org/10.1111/j.1467-7717.1977.tb00024.x
Erener, A., & Technologies, G. I. (2009). A methodology for land use change detection of high resolution pan images based on texture analysis. *Italian Journal of Remote Sensing*, *41*(2), 47–59.

https://doi.org/10.5721/ItJRS20094124

Evangelista, A. (2015). *Recovery from Typhoon Haiyan : Two Years After Pacific Typhoon Belt*. Danang, Vietnam. Retrieved from http://www.recoveryplatform.org/outfile.php?id=1237&href=http://www.recoveryplatform.org/assets/publication/Publication2015/Recovery from Typhoon Haiyan_2015.pdf

Evgeniou, T., Pontil, M., & Poggio, T. A. (2000). Regularization Networks and Support Vector Machines. *Advanced in Computational Mathematics*, 53. https://doi.org/10.1023/A:1018946025316

Fiksel, J. (2003). Designing Resilient, Sustainable Systems. *Environmental Science and Technology*, *37*(23), 5330–5339. https://doi.org/10.1021/es0344819

Foerstnow, L. P. (2017). *Functional post-disaster damage assessment in urban setting with remote sensing*. University of Twente, MSc Thesis.

Foody, G. M. (2002). Status of land cover classification accuracy assessment. *Remote Sensing of Environment*, *80*(1), 185–201. https://doi.org/10.1016/S0034-4257(01)00295-4

Foody, G. M., & Mathur, A. (2004). Toward intelligent training of supervised image classifications: Directing training data acquisition for SVM classification. *Remote Sensing of Environment*, *93*(1–2), 107–117. https://doi.org/10.1016/j.rse.2004.06.017

French, S. P., Feser, D., & Peacock, W. G. (2008). *Mid-America Earthquake Center Project SE-2*. University of Illinois at Urbana-Champaign.

Gedrange, C., Beger, R., Neubert, M., & Hecht, R. (2011). Extraction of railroad infrastructure objects from extremely high resolution aerial imagery and LiDAR data. *2nd European LiDAR Mapping Forum (ELMF)*.

Gevaert, C. M., Persello, C., Sliuzas, R., & Vosselman, G. (2016). Classification of Informal Settlements Through the Integration of 2D and 3D Features Extracted From Uav Data. *ISPRS Annals of Photogrammetry, Remote Sensing and Spatial Information Sciences*, *III-3*(July), 317–324. https://doi.org/10.5194/isprsannals-III-3-317-2016

Gevaert, C. M., Persello, C., & Vosselman, G. (2016). Optimizing multiple kernel learning for the classification of UAV data. *Remote Sensing*, *8*(12). https://doi.org/10.3390/rs8121025

Ghaffarian, S. (2016). *Post-disaster recovery assessment using remote sensing data analysis and spatial economic modeling*. Faculty of Geo-Information Science and Earth Observation (ITC) of the University of Twente Enschede, The Netherlands.

Giri, C. P. (2012). *Remote Sensing of Land Use and Land Cover;Principles and Application*. (C. P. Giri, Ed.). Indiana: Taylor & Francis Group. Retrieved from http://www.crcpress.com

Gong, X., Marklund, L. G., & Tsuji, S. (2009). Land Use Classification. *14th Meeting of the London Group on Environmental Accounting*, (April), 18. Retrieved from http://unstats.un.org/unsd/envaccounting/londongroup/meeting14/LG14_10a.pdf

Graesser, J., Cheriyadat, A., Vatsavai, R. R., Chandola, V., Long, J., & Bright, E. (2012). Image based characterization of formal and informal neighborhoods in an urban landscape. *IEEE Journal of Selected Topics in Applied Earth Observations and Remote Sensing*, *5*(4), 1164–1176. https://doi.org/10.1109/JSTARS.2012.2190383

Greene, M. (1993). Planning for Earthquakes: Risk, Politics and Policy. *Earthquake Spectra*, *9*(1), 157–159. https://doi.org/10.1193/1.1585710

Haas, J. E., Kates, R. W., & Bowden, M. J. (1977). Reconstruction Following Disaster. In 1977. Haas, J. E., R. W. Kates, and M. J. Bowden (eds.) (Ed.) (Vol. 8, pp. 327–339). The MIT Press.

Hagelman, R., Connolly, M. H., Zavar, E. M., & Khila, R. (2012). Disaster reconstruction and business geography following the 2007 Greensburg , Kansas Tornado Disaster reconstruction and business geography following the 2007 Greensburg , Kansas Tornado. *Environmental Hazards*, *7891*(December). https://doi.org/10.1080/17477891.2012.689249

Hamedianfar, A., & Shafri, H. Z. M. (2015). Detailed intra-urban mapping through transferable OBIA rule sets using WorldView-2 very-high-resolution satellite images. *International Journal of Remote Sensing*, *36*(13), 3380–3396. https://doi.org/10.1080/01431161.2015.1060645

Hansen, M. C., & Reed, B. (2000). A comparison of the IGBP DISCover and university of maryland 1 km global land cover products. *International Journal of Remote Sensing*, *21*(6–7), 1365–1373. https://doi.org/10.1080/014311600210218

Herold, M., Clarke, K. C., Hoppen, S., Gaydos, L., Marcotullio, P. J., Hughes, S., … Clarke, K. C. (2014). The role of spatial metrics in the analysis and modeling of urban land use change. *Computers, Environment and Urban Systems*, *24*(4), 369–399. https://doi.org/10.1016/j.compenvurbsys.2003.12.001

Herold, M., Gardner, M. E., & Roberts, D. a. (2003). Spectral resolution requirements for mapping urban areas. *IEEE Transactions on Geoscience and Remote Sensing*, *41*(9), 1907–1919. https://doi.org/10.1109/TGRS.2003.815238

Herold, M., Mayaux, P., Woodcock, C. E., Baccini, A., & Schmullius, C. (2008). Some challenges in global land cover mapping: An assessment of agreement and accuracy in existing 1 km datasets. *Remote Sensing of Environment*, *112*(5), 2538–2556. https://doi.org/10.1016/j.rse.2007.11.013

Hirayama, Y. (2000). Collapse and Reconstruction: Housing Recovery Policy in Kobe after the Hanshin Great Earthquake. *Housing Studies*, *15*(1), 111–128. https://doi.org/10.1080/02673030082504

Homolová, L., Malenovský, Z., Clevers, J. G. P. W., García-Santos, G., & Schaepman, M. E. (2013). Review of optical-based remote sensing for plant trait mapping. *Ecological Complexity*, *15*, 1–16. https://doi.org/10.1016/j.ecocom.2013.06.003

Hong, Y.-H., & Brain, I. (2012). Land readjustment for urban development and post-disaster reconstruction. *Land Lines, Lincoln Institute of Land Policy*, *24*, 2–9. https://doi.org/10.1016/j.cities.2018.01.009

Horney, J., Aminto, M., Berke, P., & Smith, G. (2016). Developing indicators to measure post- disaster community recovery in the United States. *Disasters*, *41*(i), 124–149. https://doi.org/10.1111/disa.12190

Hsu, C., Chang, C., & Lin, C. (2016). A Practical Guide to Support Vector Classification. *Computers & Geosciences*, *1*(1), 1–16. Retrieved from http://www.csie.ntu.edu.tw/~cjlin

Huifeng, J., & Aigong, X. (2008). the Method of Warehouse Location Selection Based on Gis and Remote Sensing Images. *Proceedings of the International Archives of the Photogrammetry, Remote Sensing and Spatial Information Sciences, XXXVII. Part B 2*, (3), 545–548.

Hussain, M., Chen, D., Cheng, A., Wei, H., & Stanley, D. (2013). Change detection from remotely sensed images: From pixel-based to object-based approaches. *ISPRS Journal of Photogrammetry and Remote Sensing*, *80*, 91–106. https://doi.org/10.1016/j.isprsjprs.2013.03.006

Iuchi, K., & Olshansky, R. (2017). Revisiting Tohoku's 5-Year Recovery: Community Rebuilding Policies, Programs and Implementation BT - The 2011 Japan Earthquake and Tsunami: Reconstruction and Restoration: Insights and Assessment after 5 Years. In V. Santiago-Fandiño, S. Sato, N. Maki, & K. Iuchi (Eds.) (pp. 91–111). Cham: Springer International Publishing. https://doi.org/10.1007/978-3-319-58691-5_6

Jansen, L. J. M., & Gregorio, A. Di. (2002). Parametric land cover and land-use classifications as tools for environmental change detection. *Agriculture, Ecosystems and Environment*, *91*(1–3), 89–100. https://doi.org/10.1016/S0167-8809(01)00243-2

Jiang, W.-G., Jia, K., Wu, J.-J., Tang, Z.-H., Wang, W.-J., & Liu, X.-F. (2015). Evaluating the Vegetation Recovery in the Damage Area of Wenchuan Earthquake Using MODIS Data. *Remote Sensing*, *7*(7), 8757–8778. https://doi.org/10.3390/rs70708757

Johansen, K., Sohlbach, M., Sullivan, B., Stringer, S., Peasley, D., & Phinn, S. (2014). Mapping banana plants from high spatial resolution orthophotos to facilitate plant health assessment. *Remote Sensing*, *6*(9), 8261–8286. https://doi.org/10.3390/rs6098261

Johnson, L. A. (2012). Synthesis Efforts in Disaster Recovery Research. *International Journal of Mass Emergencies and Disasters*, *30*(2), 212–238.

Joyce, K. E., Belliss, S. E., Sergey, V., Mcneill, S. J., & Glassey, P. J. (2009). A review of the status of satellite remote sensing and image processing techniques for mapping natural hazards and disasters. *Progress in Physical Geography*, *33*(2), 183–207. https://doi.org/10.1177/0309133309339563

Joyce, K., Wright, K., & Samsonov, S. (2009). Remote sensing and the disaster management cycle. Advances in Geoscience and Remote Sensing. In *Advances in Geoscience and Remote Sensing*. https://doi.org/10.5772/8341

Kaiser, G., Burkhard, B., Römer, H., Sangkaew, S., Graterol, R., Haitook, T., … Sakuna-Schwartz, D. (2013). Mapping tsunami impacts on land cover and related ecosystem service supply in Phang Nga, Thailand. *Natural Hazards and Earth System Sciences*, *13*(12), 3095–3111. https://doi.org/10.5194/nhess-13-3095-2013

Karen E. Joyce, Kim C. Wright, S. V. S. and V. G. A. (2009). Remote sensing and the disaster management cycle. *Advances in Geoscience and Remote Sensing*, (January 2009), 317–346.

Keck, M., & Sakdapolrak, P. (2013). What is social resilience? lessons learned and ways forward. *Erdkunde*, *67*(1), 5–19. https://doi.org/10.3112/erdkunde.2013.01.02

Kerle, N. (2016). Disasters: Risk Assessment, Management, and Post-Disaster Studies Using Remote Sensing. In N. Kerle (Ed.), *Remote Sensing of Water Resources, Disasters, and Urban Studies* (pp. 455–477).

Enschede: Taylor & Francis. Retrieved from http://taylorandfrancis.com/

Khan, M. A. U., & Sayem, M. A. (2013). Understanding recovery of small enterprises from natural disaster. *Environmental Hazards*, *12*(3–4), 218–239. https://doi.org/10.1080/17477891.2012.761593

Khan, M. M. H., Bryceson, I., Kolivras, K. N., Faruque, F., Rahman, M. M., & Haque, U. (2014). Natural disasters and land-use/land-cover change in the southwest coastal areas of Bangladesh. *Regional Environmental Change*, *15*(2), 241–250. https://doi.org/10.1007/s10113-014-0642-8

Kohli, D. (2015). *Identifying and classifying slum areas using remote sensing (Doctoral dissertation)*. ITC Printing Department Copyright, Enschede. https://doi.org/10.3990/1.9789036540087

Kohli, D., Stein, A., & Sliuzas, R. (2016). Uncertainty analysis for image interpretations of urban slums. *Computers, Environment and Urban Systems*, *60*, 37–49. https://doi.org/10.1016/j.compenvurbsys.2016.07.010

Kuffer, M., Barros, J., & Sliuzas, R. V. (2014). The development of a morphological unplanned settlement index using very-high-resolution (VHR) imagery. *Computers, Environment and Urban Systems*, *48*, 138–152. https://doi.org/10.1016/j.compenvurbsys.2014.07.012

Kuffer, M., Pfeffer, K., & Sliuzas, R. (2016). Slums from space-15 years of slum mapping using remote sensing. *Remote Sensing*, *8*(6). https://doi.org/10.3390/rs8060455

Kuffer, M., Pfeffer, K., Sliuzas, R., & Baud, I. (2016). Extraction of Slum Areas From VHR Imagery Using GLCM Variance. *IEEE Journal of Selected Topics in Applied Earth Observations and Remote Sensing*, *9*(5), 1830–1840. https://doi.org/10.1109/JSTARS.2016.2538563

Kumar, P., Gupta, D. K., Mishra, V. N., & Prasad, R. (2015). Comparison of support vector machine, artificial neural network, and spectral angle mapper algorithms for crop classification using LISS IV data. *International Journal of Remote Sensing*, *36*(6), 1604–1617. https://doi.org/10.1080/2150704X.2015.1019015

Li, M., Stein, A., Bijker, W., & Zhan, Q. (2016). Urban land use extraction from Very High Resolution remote sensing imagery using a Bayesian network. *ISPRS Journal of Photogrammetry and Remote Sensing*, *122*, 192–205. https://doi.org/10.1016/j.isprsjprs.2016.10.007

Lin, C., Wu, C. C., Tsogt, K., Ouyang, Y. C., & Chang, C. I. (2015). Effects of atmospheric correction and pansharpening on LULC classification accuracy using WorldView-2 imagery. *Information Processing in Agriculture*, *2*(1), 25–36. https://doi.org/10.1016/j.inpa.2015.01.003

Lin, P., & Wang, N. (2017). Stochastic post-disaster functionality recovery of community building portfolios II: Application. *Structural Safety*, *69*, 106–117. https://doi.org/10.1016/j.strusafe.2017.05.004

Lindell, M. K. (2013). Encyclopedia of Natural Hazards. In P. T. Bobrowsky (Ed.), *Encyclopedia of Natural Hazards* (pp. 812–824). Texas. https://doi.org/10.1007/978-1-4020-4399-4

Liu, W., Matsuoka, M., Adriano, B., Mas, E., & Koshimura, S. (2014). Damage detection due to the typhoon haiyan from high-resolution SAR images. *International Geoscience and Remote Sensing Symposium (IGARSS)*, 4828–4831. https://doi.org/10.1109/IGARSS.2014.6947575

Lu, D., & Weng, Q. (2007). A survey of image classification methods and techniques for improving classification performance. *International Journal of Remote Sensing*, *28*(5), 823–870. https://doi.org/10.1080/01431160600746456

Mader, G. G., Spangle, W. E., Blair, M. L., Meehan, R. L., Bilodeau, S. W., Degenkolb, H. J., … Williams, N. J. (1980). *Land use planning after earthquakes*. Washington: Office of Planning and Resources Management (OPRM).

Maly, E. (2017). Rethinking "build Back Better" in housing reconstruction: A proposal for "people Centered Housing Recovery." *IOP Conference Series: Earth and Environmental Science*, *56*(1). https://doi.org/10.1088/1755-1315/56/1/012025

Manandhar, R., Odeh, I. O. A., & Ancev, T. (2009). Improving the Accuracy of Land Use and Land Cover Classification of Landsat Data Using Post-Classification Enhancement. *Remote Sensing*, *1*(3), 330–344. https://doi.org/10.3390/rs1030330

Mansaray, L. R., Huang, W., Zhang, D., Huang, J., & Li, J. (2017). Mapping rice fields in urban Shanghai, southeast China, using Sentinel-1A and Landsat 8 datasets. *Remote Sensing*, *9*(3). https://doi.org/10.3390/rs9030257

Mas, E., Bricker, J., Kure, S., Adriano, B., Yi, C., Suppasri, A., & Koshimura, S. (2015). Field survey report and satellite image interpretation of the 2013 Super Typhoon Haiyan in the Philippines. *Natural Hazards and Earth System Sciences*, *15*(4), 805–816. https://doi.org/10.5194/nhess-15-805-2015

Mathur, A., & Foody, G. M. (2008). Crop classification by support vector machine with intelligently selected training data for an operational application. *International Journal of Remote Sensing*, *29*(8), 2227–

2240. https://doi.org/10.1080/01431160701395203

Maxwell, A. E., Warner, T. A., Strager, M. P., Conley, J. F., & Sharp, A. L. (2015). Assessing machine-learning algorithms and image- and lidar-derived variables for GEOBIA classification of mining and mine reclamation. *International Journal of Remote Sensing*, *36*(4), 954–978. https://doi.org/10.1080/01431161.2014.1001086

Mayans, J. (2014). *Food Security and Livelihood Rapid Assessment in inland municipalities of Leyte*. FSL Rapid Assessment Leyte.

Mboga, N. O. (2017). *DETECTION OF INFORMAL SETTLEMENTS FROM VHR SATELLITE IMAGES USING CONVOLUTIONAL NEURAL NETWORKS DETECTION OF INFORMAL SETTLEMENTS FROM VHR SATELLITE IMAGES USING*. University of Twente (ITC), MSc thesis.

Mboga, N., Persello, C., Bergado, J., & Stein, A. (2017). Detection of Informal Settlements from VHR Images Using Convolutional Neural Networks. *Remote Sensing*, *9*(11), 1106. https://doi.org/10.3390/rs9111106

Mejri, O., Menoni, S., Matias, K., & Aminoltaheri, N. (2017). Crisis information to support spatial planning in post disaster recovery. *International Journal of Disaster Risk Reduction*, *22*(June 2016), 46–61. https://doi.org/10.1016/j.ijdrr.2017.02.007

Metzger, M. J., Rounsevell, M. D. A., Acosta-Michlik, L., Leemans, R., & Schröter, D. (2006). The vulnerability of ecosystem services to land use change. *Agriculture, Ecosystems & Environment*, *114*(1), 69–85. https://doi.org/10.1016/j.agee.2005.11.025

Miles, S. B., & Chang, S. E. (2006). Modeling Community Recovery from Earthquakes. *Earthquake Spectra*, *22*(2), 439–458. https://doi.org/10.1193/1.2192847

Miles, S., & Chang, S. E. (2007). A Simulation Model of Urban Disaster Recovery and Resilience: Implementation for the 1994 Northridge Earthquake. *Earthquake Engineering*, 130. Retrieved from c:%5CCS%5Call refs%5Ctechnical%5CMCEER reports%5C07-0014.pdf

Mileti, D. (1999). DISASTERS BY DESIGN. *An Activity of the International Decade for Natural Disaster Reduction*, (1975), 1–16.

Nakabayashi, I. (2014). East Japan Mega Earthquake and Dual Reconstruction Scheme-Regional and National Planning of Post-Disaster and Pre-Disaster Recovery. In *Traditional Wisdom and Modern Knowledge for the Earth's Future: Lectures given at the plenary sessions of the international geographical conference, 2013* (pp. 135–165). https://doi.org/10.1007/978-4-431-54406-7

Ojala, T., Pietikäinen, M., & Mäenpää, T. (2002). Multiresolution gray-scale and rotation invariant texture classification with local binary patterns. *IEEE Transactions on Pattern Analysis and Machine Intelligence*, *24*(7), 971–987. https://doi.org/10.1109/TPAMI.2002.1017623

Olshansky, R. B. (2006). Planning after Hurricane Katrina. *Journal of the American Planning Association*, *72*(2), 147–153. https://doi.org/10.1080/01944360608976735

Olshansky, R. B., Hopkins, L. D., & Johnson, L. A. (2012). Disaster and Recovery: Processes Compressed in Time. *Natural Hazards Review*, *13*(3), 173–178. https://doi.org/10.1061/(ASCE)NH.1527-6996.0000077

Ozdogan, M., Yang, Y., Allez, G., & Cervantes, C. (2010). Remote sensing of irrigated agriculture: Opportunities and challenges. *Remote Sensing*, *2*(9), 2274–2304. https://doi.org/10.3390/rs2092274

Pagot, E., Pesaresi, M., Buda, D., & Ehrlich, D. (2008). Development of an object-oriented classification model using very high resolution satellite imagery for monitoring diamond mining activity. *International Journal of Remote Sensing*, *29*(June 2014), 499–512. https://doi.org/10.1080/01431160601047771

Pal, M., & Foody, G. M. (2010). Feature selection for classification of hyperspectral data by SVM. *IEEE Transactions on Geoscience and Remote Sensing*, *48*(5), 2297–2307. https://doi.org/10.1109/TGRS.2009.2039484

Parsons, M., Glavac, S., Hastings, P., Marshall, G., McGregor, J., McNeill, J., … Stayner, R. (2016). Top-down assessment of disaster resilience: A conceptual framework using coping and adaptive capacities. *International Journal of Disaster Risk Reduction*, *19*, 1–11. https://doi.org/10.1016/j.ijdrr.2016.07.005

Passerini, E. (2000). Disasters as Agents of Social Change in Recovery and Reconstruction. *Natural Hazards Review*. https://doi.org/https://doi.org/10.1061/(ASCE)1527-6988(2000)1:2(67)

Pelizari, P., Spröhnle, K., Geiß, C., Schoepfer, E., Plank, S., & Taubenbock, H. (2017). Multi-sensor feature fusion for very high spatial resolution built-up area extraction in temporary settlements. *Remote Sensing of Environment*.

Persello, C., & Bruzzone, L. (2016). Kernel-Based Domain-Invariant Feature Selection in Hyperspectral Images for Transfer Learning. *IEEE Transactions on Geoscience and Remote Sensing*, *54*(5), 2615–2626.

Philippines, I. (2014). *IOM Philippines - Typhoon Hagupit Response*. Tacloban. Retrieved from http://philippineresponse.iom.int

Pitts, D. A. D. A., & So, E. (2017). Enhanced change detection index for disaster response , recovery assessment and monitoring of accessibility and open spaces ( camp. *International Journal of Applied Earth Observations and Geoinformation*, *57*, 49–60. https://doi.org/10.1016/j.jag.2016.12.004

Platt, S., Brown, D., & Hughes, M. (2016). Measuring resilience and recovery. *International Journal of Disaster Risk Reduction*, *19*(May), 447–460. https://doi.org/10.1016/j.ijdrr.2016.05.006

Platt, S., & Drinkwater, B. D. (2016). Post-earthquake decision making in Turkey: Studies of Van and I˙zmir. *International Journal of Disaster Risk Reduction*, *17*, 220–237. https://doi.org/10.1016/j.ijdrr.2016.03.010

Pontius, R. G., Boersma, W., Castella, J. C., Clarke, K., Nijs, T., Dietzel, C., … Verburg, P. H. (2008). Comparing the input, output, and validation maps for several models of land change. *Annals of Regional Science*, *42*(1), 11–37. https://doi.org/10.1007/s00168-007-0138-2

Rao, P. V. N., Sai, M. V. R. S., Sreenivas, K., Rao, M. V. K., Rao, B. R. M., Dwivedi, R. S., … Sesha Sai, M. V. R. (2002). International Journal of Remote Sensing Textural analysis of IRS-1D panchromatic data for land cover classification Textural analysis of IRS-1D panchromatic data for land cover classi cation. *International Journal of Remote Sensing Int. J. Remote Sensing*, *2317*(17), 3327–3345. https://doi.org/10.1080/01431160110104665

Rathfon, D., Davidson, R., Bevington, J., Vicini, A., & Hill, A. (2013). Quantitative assessment of post-disaster housing recovery: a case study of Punta Gorda, Florida, after Hurricane Charley. *Disasters*, *37*(2), 333–355. https://doi.org/10.1111/j.1467-7717.2012.01305.x

Richards, J. a, & Jia, X. (2006). *Remote Sensing Digital Image Analysis*. *Methods*. https://doi.org/10.1007/3-540-29711-1

Rodríguez, H., Quarantelli, E. L., & Dynes, R. R. (2007). *Handbook of Disaster Research*. https://doi.org/10.1007/978-0-387-32353-4

Rubin, C. B., Saperstein, M. D., & Barbee, D. G. (1985). Community recovery from a major natural disaster.

Ruiter, M. (2011). *Post-Disaster Community Recovery Linking Environmental and Economic*. THE UNIVERSITY OF BRITISH COLUMBIA,MSc Thesis.

Saito, K., Brown, D., Spence, R., Chenvidyakarn, T., Adams, B., Bevington, J., & Platt, S. (2009). Monitoring and evaluating recovery from natural disasters using remote sensing – towards creating guidelines on the use of satellite images in the context of disaster recovery. *Assembly*, *11*(February).

Salehi, B., Zhang, Y., & Zhong, M. (2011). Combination of object-based and pixel-based image analysis for classification of vhr imagery over urban areas. *American Society for Photogrammetry and Remote Sensing Annual Conference 2011*, (2006), 454–460. Retrieved from http://www.scopus.com/inward/record.url?eid=2-s2.0-84868613965&partnerID=40&md5=f2c756d1a03f5f319f4db065d2a4e134

Santoso, H., Tani, H., & Wang, X. (2016). A simple method for detection and counting of oil palm trees using high-resolution multispectral satellite imagery. *International Journal of Remote Sensing*, *37*(21), 5122–5134. https://doi.org/10.1080/01431161.2016.1226527

Saunders, W. S. A., & Becker, J. S. (2015). A discussion of resilience and sustainability: Land use planning recovery from the Canterbury earthquake sequence, New Zealand. *International Journal of Disaster Risk Reduction*, *14*, 73–81. https://doi.org/10.1016/j.ijdrr.2015.01.013

Shaker, I. F., Abd-Elrahman, A., Abdel-Gawad, A. K., & Sherief, M. A. (2011). Building extraction from high resolution space images in high density residential areas in the Great Cairo region. *Remote Sensing*, *3*(4), 781–791. https://doi.org/10.3390/rs3040781

Sharif Razavian, A., Azizpour, H., Sullivan, J., & Carlsson, S. (2014). CNN Features Off-the-Shelf: An Astounding Baseline for Recognition. *IEEE Computer Society Conference on Computer Vision and Pattern Recognition Workshops*, 806–813. https://doi.org/http://doi.org/10.1109/CVPRW.2014.131

Sliuzas, R. R. V. (2004). *Managing Informal Settlements: A Study Using Geo-Information in Dar es Salaam, Tanzania*. *Urban Planning and Geoinformation Management*.

Song, L., Smola, A., Gretton, A., Bedo, J., & Borgwardt, K. (2012). Feature selection via dependence maximization. *Journal of Machine Learning Research*, *13*, 1393–1434. https://doi.org/10.1145/1273496.1273600

Song, L., Smola, A., Gretton, A., Borgwardt, K. M., & Bedo, J. (2007). Supervised feature selection via dependence estimation. *Proceedings of the 24th International Conference on Machine Learning - ICML '07*, 823–830. https://doi.org/10.1145/1273496.1273600

Song, Y., & Knapp, G.-J. (2004). Song_Measuring urban form - Is Portland winning the war on sprawl.pdf. *Journal of American Planning Asscociation*. https://doi.org/10.1080/01944360408976371

Song, Y., Li, C., Olshansky, R., Zhang, Y., & Xiao, Y. (2017). Are we planning for sustainable disaster recovery? Evaluating recovery plans after the Wenchuan earthquake. *Journal of Environmental Planning and Management*, *60*(12), 2192–2216. https://doi.org/10.1080/09640568.2017.1282346

Statistics, J. of P. (2012). *JOURNAL OF PHILIPPINE STATISTICS*. Manila. https://doi.org/ISSN 0022-3603

Strahler, A. H., Boschetti, L., Foody, G. M., Friedl, M. a., Hansen, M. C., Herold, M., … Woodcock, C. E. (2006). Global Land Cover Validation: Recommendations for Evaluation and Accuracy Assessment of Global Land Cover Maps. *Change*, *48pp*(25), 51. https://doi.org/10.1080/01431160512331326521

Stumpf, A., & Kerle, N. (2011). Combining Random Forests and object-oriented analysis for landslide mapping from very high resolution imagery. *Procedia Environmental Sciences*, *3*, 123–129. https://doi.org/10.1016/j.proenv.2011.02.022

Sutton, P., Elvidge, C., & Ghosh, T. (2007). Estimation of gross domestic product at sub-national scales using nighttime satellite imagery. *International Journal of Ecological Economics & Statistics*, *8*(S07), 5–21. Retrieved from http://urizen-geography.nsm.du.edu/~psutton/AAA_Sutton_WebPage/Sutton/Publications/Sut_Pub_13.pdf

Tacloban Recovery and Sustainable Development Group. (2014). *Proposed Tacloban Recovery and Rehabilitation Plan*. Tacloban.

Takahashi, B., Tandoc, E. C., & Carmichael, C. (2015). Communicating on Twitter during a disaster: An analysis of tweets during Typhoon Haiyan in the Philippines. *Computers in Human Behavior*, *50*, 392–398. https://doi.org/10.1016/j.chb.2015.04.020

Tewkesbury, A. P., Comber, A. J., Tate, N. J., Lamb, A., & Fisher, P. F. (2015). A critical synthesis of remotely sensed optical image change detection techniques. *Remote Sensing of Environment*, *160*, 1–14. https://doi.org/10.1016/j.rse.2015.01.006

Tolpkein, V. A., & A.Stein. (2013). *The core of GIScience: a process-based approach. The core of GIScience: a process-based apprach*. Enschede: University of Twente Faculty of Geo-Information and Earth Observation (ITC).

Tomowski, D., Ehlers, M., & Klonus, S. (2011). Colour and texture based change detection for urban disaster analysis. *2011 Joint Urban Remote Sensing Event, JURSE 2011 - Proceedings*, 329–332. https://doi.org/10.1109/JURSE.2011.5764786

Townshend, I., Awosoga, O., Kulig, J., & Fan, H. Y. (2015). Social cohesion and resilience across communities that have experienced a disaster. *Natural Hazards*, *76*(2), 913–938. https://doi.org/10.1007/s11069-014-1526-4

Uba, N. K. (2016). *Land Use and Land Cover Classification Using Deep Learning Techniques*. ARIZONA STATE UNIVERSITY, MSc thesis.

UNDP. (1993). *Rehabilitation and Reconstruction*. Disaster Management Training Programme (DMTP) in association with the University of Wisconsin Disaster Management Center.

UNDP. (2013). *Livelihoods & Economic Recovery in Crisis Situations*. Retrieved from http://www.undp.org/content/undp/en/home/librarypage/crisis-prevention-and-recovery/guide-on-livelihoods-and- economic-recovery-programming-in-crisis.html

UNISDR. (2009). Terminology on Disaster Risk Reduction. https://doi.org/978-600-6937-11-3

UNISDR. (2015a). Proposed Updated Terminology on Disaster Risk Reduction: A Technical Review. Retrieved May 30, 2017, from http://www.preventionweb.net/english/

UNISDR. (2015b). Sendai Framework for Disaster Risk Reduction 2015 - 2030. *Third World Conference on Disaster Risk Reduction, Sendai, Japan, 14-18 March 2015.*, (March), 1–25. https://doi.org/A/CONF.224/CRP.1

UNOCHA. (2008). *Guidance note on early recovery*.

Vapnik, V. N. (1995). The nature of statistical learning theory. *IEEE Transactions on Neural Networks*, *8*(6), 1564–1564. https://doi.org/10.1109/TNN.1997.641482

Verburg, P. H., van de Steeg, J., Veldkamp, A., & Willemen, L. (2009). From land cover change to land function dynamics: A major challenge to improve land characterization. *Journal of Environmental Management*, *90*(3), 1327–1335. https://doi.org/10.1016/j.jenvman.2008.08.005

Vetrivel, A., Gerke, M., Kerle, N., Nex, F., & Vosselman, G. (2016). Disaster damage detection through synergistic use of deep learning and 3D point cloud features derived from very high resolution oblique aerial images, and multiple-kernel-learning. *ISPRS Journal of Photogrammetry and Remote Sensing*. https://doi.org/10.1016/j.isprsjprs.2017.03.001

Vetrivel, A., Gerke, M., Kerle, N., & Vosselman, G. (2016). Identification of structurally damaged areas in airborne oblique images using a Visual-Bag-of-Words approach. *Remote Sensing*, *8*(3), 1–22. https://doi.org/10.3390/rs8030231

Vetrivel, A., Kerle, N., Gerke, M., & Vosselman, G. (2016). Towards Automated Satellite Image Segmentation and Classification for Assessing Disaster Damage Using Data-Specific Features with Incremental Learning. *GEOB IA 2016 - Solutions & Synergies*.

Viratkapan, V., & Perera, R. (2006). Slum relocation projects in Bangkok: What has contributed to their success or failure? *Habitat International*, *30*(1), 157–174. https://doi.org/10.1016/j.habitatint.2004.09.002

Volpi, M., Tuia, D., Bovolo, F., Kanevski, M., & Bruzzone, L. (2013). Supervised change detection in VHR images using contextual information and support vector machines. *International Journal of Applied Earth Observation and Geoinformation*, *20*, 77–85. https://doi.org/10.1016/j.jag.2011.10.013

Wagner, M. A., Myint, S. W., & Cerveny, R. S. (2012). Geospatial assessment of recovery rates following a tornado disaster. *IEEE Transactions on Geoscience and Remote Sensing*, *50*(11 PART1), 4313–4322. https://doi.org/10.1109/TGRS.2012.2191973

Webb, G. R., Tierney, K. J., & Dahlhamer, J. M. (2000). Businesses and disasters: Empirical patterns and unanswered questions. *Natural Hazards Review*, *1*(2), 83–90. https://doi.org/10.1061/(ASCE)1527-6988(2000)1:2(83)

Wei, H., Zhou, G., & Zhang, Y. (2013). Vehicle detection from parkinglot aerial images. *IEEE Geoscience and Remote Sensing Letters*, *86*(773), 4002–4005.

Weng, Q. (2012). Remote sensing of impervious surfaces in the urban areas: Requirements, methods, and trends. *Remote Sensing of Environment*, *117*, 34–49. https://doi.org/10.1016/j.rse.2011.02.030

Wisner, B., Cannon, T., Davis, I. & Blaikie, P. (2005). *At Risk: Natural Hazards, People's Vulnerability, and Disasters*. *Journal of Homeland Security and Emergency Management* (second, Vol. 2). New York and London: Routledge. https://doi.org/10.2202/1547-7355.1131

Woolf, S., Twigg, J., Parikh, P., Karaoglou, A., & Cheab, T. (2016). Towards measurable resilience: A novel framework tool for the assessment of resilience levels in slums. *International Journal of Disaster Risk Reduction*, *19*, 280–302. https://doi.org/10.1016/j.ijdrr.2016.08.003

Xiao, W., Vallet, B., Schindler, K., & Paparoditis, N. (2016). Street-side vehicle detection, classification and change detection using mobile laser scanning data. *ISPRS Journal of Photogrammetry and Remote Sensing*, *114*, 166–178. https://doi.org/10.1016/j.isprsjprs.2016.02.007

Xie, J., & Zhou, J. (2017). Classification of Urban Building Type from High Spatial Resolution Remote Sensing Imagery Using Extended MRS and Soft BP Network. *IEEE Journal of Selected Topics in Applied Earth Observations and Remote Sensing*, *10*(8), 3515–3528. https://doi.org/10.1109/JSTARS.2017.2686422

Xu, C., Zhang, D., Zhang, Z., & Feng, Z. (2014). BgCut: Automatic ship detection from UAV images. *The Scientific World Journal*, *2014*. https://doi.org/10.1155/2014/171978

Yan, Y., Eckle, M., Kuo, C., Herfort, B., & Fan, H. (2017). Monitoring and Assessing Post-Disaster Tourism Recovery Using Geotagged Social Media Data. *ISPRS International Journal of Geo-Information*, *6*(5), 144. https://doi.org/10.3390/ijgi6050144

Yi, C. J., Suppasri, A., Kure, S., Bricker, J. D., Mas, E., Quimpo, M., & Yasuda, M. (2015). Storm surge mapping of typhoon Haiyan and its impact in Tanauan, Leyte, Philippines. *International Journal of Disaster Risk Reduction*, *13*, 207–214. https://doi.org/10.1016/j.ijdrr.2015.05.007

Yu, H., Liu, S., Guo, S., Hu, Y., Zheng, Z., & She, T. (2012). The impact of catastrophic natural disaster on land-use changes of Qingping town and the selection of suitable land for settlement construction. *Journal of Mountain Science*, *9*(6), 827–834. https://doi.org/10.1007/s11629-012-2370-1

Zakharova, M. (2017). *Automated Coconut Tree Detection In Aerial Imagery Using Deep Learning*. KU Leuven.

Zhang, Y., Zhang, C., Drake, W., & Olshansky, R. (2014). Planning and Recovery Following the Great 1976 Tangshan Earthquake. *Journal of Planning History*, *14*(3), 224–243. https://doi.org/10.1177/1538513214549435

Zorn, C. R., & Shamseldin, A. Y. (2015). International Journal of Disaster Risk Reduction Post-disaster infrastructure restoration : A comparison of events for future planning. *International Journal of Disaster Risk Reduction*, *13*, 158–166. https://doi.org/10.1016/j.ijdrr.2015.04.004

# ANNEX

## Annex 1: A complete list of LC-based transition patterns in the study area

| ID | T0 | T1 | T2 | Transition ID |
|---|---|---|---|---|
| 1 | Building | Building | Building | 111 |
| 2 | Building | Building | Impervious surface | 112 |
| 3 | Building | Building | Bare Land | 113 |
| 4 | Building | Building | Inland Water | 114 |
| 5 | Building | Building | Tree | 115 |
| 6 | Building | Building | Non-Tree (Vegetation) | 116 |
| 7 | Building | Rubble | Building | 181 |
| 8 | Building | Rubble | Impervious surface | 182 |
| 9 | Building | Rubble | Bare Land | 183 |
| 10 | Building | Rubble | Inland Water | 184 |
| 11 | Building | Rubble | Tree | 185 |
| 12 | Building | Rubble | Non-Tree (Vegetation) | 186 |
| 13 | Impervious surface | Impervious surface | Building | 221 |
| 14 | Impervious surface | Impervious surface | Impervious surface | 222 |
| 15 | Impervious surface | Impervious surface | Bare Land | 223 |
| 16 | Impervious surface | Impervious surface | Inland Water | 224 |
| 17 | Impervious surface | Impervious surface | Tree | 225 |
| 18 | Impervious surface | Impervious surface | Non-Tree (Vegetation) | 226 |
| 19 | Impervious surface | Inundated Land | Building | 241 |
| 20 | Impervious surface | Inundated Land | Impervious surface | 242 |
| 21 | Impervious surface | Inundated Land | Bare Land | 243 |
| 22 | Impervious surface | Inundated Land | Inland Water | 244 |
| 23 | Impervious surface | Inundated Land | Tree | 245 |
| 24 | Impervious surface | Inundated Land | Non-Tree (Vegetation) | 246 |
| 25 | Impervious surface | Rubble | Building | 281 |
| 26 | Impervious surface | Rubble | Impervious surface | 282 |
| 27 | Impervious surface | Rubble | Bare Land | 283 |
| 28 | Impervious surface | Rubble | Inland Water | 284 |
| 29 | Impervious surface | Rubble | Tree | 285 |
| 30 | Impervious surface | Rubble | Non-Tree (Vegetation) | 286 |
| 31 | Bare Land | Bare Land | Building | 331 |
| 32 | Bare Land | Bare Land | Impervious surface | 332 |
| 33 | Bare Land | Bare Land | Bare Land | 333 |
| 34 | Bare Land | Bare Land | Inland Water | 334 |
| 35 | Bare Land | Bare Land | Tree | 335 |
| 36 | Bare Land | Bare Land | Non-Tree (Vegetation) | 336 |
| 37 | Bare Land | Inundated Land | Building | 341 |
| 38 | Bare Land | Inundated Land | Impervious surface | 342 |
| 39 | Bare Land | Inundated Land | Bare Land | 343 |

| ID | T0 | T1 | T2 | Transition ID |
|---|---|---|---|---|
| 40 | Bare Land | Inundated Land | Inland Water | 344 |
| 41 | Bare Land | Inundated Land | Tree | 345 |
| 42 | Bare Land | Inundated Land | Non-Tree (Vegetation) | 346 |
| 43 | Bare Land | Rubble | Building | 381 |
| 44 | Bare Land | Rubble | Impervious surface | 382 |
| 45 | Bare Land | Rubble | Bare Land | 383 |
| 46 | Bare Land | Rubble | Inland Water | 384 |
| 47 | Bare Land | Rubble | Tree | 385 |
| 48 | Bare Land | Rubble | Non-Tree (Vegetation) | 386 |
| 49 | Inland Water | Inundated Land | Building | 441 |
| 50 | Inland Water | Inundated Land | Impervious surface | 442 |
| 51 | Inland Water | Inundated Land | Bare Land | 443 |
| 52 | Inland Water | Inundated Land | Inland Water | 444 |
| 53 | Inland Water | Inundated Land | Tree | 445 |
| 54 | Inland Water | Inundated Land | Non-Tree (Vegetation) | 446 |
| 55 | Inland Water | Rubble | Building | 481 |
| 56 | Inland Water | Rubble | Impervious surface | 482 |
| 57 | Inland Water | Rubble | Bare Land | 483 |
| 58 | Inland Water | Rubble | Inland Water | 484 |
| 59 | Inland Water | Rubble | Tree | 485 |
| 60 | Inland Water | Rubble | Non-Tree (Vegetation) | 486 |
| 61 | Tree | Flattened Tree | Building | 551 |
| 62 | Tree | Flattened Tree | Impervious surface | 552 |
| 63 | Tree | Flattened Tree | Bare Land | 553 |
| 64 | Tree | Flattened Tree | Inland Water | 554 |
| 65 | Tree | Flattened Tree | Tree | 555 |
| 66 | Tree | Flattened Tree | Non-Tree (Vegetation) | 556 |
| 67 | Non-Tree (Vegetation) | Non-Tree (Vegetation) | Building | 661 |
| 68 | Non-Tree (Vegetation) | Non-Tree (Vegetation) | Impervious surface | 662 |
| 69 | Non-Tree (Vegetation) | Non-Tree (Vegetation) | Bare Land | 663 |
| 70 | Non-Tree (Vegetation) | Non-Tree (Vegetation) | Inland Water | 664 |
| 71 | Non-Tree (Vegetation) | Non-Tree (Vegetation) | Tree | 665 |
| 72 | Non-Tree (Vegetation) | Non-Tree (Vegetation) | Non-Tree (Vegetation) | 666 |
| 73 | Non-Tree (Vegetation) | Inundated Land | Building | 641 |
| 74 | Non-Tree (Vegetation) | Inundated Land | Impervious surface | 642 |
| 75 | Non-Tree (Vegetation) | Inundated Land | Bare Land | 643 |
| 76 | Non-Tree (Vegetation) | Inundated Land | Inland Water | 644 |
| 77 | Non-Tree (Vegetation) | Inundated Land | Tree | 645 |
| 78 | Non-Tree (Vegetation) | Inundated Land | Non-Tree (Vegetation) | 646 |

## Annex 2: A complete list of LU-based transition patterns in the study area

| ID | T0 | T1 | T2 | Transition ID |
|---|---|---|---|---|
| 1 | LSI | LSI | LSI | 111 |
| 2 | LSI | LSI | IBA | 112 |
| 3 | LSI | LSI | FBA | 113 |
| 4 | LSI | LSI | Palm Tree | 114 |
| 5 | LSI | LSI | Other Tree | 115 |
| 6 | LSI | LSI | Recreation Area | 116 |
| 7 | LSI | LSI | Crop Land | 117 |
| 8 | LSI | LSI | Grass Land | 118 |
| 9 | LSI | LSI | Inland Water | 119 |
| 10 | LSI | LSI | Bare Land | 1110 |
| 11 | LSI | LSI | Impervious Surface | 1111 |
| 12 | LSI | Rubble | LSI | 151 |
| 13 | LSI | Rubble | IBA | 152 |
| 14 | LSI | Rubble | FBA | 153 |
| 15 | LSI | Rubble | Palm Tree | 154 |
| 16 | LSI | Rubble | Other Tree | 155 |
| 17 | LSI | Rubble | Recreation Area | 156 |
| 18 | LSI | Rubble | Crop Land | 157 |
| 19 | LSI | Rubble | Grass Land | 158 |
| 20 | LSI | Rubble | Inland Water | 159 |
| 21 | LSI | Rubble | Bare Land | 1510 |
| 22 | LSI | Rubble | Impervious Surface | 1511 |
| 23 | IBA | IBA | LSI | 221 |
| 24 | IBA | IBA | IBA | 222 |
| 25 | IBA | IBA | FBA | 223 |
| 26 | IBA | IBA | Palm Tree | 224 |
| 27 | IBA | IBA | Other Tree | 225 |
| 28 | IBA | IBA | Recreation Area | 226 |
| 29 | IBA | IBA | Crop Land | 227 |
| 30 | IBA | IBA | Grass Land | 228 |
| 31 | IBA | IBA | Inland Water | 229 |
| 32 | IBA | IBA | Bare Land | 2210 |
| 33 | IBA | IBA | Impervious Surface | 2211 |
| 34 | IBA | Rubble | LSI | 251 |
| 35 | IBA | Rubble | IBA | 252 |
| 36 | IBA | Rubble | FBA | 253 |
| 37 | IBA | Rubble | Palm Tree | 254 |
| 38 | IBA | Rubble | Other Tree | 255 |

| ID | T0 | T1 | T2 | Transition ID |
|---|---|---|---|---|
| 39 | IBA | Rubble | Recreation Area | 256 |
| 40 | IBA | Rubble | Crop Land | 257 |
| 41 | IBA | Rubble | Grass Land | 258 |
| 42 | IBA | Rubble | Inland Water | 259 |
| 43 | IBA | Rubble | Bare Land | 2510 |
| 44 | IBA | Rubble | Impervious Surface | 2511 |
| 45 | IBA | Inundated Land | LSI | 291 |
| 46 | IBA | Inundated Land | IBA | 292 |
| 47 | IBA | Inundated Land | FBA | 293 |
| 48 | IBA | Inundated Land | Palm Tree | 294 |
| 49 | IBA | Inundated Land | Other Tree | 295 |
| 50 | IBA | Inundated Land | Recreation Area | 296 |
| 51 | IBA | Inundated Land | Crop Land | 297 |
| 52 | IBA | Inundated Land | Grass Land | 298 |
| 53 | IBA | Inundated Land | Inland Water | 299 |
| 54 | IBA | Inundated Land | Bare Land | 2910 |
| 55 | IBA | Inundated Land | Impervious Surface | 2911 |
| 56 | FBA | FBA | LSI | 331 |
| 57 | FBA | FBA | IBA | 332 |
| 58 | FBA | FBA | FBA | 333 |
| 59 | FBA | FBA | Palm Tree | 334 |
| 60 | FBA | FBA | Other Tree | 335 |
| 61 | FBA | FBA | Recreation Area | 336 |
| 62 | FBA | FBA | Crop Land | 337 |
| 63 | FBA | FBA | Grass Land | 338 |
| 64 | FBA | FBA | Inland Water | 339 |
| 65 | FBA | FBA | Bare Land | 3310 |
| 66 | FBA | FBA | Impervious Surface | 3311 |
| 67 | FBA | Rubble | LSI | 351 |
| 68 | FBA | Rubble | IBA | 352 |
| 69 | FBA | Rubble | FBA | 353 |
| 70 | FBA | Rubble | Palm Tree | 354 |
| 71 | FBA | Rubble | Other Tree | 355 |
| 72 | FBA | Rubble | Recreation Area | 356 |
| 73 | FBA | Rubble | Crop Land | 357 |
| 74 | FBA | Rubble | Grass Land | 358 |
| 75 | FBA | Rubble | Inland Water | 359 |
| 76 | FBA | Rubble | Bare Land | 3510 |

| ID | T0 | T1 | T2 | Transition ID |
|---|---|---|---|---|
| 77 | FBA | Rubble | Impervious Surface | 3511 |
| 78 | Palm Tree | Flattened Tree | LSI | 441 |
| 79 | Palm Tree | Flattened Tree | IBA | 442 |
| 80 | Palm Tree | Flattened Tree | FBA | 443 |
| 81 | Palm Tree | Flattened Tree | Palm Tree | 444 |
| 82 | Palm Tree | Flattened Tree | Other Tree | 445 |
| 83 | Palm Tree | Flattened Tree | Recreation Area | 446 |
| 84 | Palm Tree | Flattened Tree | Crop Land | 447 |
| 85 | Palm Tree | Flattened Tree | Grass Land | 448 |
| 86 | Palm Tree | Flattened Tree | Inland Water | 449 |
| 87 | Palm Tree | Flattened Tree | Bare Land | 4410 |
| 88 | Palm Tree | Flattened Tree | Impervious Surface | 4411 |
| 89 | Other Tree | Flattened Tree | LSI | 541 |
| 90 | Other Tree | Flattened Tree | IBA | 542 |
| 91 | Other Tree | Flattened Tree | FBA | 543 |
| 92 | Other Tree | Flattened Tree | Palm Tree | 544 |
| 93 | Other Tree | Flattened Tree | Other Tree | 545 |
| 94 | Other Tree | Flattened Tree | Recreation Area | 546 |
| 95 | Other Tree | Flattened Tree | Crop Land | 547 |
| 96 | Other Tree | Flattened Tree | Grass Land | 548 |
| 97 | Other Tree | Flattened Tree | Inland Water | 549 |
| 98 | Other Tree | Flattened Tree | Bare Land | 5410 |
| 99 | Other Tree | Flattened Tree | Impervious Surface | 5411 |
| 100 | Recreation Area | Recreation Area | LSI | 661 |
| 101 | Recreation Area | Recreation Area | IBA | 662 |
| 102 | Recreation Area | Recreation Area | FBA | 663 |
| 103 | Recreation Area | Recreation Area | Palm Tree | 664 |
| 104 | Recreation Area | Recreation Area | Other Tree | 665 |
| 105 | Recreation Area | Recreation Area | Recreation Area | 666 |
| 106 | Recreation Area | Recreation Area | Crop Land | 667 |
| 107 | Recreation Area | Recreation Area | Grass Land | 668 |
| 108 | Recreation Area | Recreation Area | Inland Water | 669 |
| 109 | Recreation Area | Recreation Area | Bare Land | 6610 |
| 110 | Recreation Area | Recreation Area | Impervious Surface | 6611 |
| 111 | Recreation Area | Rubble | LSI | 651 |
| 112 | Recreation Area | Rubble | IBA | 652 |
| 113 | Recreation Area | Rubble | FBA | 653 |
| 114 | Recreation Area | Rubble | Palm Tree | 654 |

| ID | T0 | T1 | T2 | Transition ID |
|---|---|---|---|---|
| 115 | Recreation Area | Rubble | Other Tree | 655 |
| 116 | Recreation Area | Rubble | Recreation Area | 656 |
| 117 | Recreation Area | Rubble | Crop Land | 657 |
| 118 | Recreation Area | Rubble | Grass Land | 658 |
| 119 | Recreation Area | Rubble | Inland Water | 659 |
| 120 | Recreation Area | Rubble | Bare Land | 6510 |
| 121 | Recreation Area | Rubble | Impervious Surface | 6511 |
| 122 | Recreation Area | Inundated Land | LSI | 691 |
| 123 | Recreation Area | Inundated Land | IBA | 692 |
| 124 | Recreation Area | Inundated Land | FBA | 693 |
| 125 | Recreation Area | Inundated Land | Palm Tree | 694 |
| 126 | Recreation Area | Inundated Land | Other Tree | 695 |
| 127 | Recreation Area | Inundated Land | Recreation Area | 696 |
| 128 | Recreation Area | Inundated Land | Crop Land | 697 |
| 129 | Recreation Area | Inundated Land | Grass Land | 698 |
| 130 | Recreation Area | Inundated Land | Inland Water | 699 |
| 131 | Recreation Area | Inundated Land | Bare Land | 6910 |
| 132 | Recreation Area | Inundated Land | Impervious Surface | 6911 |
| 133 | Crop Land | Crop Land | LSI | 771 |
| 134 | Crop Land | Crop Land | IBA | 772 |
| 135 | Crop Land | Crop Land | FBA | 773 |
| 136 | Crop Land | Crop Land | Palm Tree | 774 |
| 137 | Crop Land | Crop Land | Other Tree | 775 |
| 138 | Crop Land | Crop Land | Recreation Area | 776 |
| 139 | Crop Land | Crop Land | Crop Land | 777 |
| 140 | Crop Land | Crop Land | Grass Land | 778 |
| 141 | Crop Land | Crop Land | Inland Water | 779 |
| 142 | Crop Land | Crop Land | Bare Land | 7710 |
| 143 | Crop Land | Crop Land | Impervious Surface | 7711 |
| 144 | Crop Land | Inundated Land | LSI | 791 |
| 145 | Crop Land | Inundated Land | IBA | 792 |
| 146 | Crop Land | Inundated Land | FBA | 793 |
| 147 | Crop Land | Inundated Land | Palm Tree | 794 |
| 148 | Crop Land | Inundated Land | Other Tree | 795 |
| 149 | Crop Land | Inundated Land | Recreation Area | 796 |
| 150 | Crop Land | Inundated Land | Crop Land | 797 |
| 151 | Crop Land | Inundated Land | Grass Land | 798 |
| 152 | Crop Land | Inundated Land | Inland Water | 799 |

| ID | T0 | T1 | T2 | Transition ID |
|---|---|---|---|---|
| 153 | Crop Land | Inundated Land | Bare Land | 7910 |
| 154 | Crop Land | Inundated Land | Impervious Surface | 7911 |
| 155 | Grass Land | Grass Land | LSI | 881 |
| 156 | Grass Land | Grass Land | IBA | 882 |
| 157 | Grass Land | Grass Land | FBA | 883 |
| 158 | Grass Land | Grass Land | Palm Tree | 884 |
| 159 | Grass Land | Grass Land | Other Tree | 885 |
| 160 | Grass Land | Grass Land | Recreation Area | 886 |
| 161 | Grass Land | Grass Land | Crop Land | 887 |
| 162 | Grass Land | Grass Land | Grass Land | 888 |
| 163 | Grass Land | Grass Land | Inland Water | 889 |
| 164 | Grass Land | Grass Land | Bare Land | 8810 |
| 165 | Grass Land | Grass Land | Impervious Surface | 8811 |
| 166 | Grass Land | Rubble | LSI | 851 |
| 167 | Grass Land | Rubble | IBA | 852 |
| 168 | Grass Land | Rubble | FBA | 853 |
| 169 | Grass Land | Rubble | Palm Tree | 854 |
| 170 | Grass Land | Rubble | Other Tree | 855 |
| 171 | Grass Land | Rubble | Recreation Area | 856 |
| 172 | Grass Land | Rubble | Crop Land | 857 |
| 173 | Grass Land | Rubble | Grass Land | 858 |
| 174 | Grass Land | Rubble | Inland Water | 859 |
| 175 | Grass Land | Rubble | Bare Land | 8510 |
| 176 | Grass Land | Rubble | Impervious Surface | 8511 |
| 177 | Grass Land | Inundated Land | LSI | 891 |
| 178 | Grass Land | Inundated Land | IBA | 892 |
| 179 | Grass Land | Inundated Land | FBA | 893 |
| 180 | Grass Land | Inundated Land | Palm Tree | 894 |
| 181 | Grass Land | Inundated Land | Other Tree | 895 |
| 182 | Grass Land | Inundated Land | Recreation Area | 896 |
| 183 | Grass Land | Inundated Land | Crop Land | 897 |
| 184 | Grass Land | Inundated Land | Grass Land | 898 |
| 185 | Grass Land | Inundated Land | Inland Water | 899 |
| 186 | Grass Land | Inundated Land | Bare Land | 8910 |
| 187 | Grass Land | Inundated Land | Impervious Surface | 8911 |

**Annex 3: LU plan of study area (CLP, 2016)**

| LAND USE | EXISTING LAND USE 2016 | PROPOSED LAND USE2025 | STATUS |
|---|---|---|---|
| Residential | 1,190.63 | 1,400.00 | increase |
| Socialized Housing | 151.65 | 253.52 | increase |
| Commercial | 505.30 | 618.18 | increase |
| Agri-Industrial | 27.72 | 27.72 | same |
| Light Industrial | 74.92 | 74.92 | same |
| Institutional | 138.98 | 290.97 | increase |
| Special Institution | 22.51 | 22.51 | same |
| Parks | 38.98 | 272.79 | increase |
| Tourism Zone | 72.18 | 212.82 | increase |
| Buffer zone | 373.41 | 405.12 | increase |
| Roads | 514.85 | 898.90 | increase |
| Protection Forest | 1,993.43 | 1,993.43 | same |
| Production Forest | 1,910.11 | 1,910.11 | same |
| Industrial Forest | 81.99 | 81.99 | same |
| Agricultural | 3,013.93 | 1,598.92 | decrease |
| Cemeteries | 20.00 | 29.67 | increase |
| Sanitary Landfill | 4.00 | 5.00 | increase |
| Utilities | 102.08 | 125.07 | increase |
| Rivers | 67.03 | 67.03 | same |
| Mangroves | 190.54 | 190.54 | same |
| Aquaculture | 17.63 | 17.63 | same |
| Lake | - | 15.04 | increase |
| Cancabato Marine Protection | 562.76 | 562.76 | same |
| Dio Fish Sanctuary | 50.00 | 50.00 | same |
| San Juanico Mariculture Zone | 1,023.85 | 1,023.85 | same |
| San Pedro Bay | 8,023.51 | 8,023.51 | same |
| **TOTAL** | **20,172.00** | **20,172.00** | |